Neutronenradiographie und Tomographie am Instrument ANTARES

Forschungsreaktor München II

Technische Universität München

Dr. Burkhard Schillinger

Mass attenuation coefficient for X-rays, gamms, fast and thermal neutrons

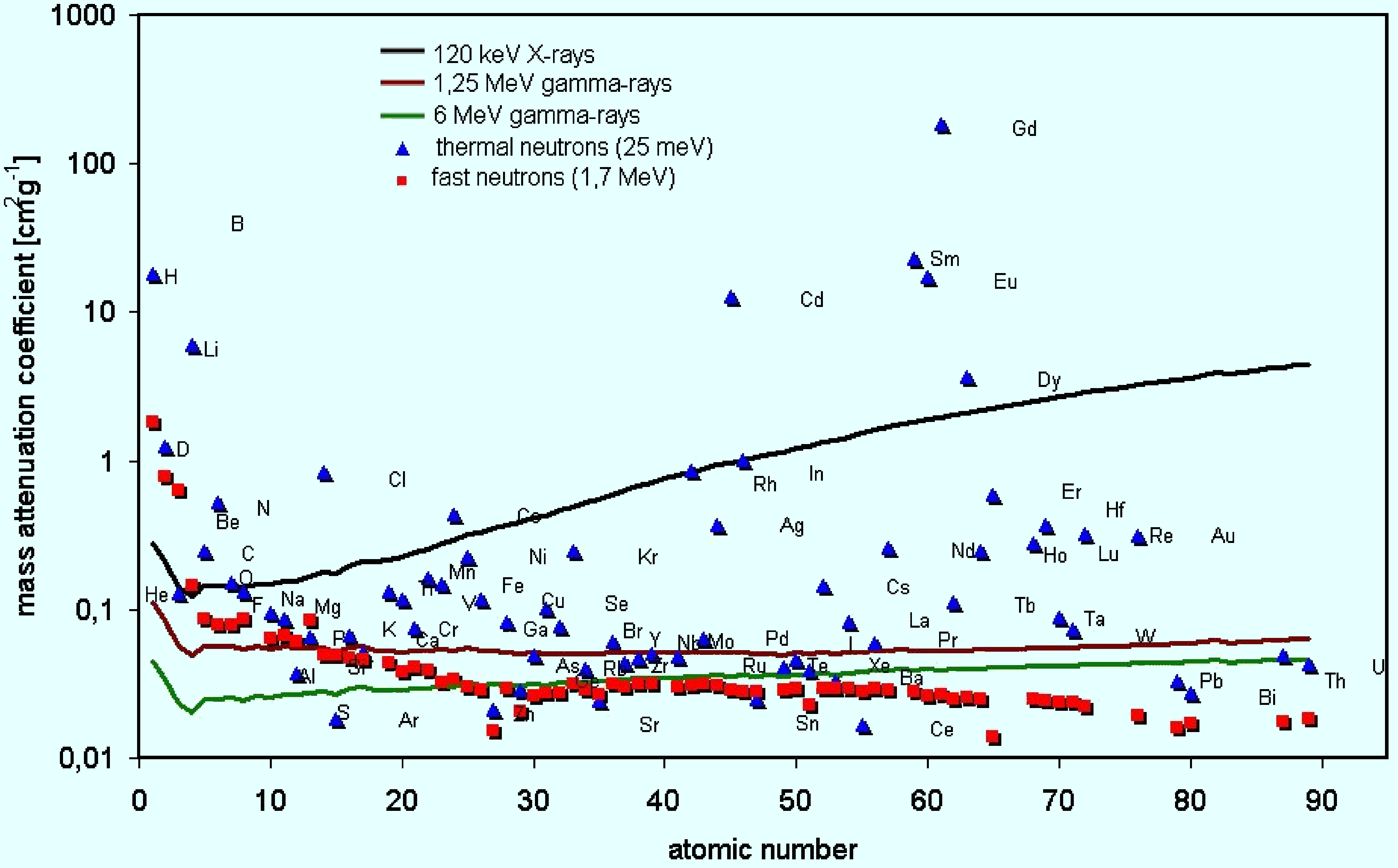

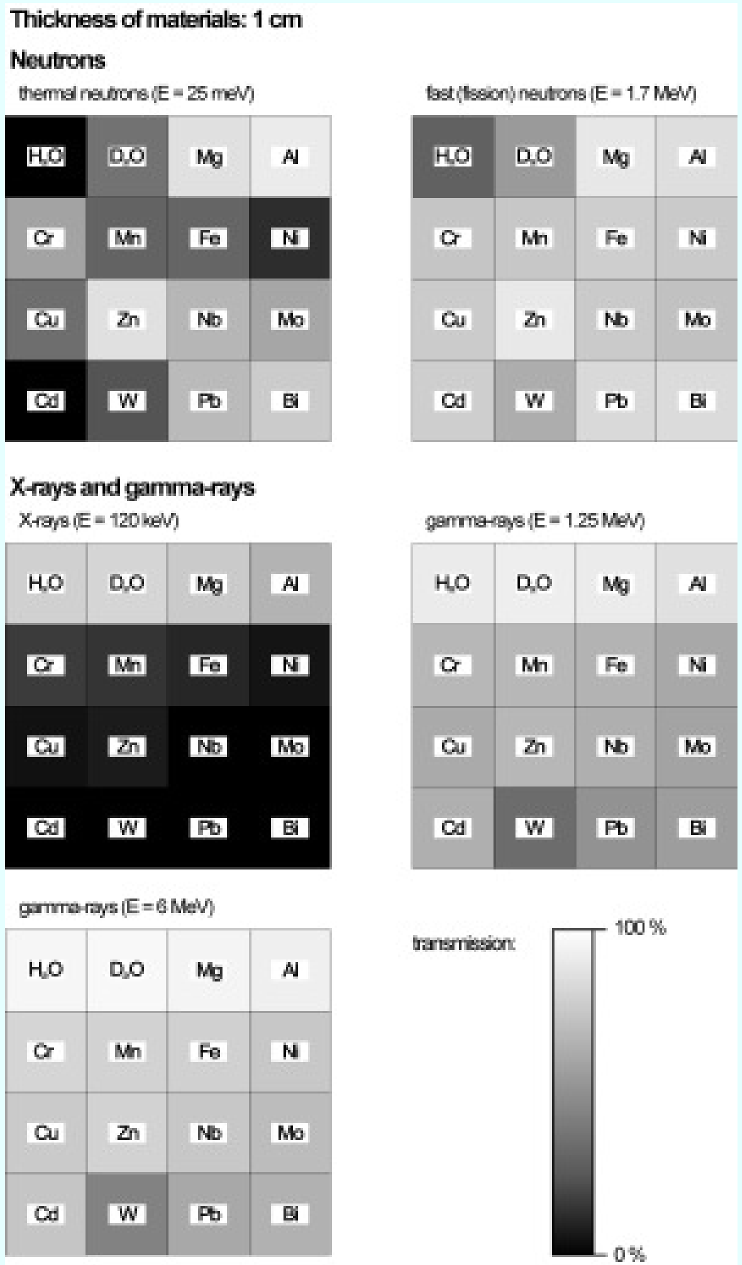
Thickness of materials: 1 cm
Neutrons
thermal neutrons (E = 25 meV)
fast (fission) neutrons (E = 1.7 MeV)
X-rays and gamma-rays
X-rays (E = 120 keV)
gamma-rays (E = 1.25 MeV)
gamma-rays (E = 6 MeV)
H2O D2O Mg Al
Cr Mn Fe Ni
Cu Zn Nb Mo
Cd W Pb Bi
transmission:
100 %
0 %

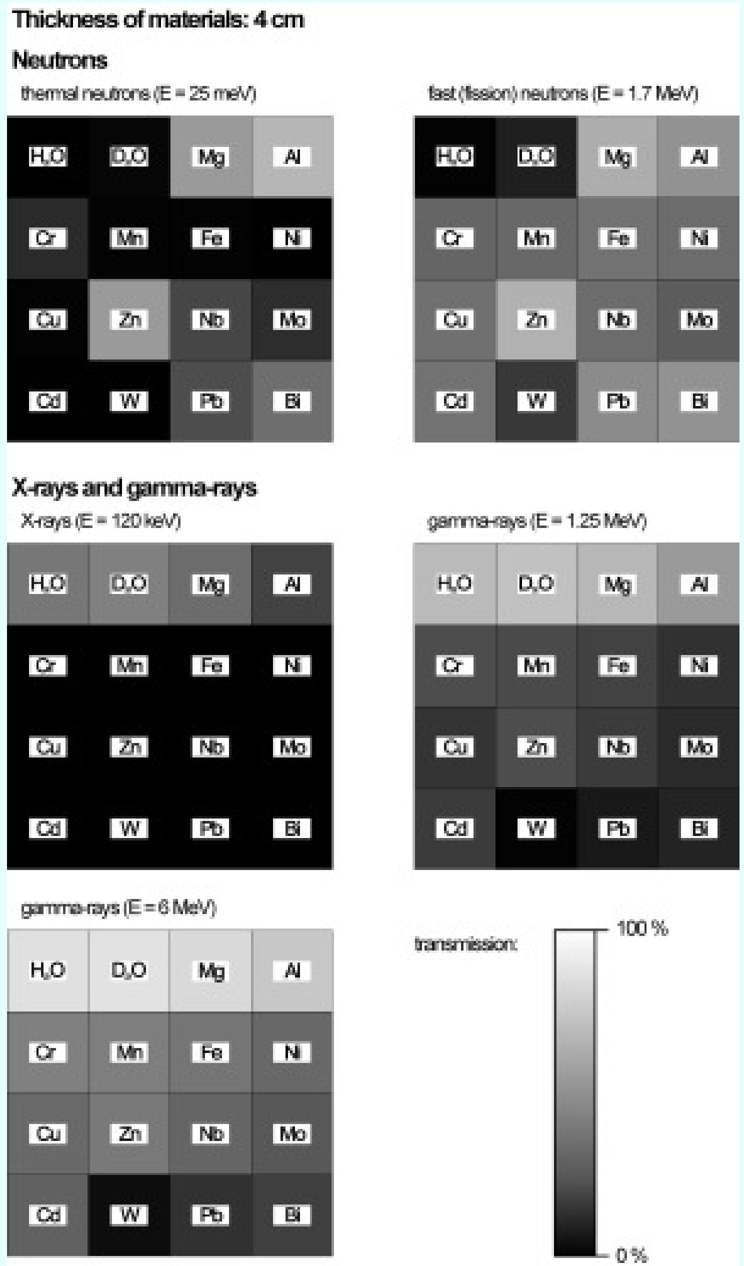
Thickness of materials: 4 cm
Neutrons
thermal neutrons (E = 25 meV)
fast (fission) neutrons (E = 1.7 MeV)
X-rays and gamma-rays
X-rays (E = 120 keV)
gamma-rays (E = 1.25 MeV)
gamma-rays (E = 6 MeV)
H2O D2O Mg Al
Cr Mn Fe Ni
Cu Zn Nb Mo
Cd W Pb Bi
transmission:
100 %
0 %

Antares

Advanced **N**eutron **T**omography **A**nd **R**adiography **E**xperimental **S**ystem

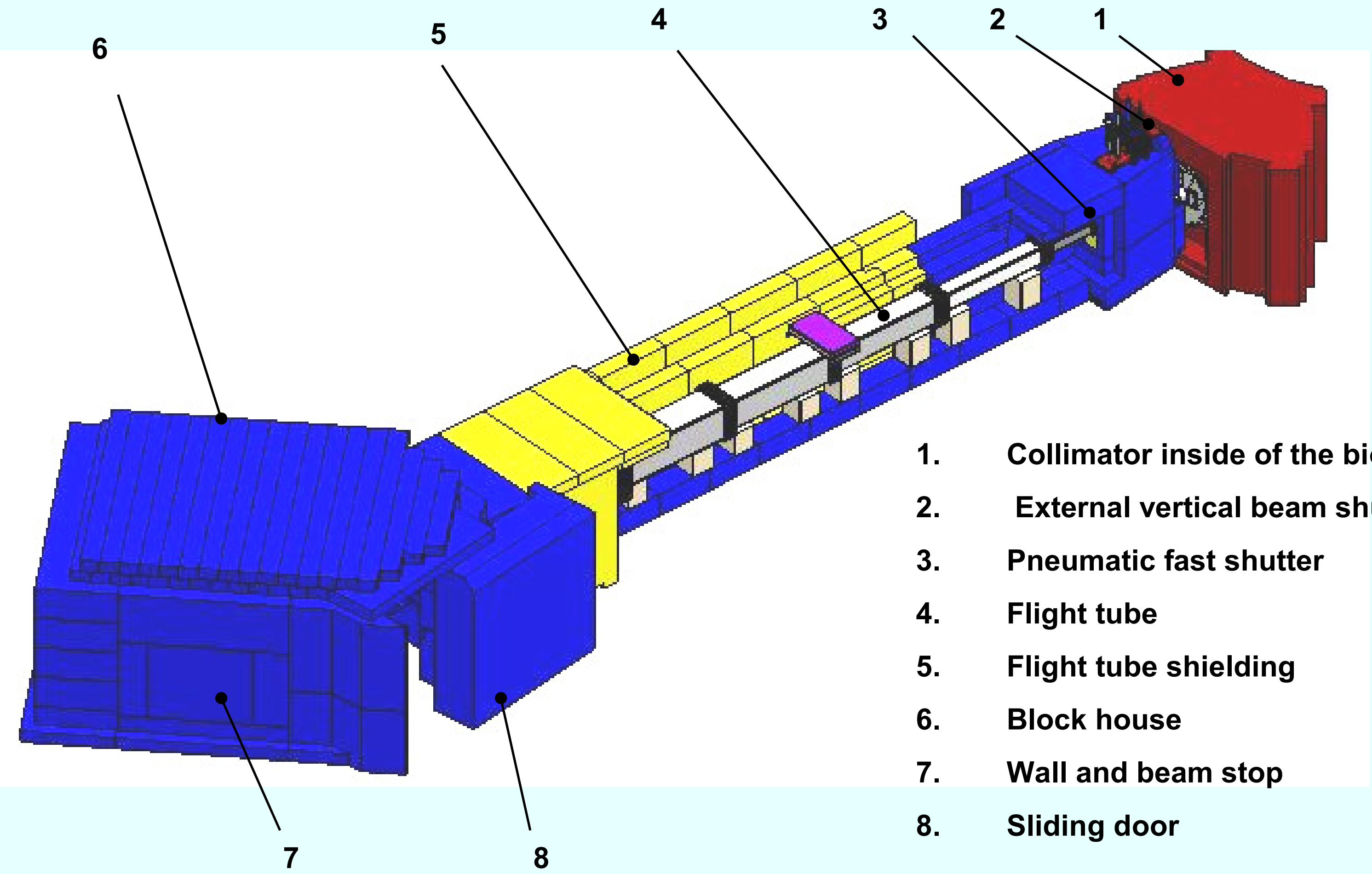

1. Collimator inside of the biological shielding
2. External vertical beam shutter
3. Pneumatic fast shutter
4. Flight tube
5. Flight tube shielding
6. Block house
7. Wall and beam stop
8. Sliding door


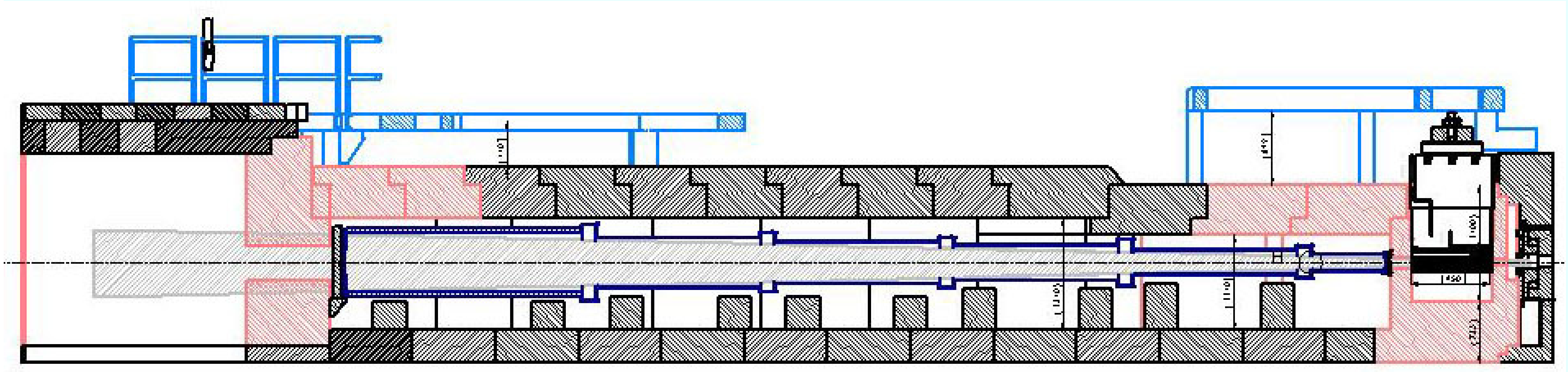

Cross section of the ANTARES facility.
The roof components were positioned with the hall crane on the lateral walls situated between the two platforms of the positron source, then slid under the platform on retractable ball rollers.

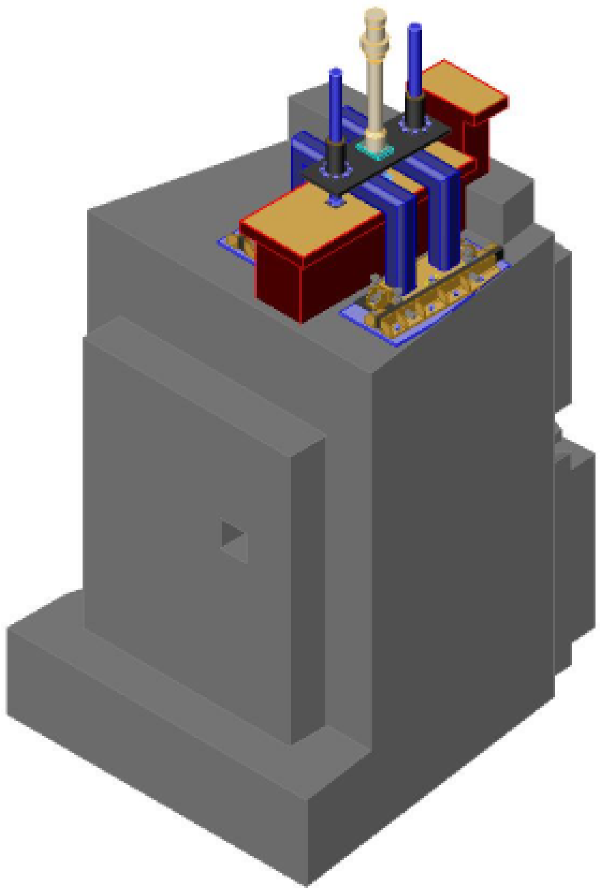

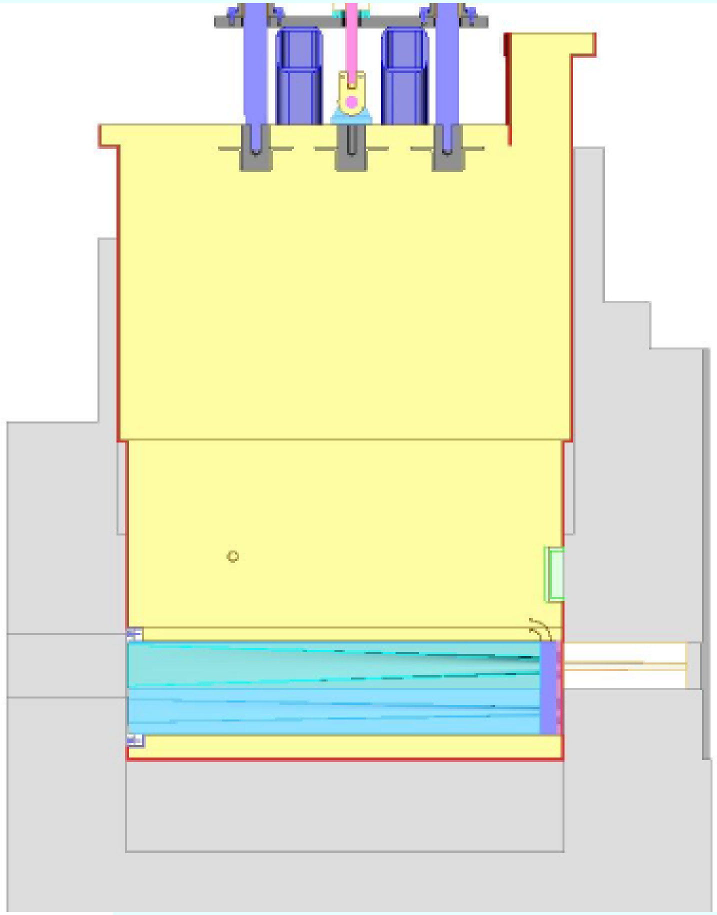

External hydraulic shutter of the ANTARES facility.
The slider contains two different collimators that can be positioned and locked in place by a position-controlled hydraulic system and hydraulic clamps.

Locking Units:

Clamping by spring action, release by hydraulic pressure

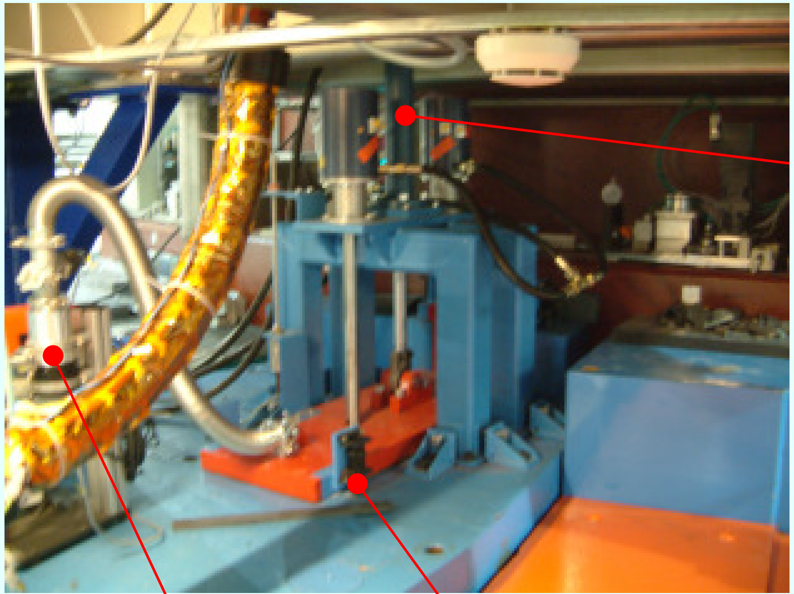

Hydraulic cylinnder

Vacuum pump **shock absorber**

Two collimators:
With a different collimation ratio of L/D=400 and L/D=800.

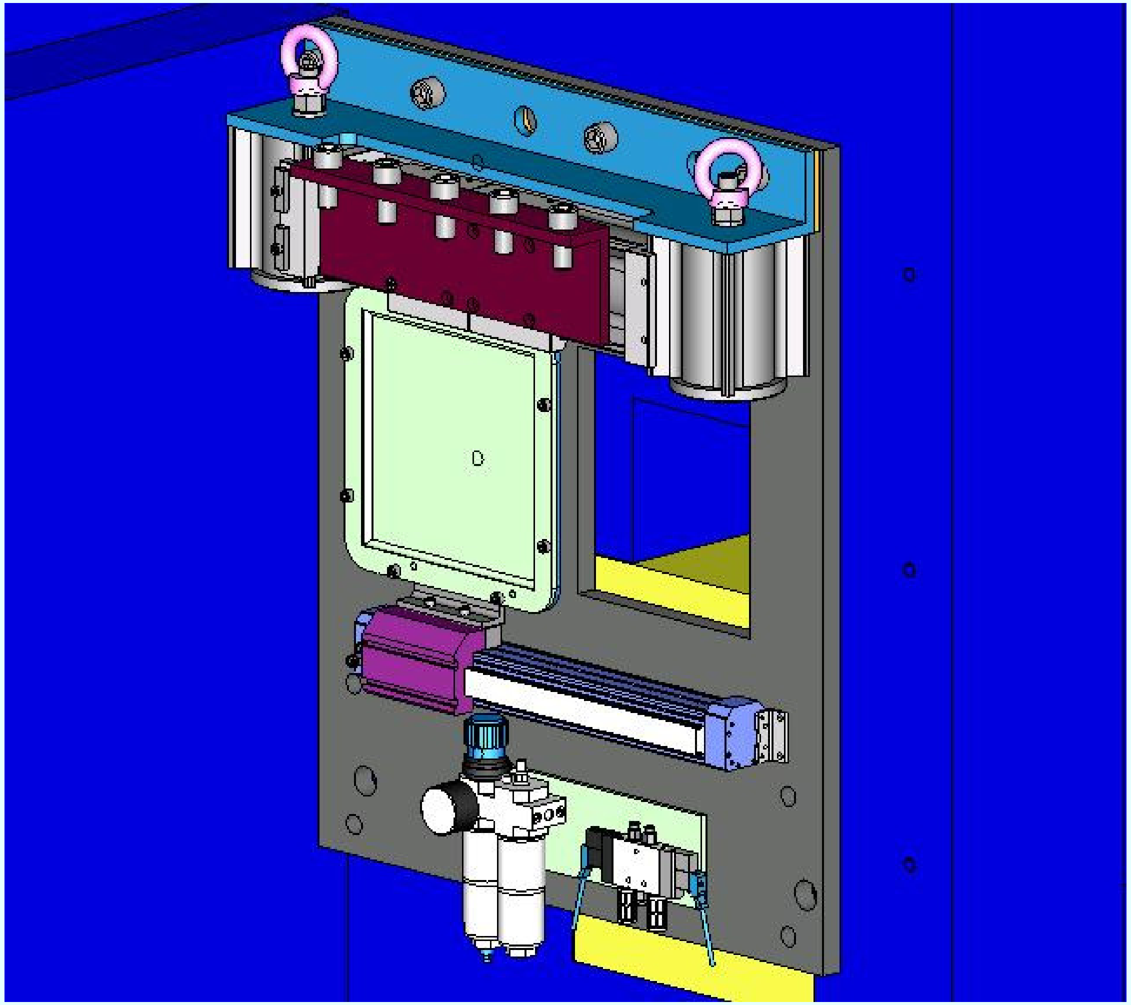

A pneumatic fast shutter at the beginning of the flight tube is used to shut off the thermal beam between exposures in order to minimize activation of the sample .

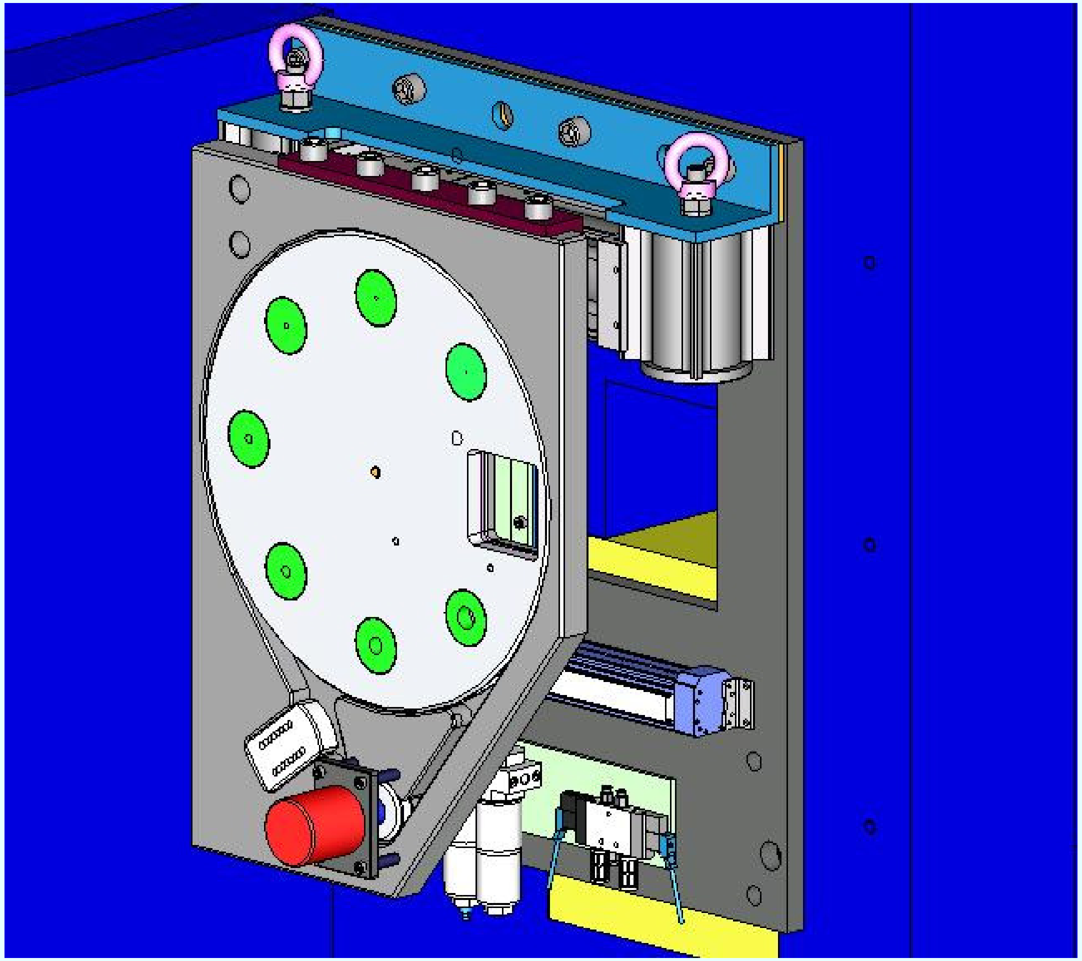

A selector wheel with different masks for will allow to switch the facility
to phase contrast imaging within seconds .

The sample manipulator can carry up to 500 kg samples up to 1 m diameter.

A standard neutron radiography: A diesel injector pump

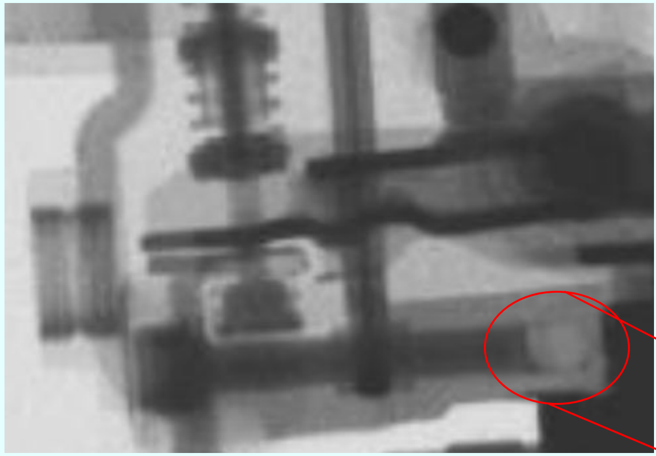

Oil remains

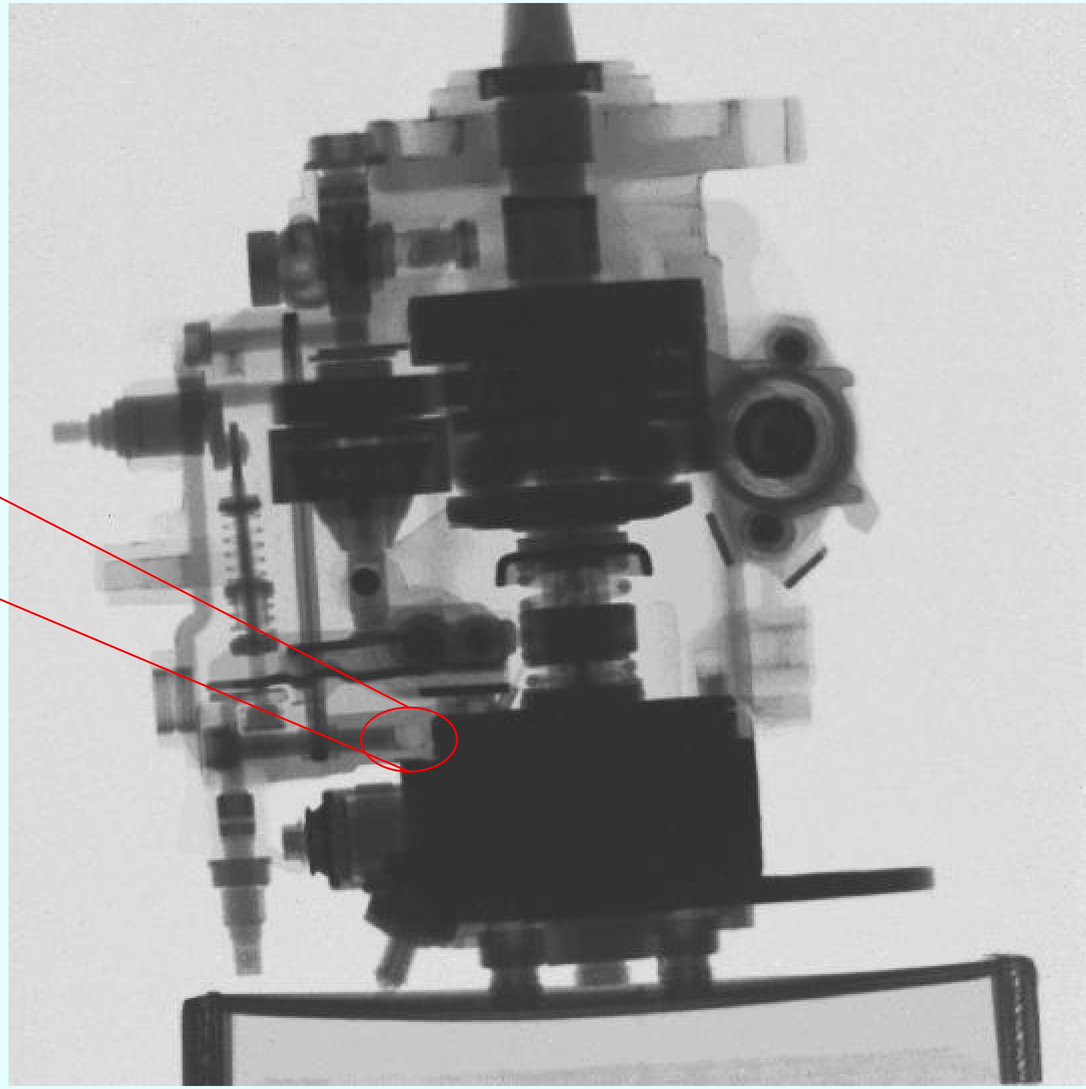

Typical static radiography: A gas pressure reducer with sealants and o-rings

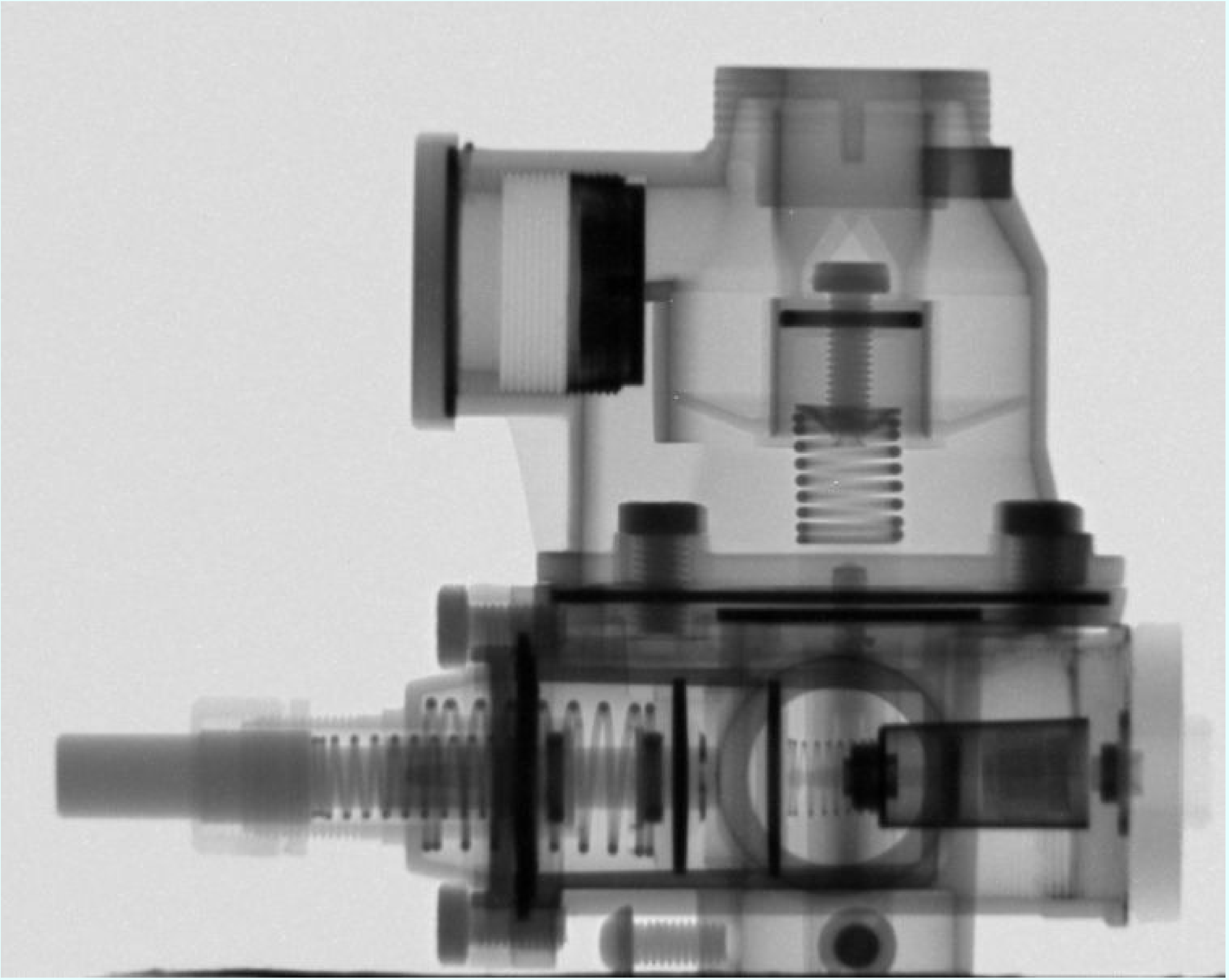

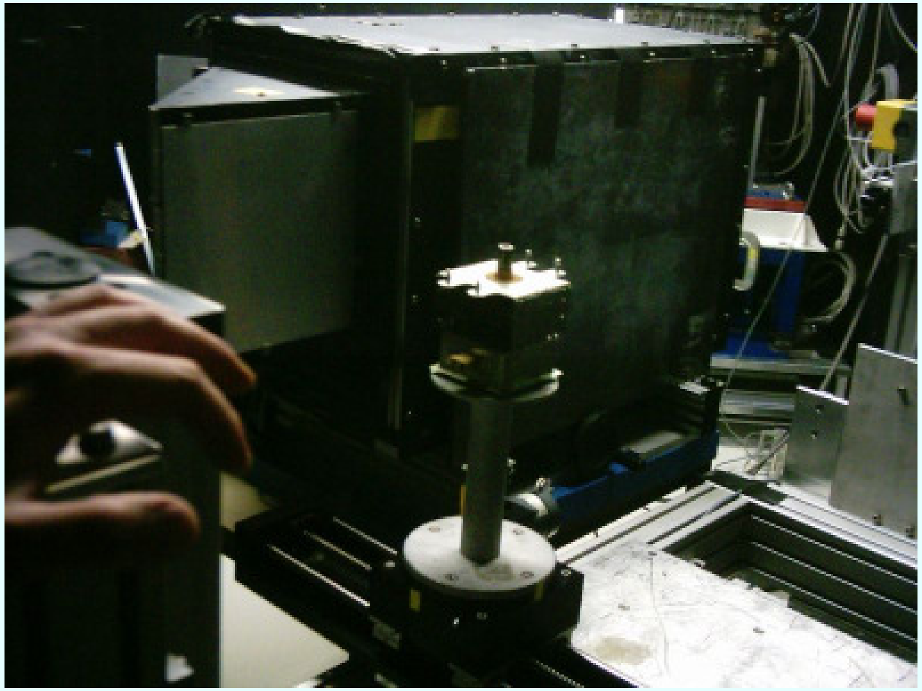

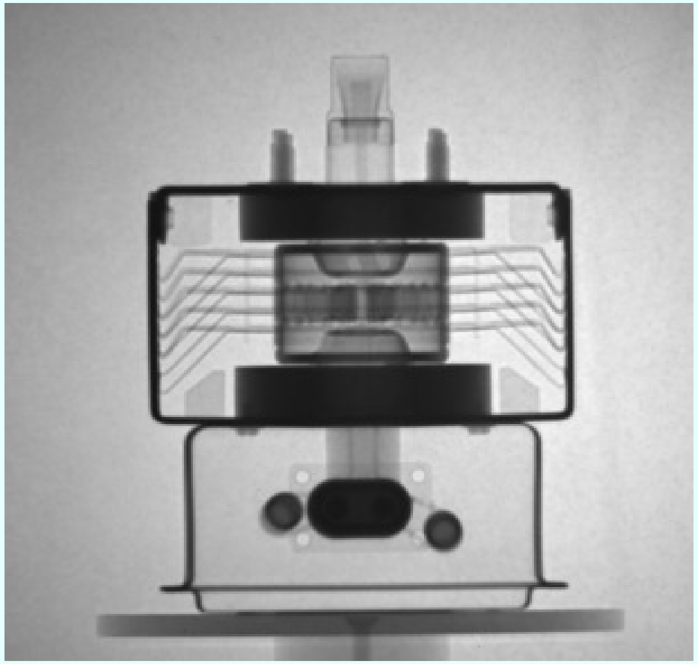

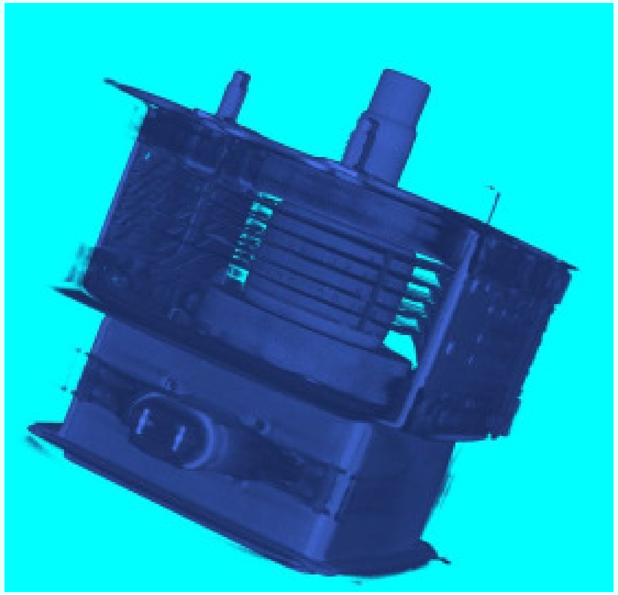

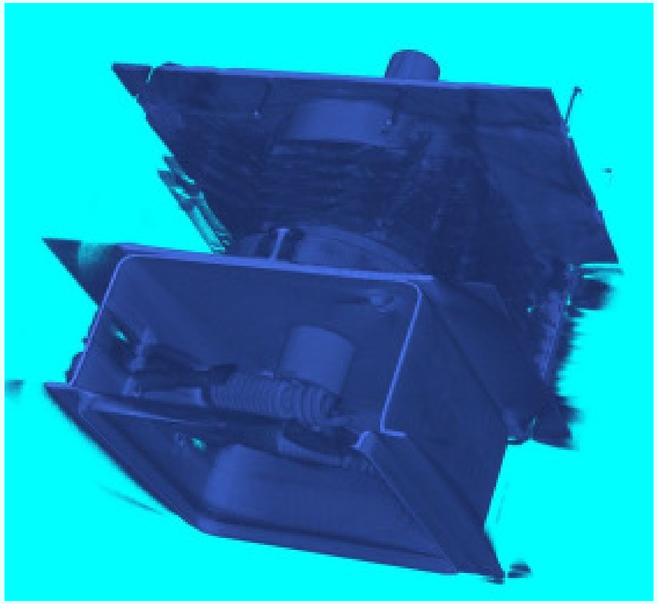

Radiography and tomography of a microwave klystron

Einige technische Beispiele

Ein schon älteres Beispiel:

Diese Rohrbombe hat uns das Bundeskriminalamt zum Ausprobieren gebaut – ohne Sprengstoff.

Das Stahlrohr ist 8 mm dick.

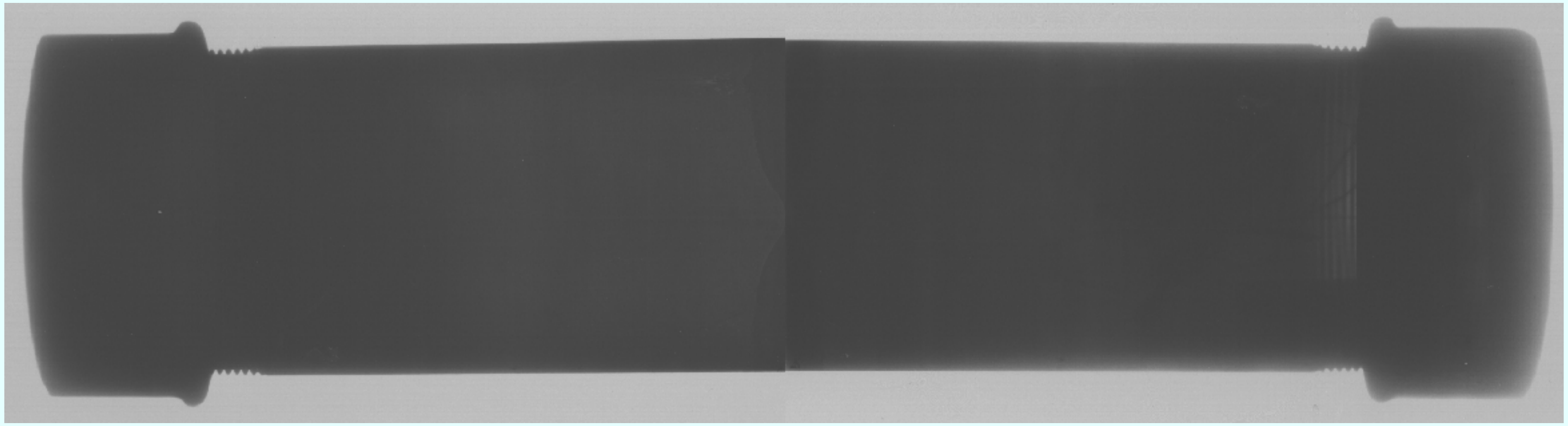

Mit 150 kV-Röntgenstrahlen ist die Wandung kaum zu durchdringen.

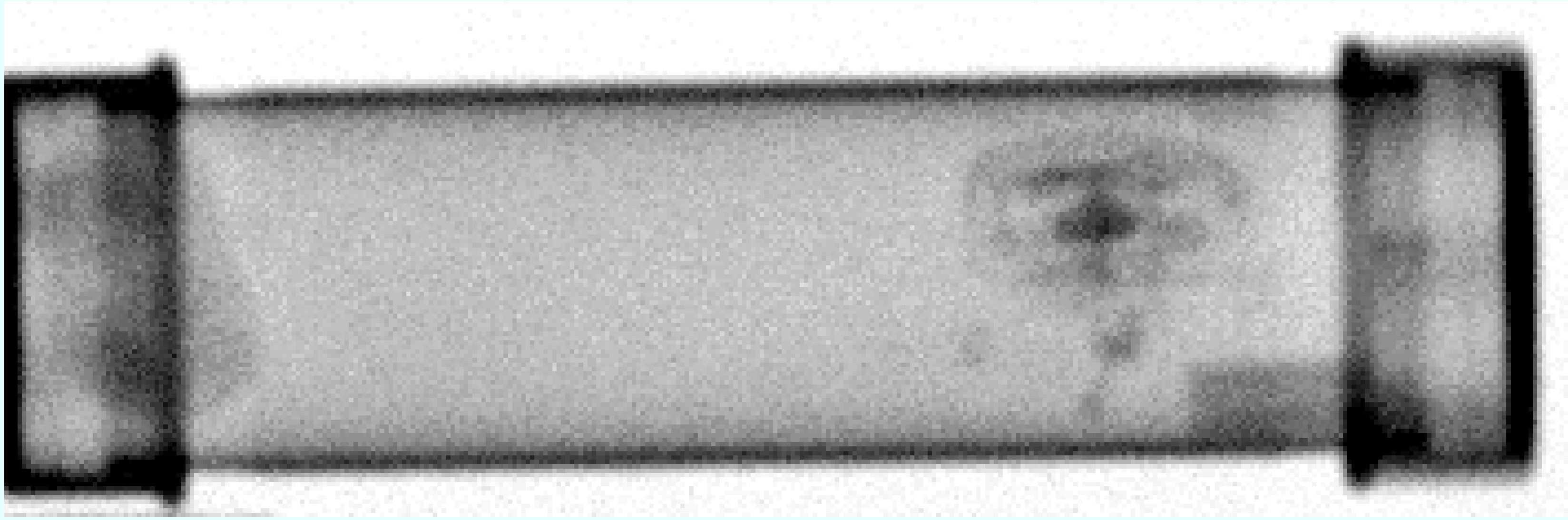

Für harte Gammastrahlung (Kobalt-60, 1,2 MeV)
wird zwar das Stahlrohr transparent, jedoch auch der Inhalt.

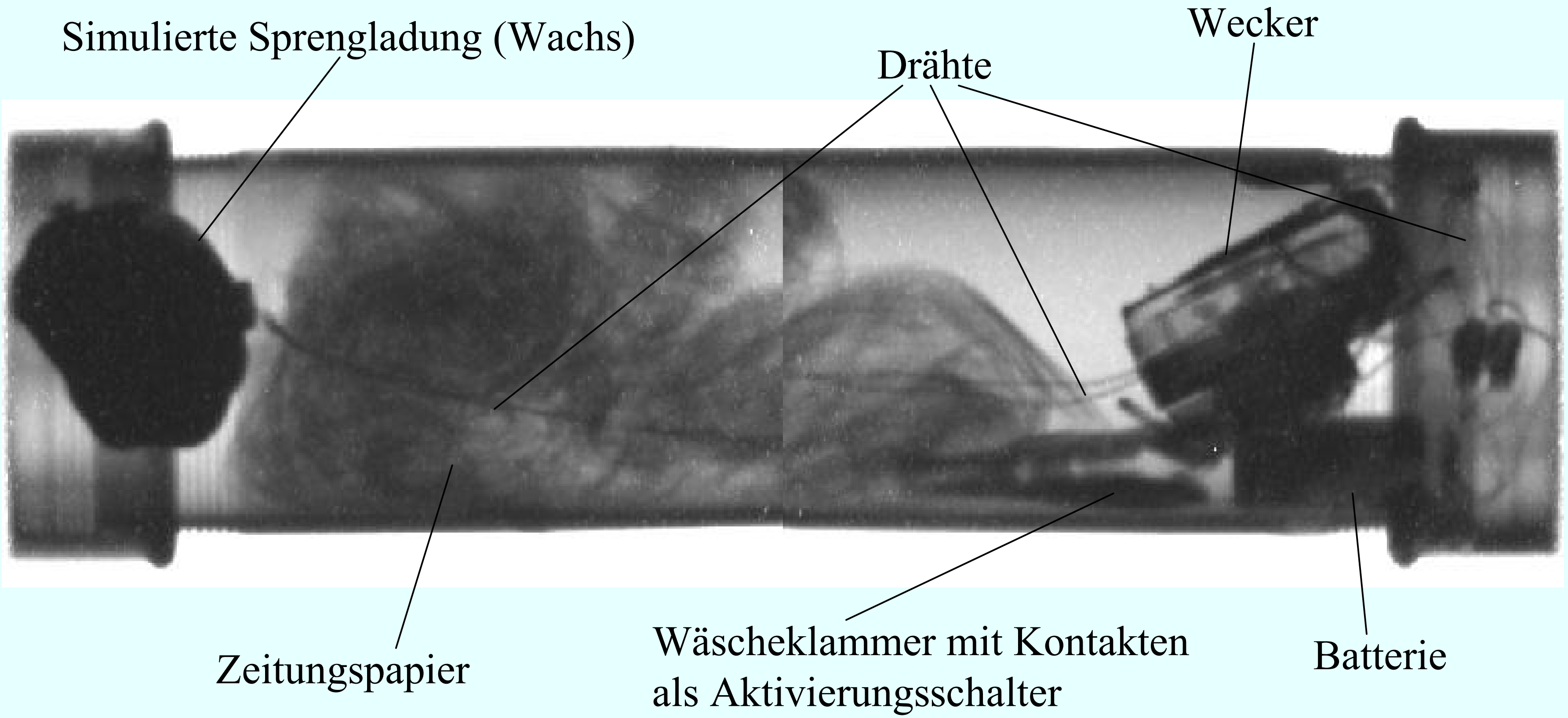

Mit thermischen Neutronen sieht man umso mehr!

Extension: Planning accessories and more possibilities

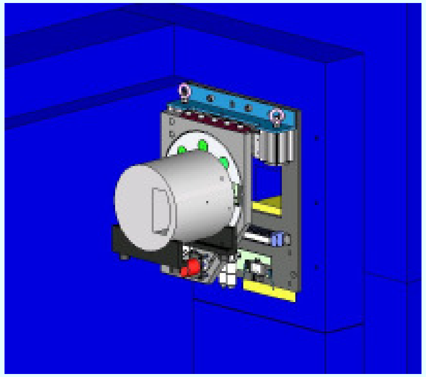

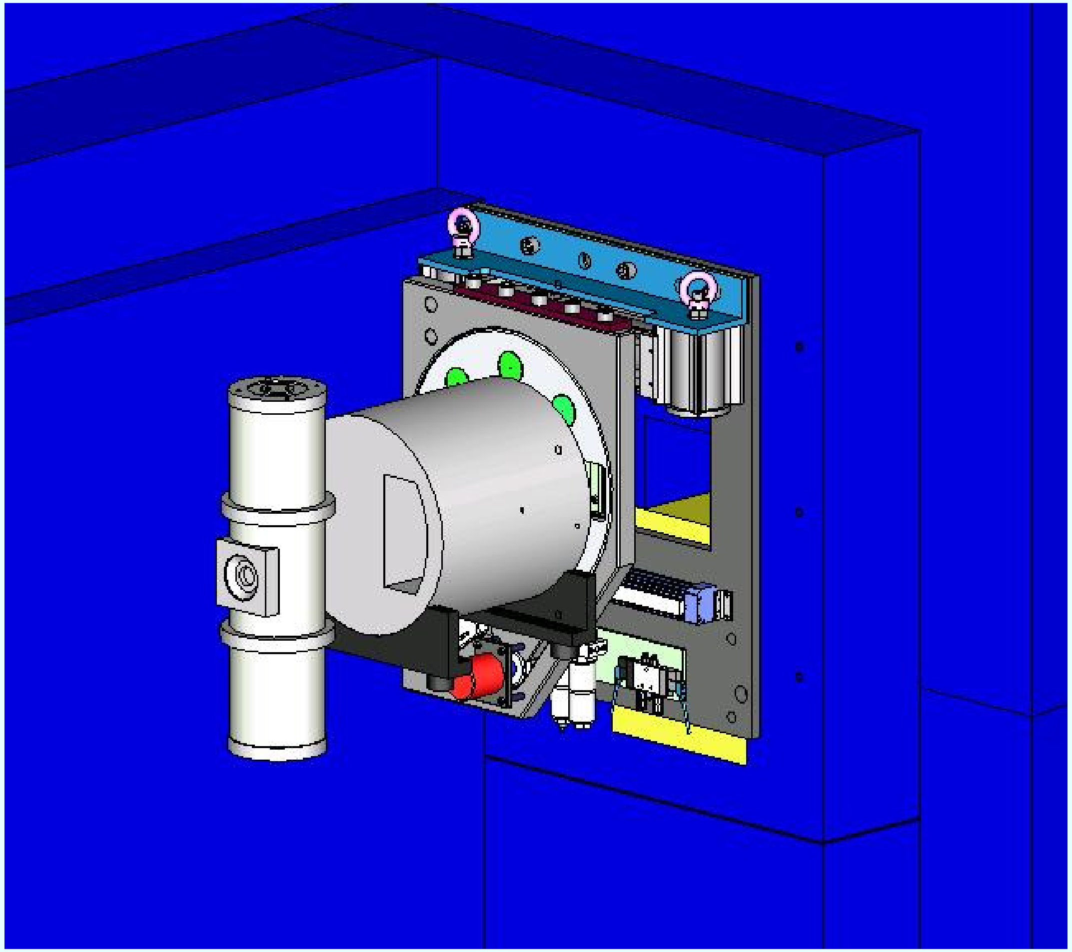

A removable 320 kV X-ray tube has been mounted before the flight tube.
This allows for alternate X-ray tomography in the identical beam geometry!

4. Extension: Planning accessories and more possibilities

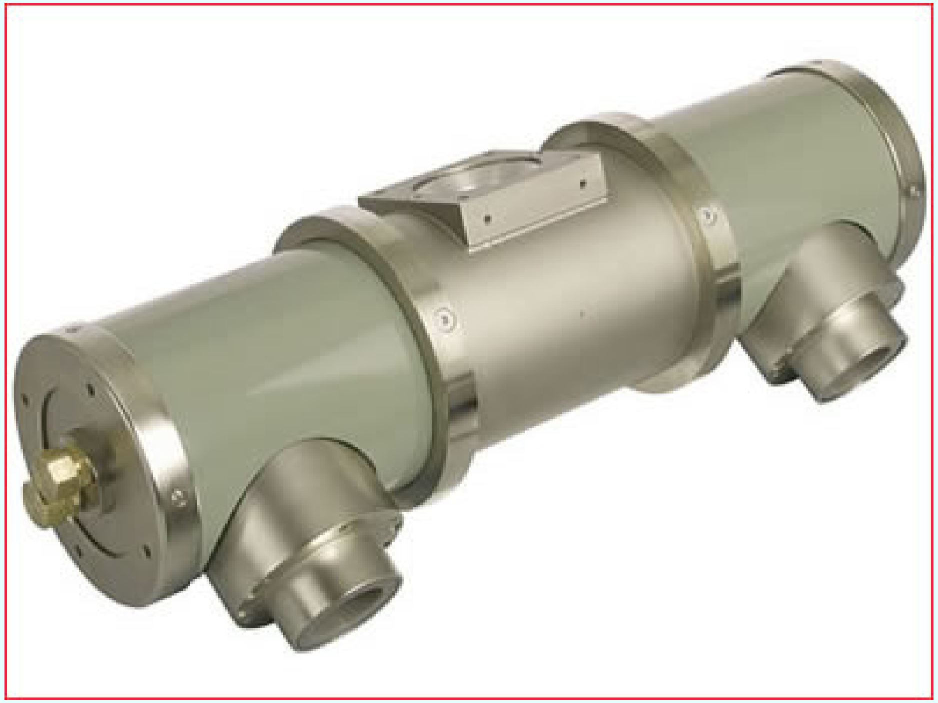

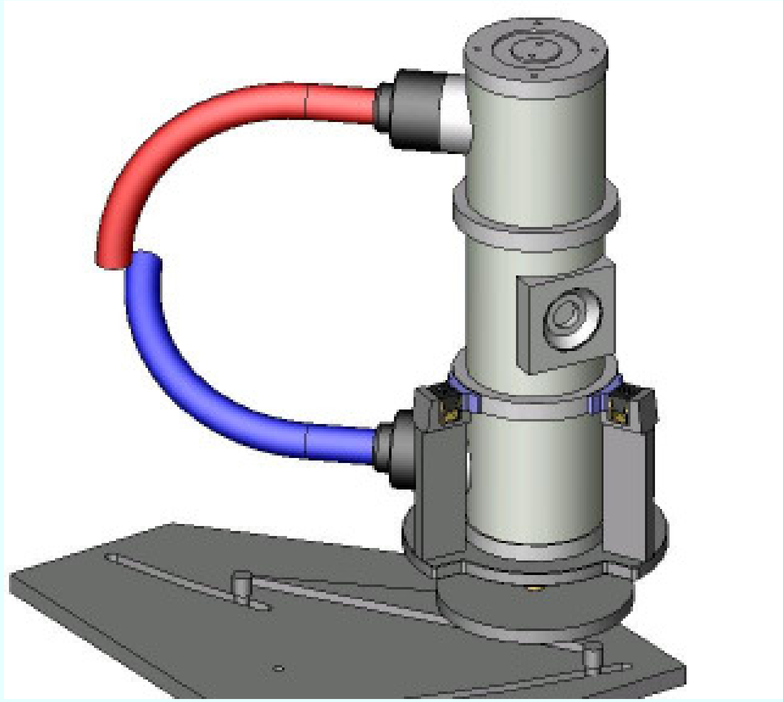

A removable 320 kV X-ray tube has been mounted before the flight tube.
This allows for alternate X-ray tomography in the identical beam geometry!

Comparison and combination of X-ray and neutron images

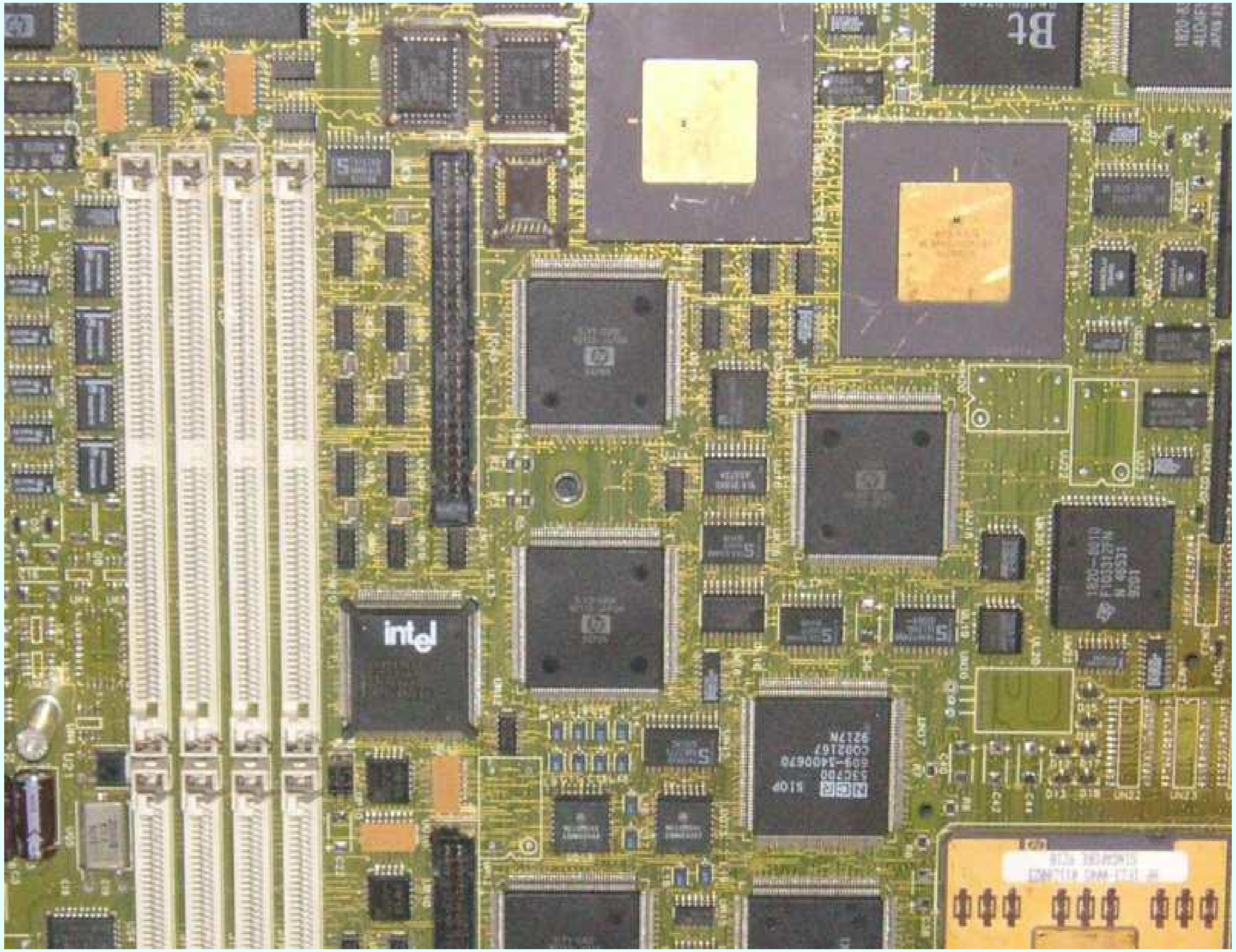

Images
M. Schulz,
TUM

Photo of a printed circuit board.
Note many parts with plastic or ceramic cases and lots of pins.

Comparison and combination of X-ray and neutron images

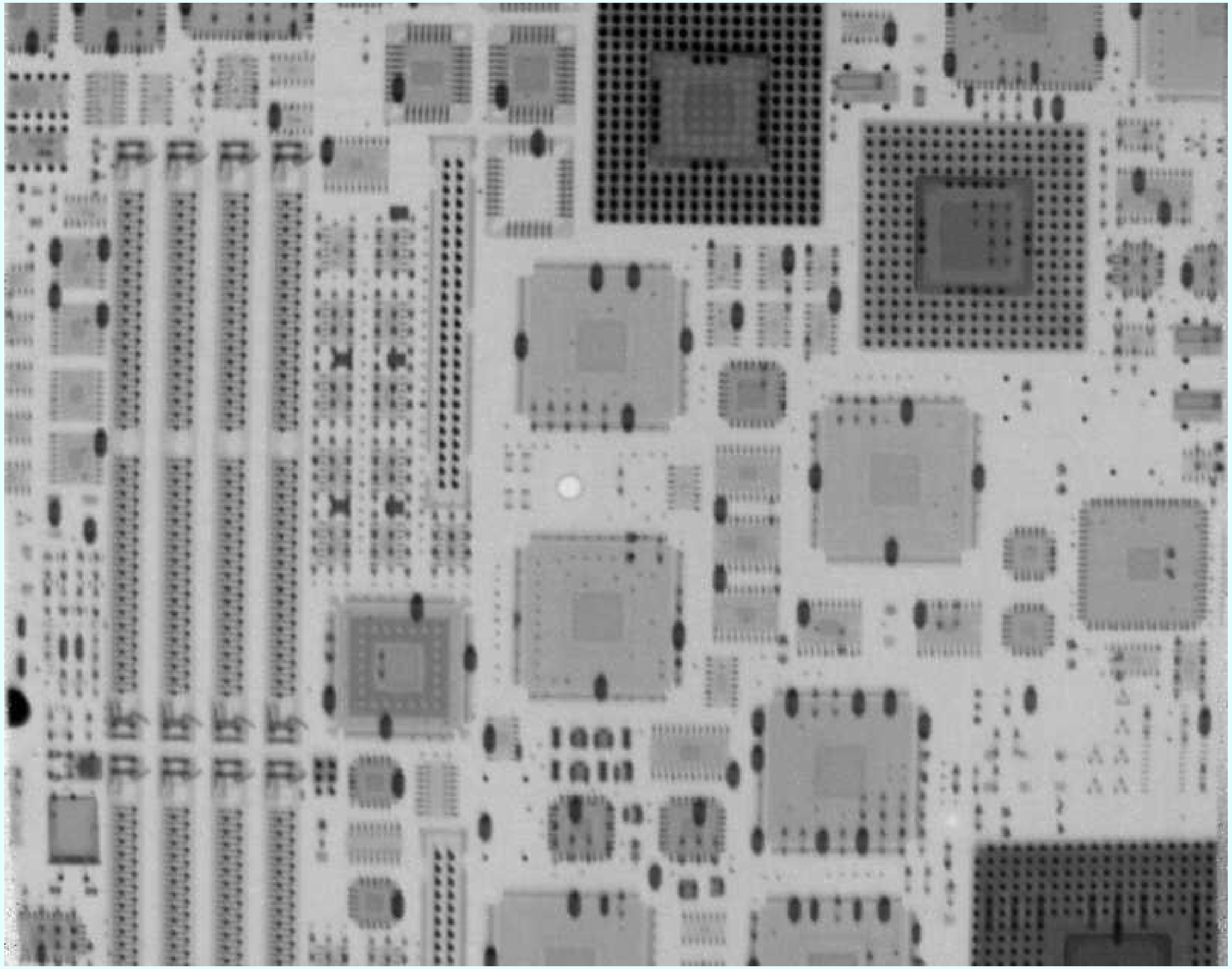

X-ray image.
Most contrast is given by the metal pins.

Comparison and combination of X-ray and neutron images

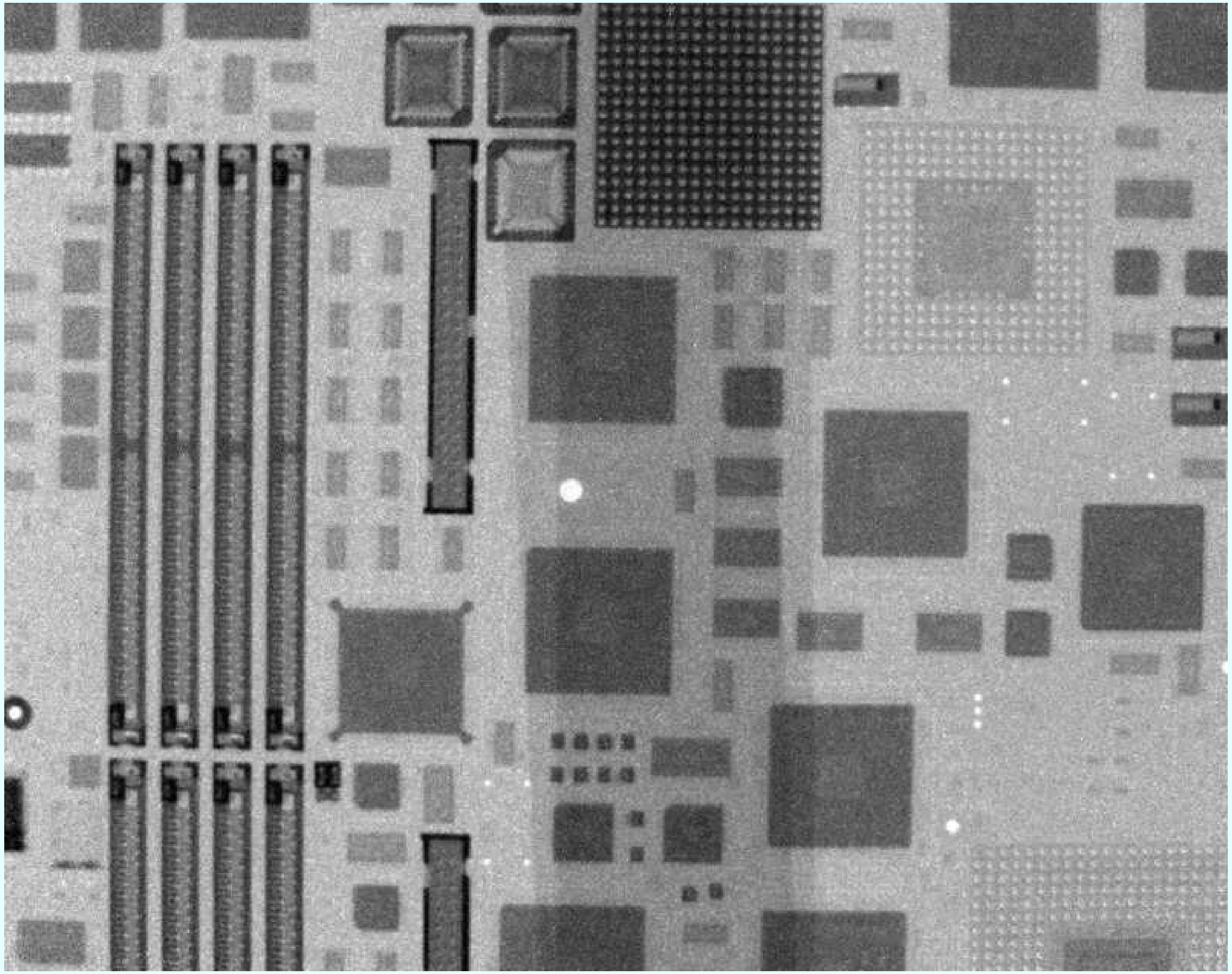

Neutron image.
Most contrast is given by plastic parts, the metal pins are nearly transparent.

Comparison and combination of X-ray and neutron images

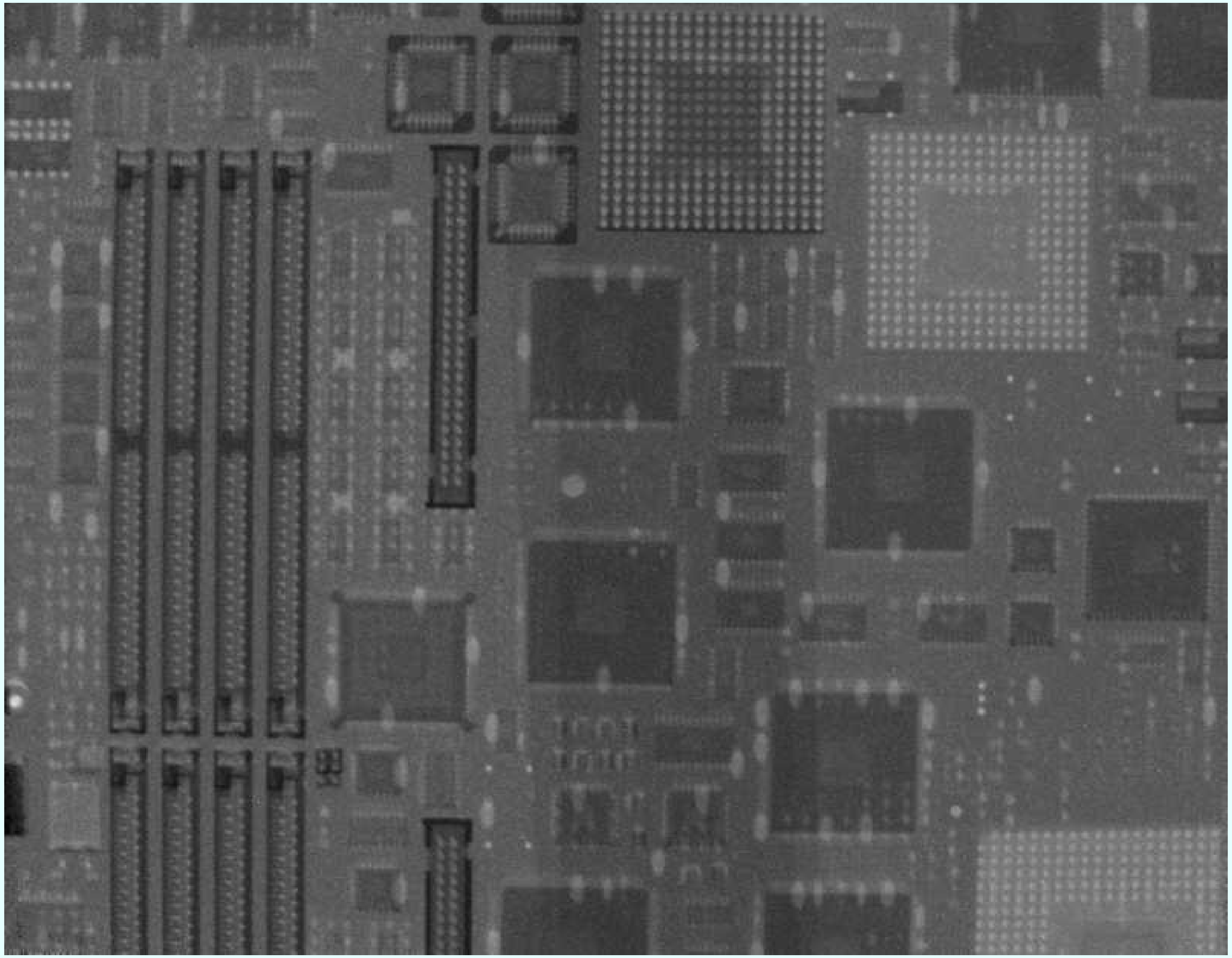

Combination of both images.
The X-ray image was subtracted from the neutron image.

Comparison and combination of X-ray and neutron images

Photo of an unfinished ice hockey knee protector containg a chainmail mesh.

Comparison and combination of X-ray and neutron images

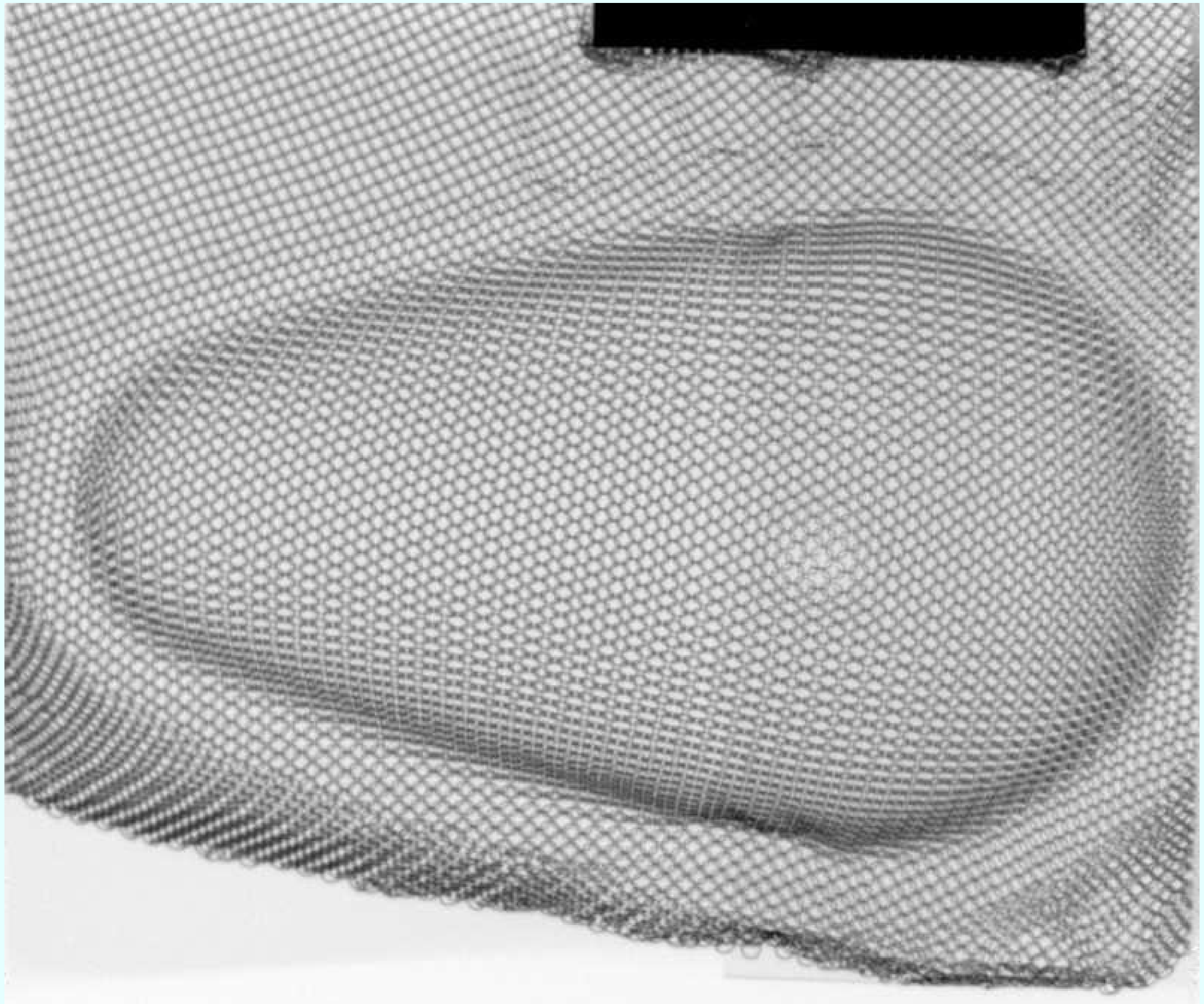

The X-ray image shows dents and even some faults without revealing the causes.

Comparison and combination of X-ray and neutron images

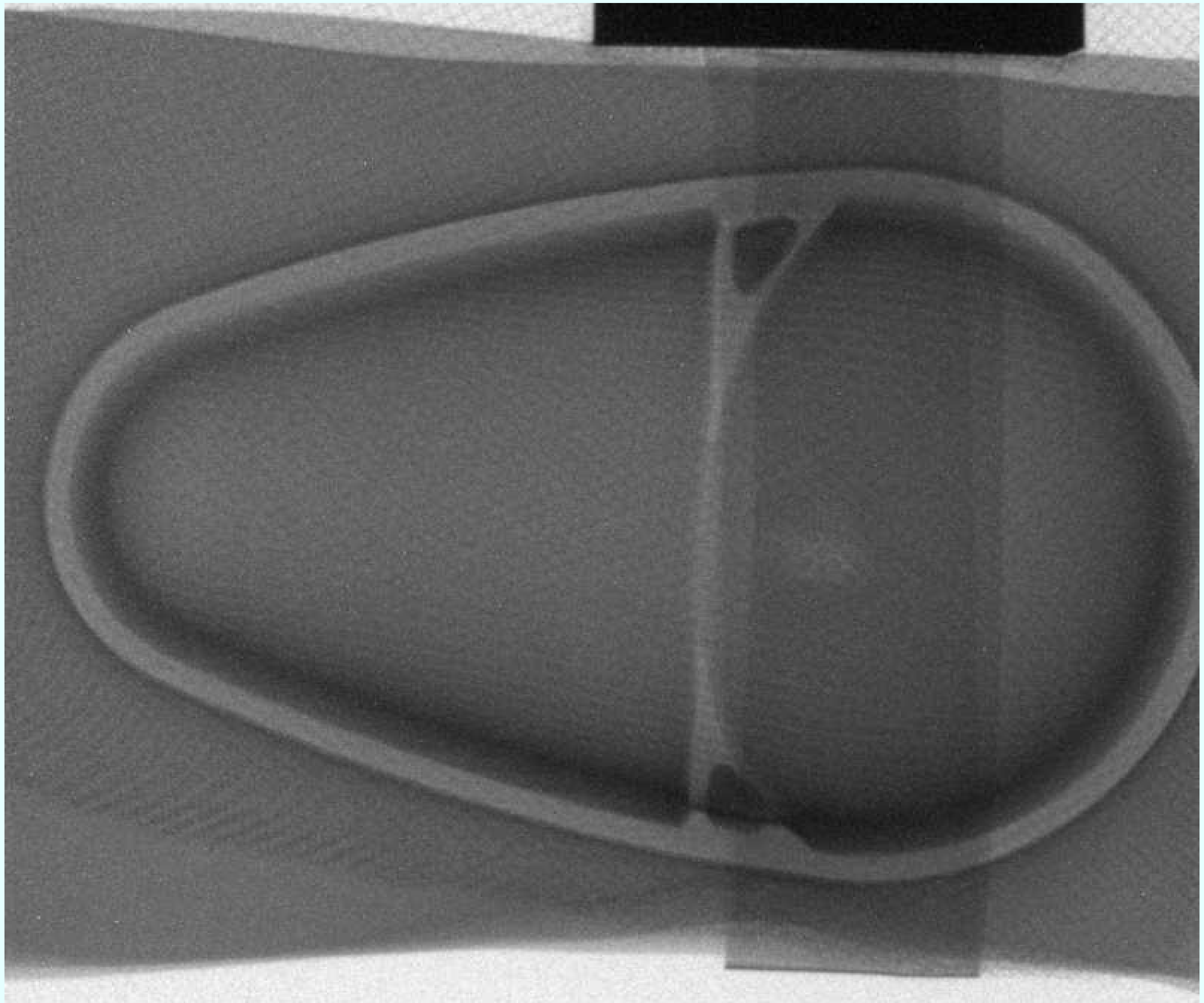

The Neutron image gives very gould contrast on the hydrogen of the foam material, but rather low contrast on the chain mail.

Comparison and combination of X-ray and neutron images

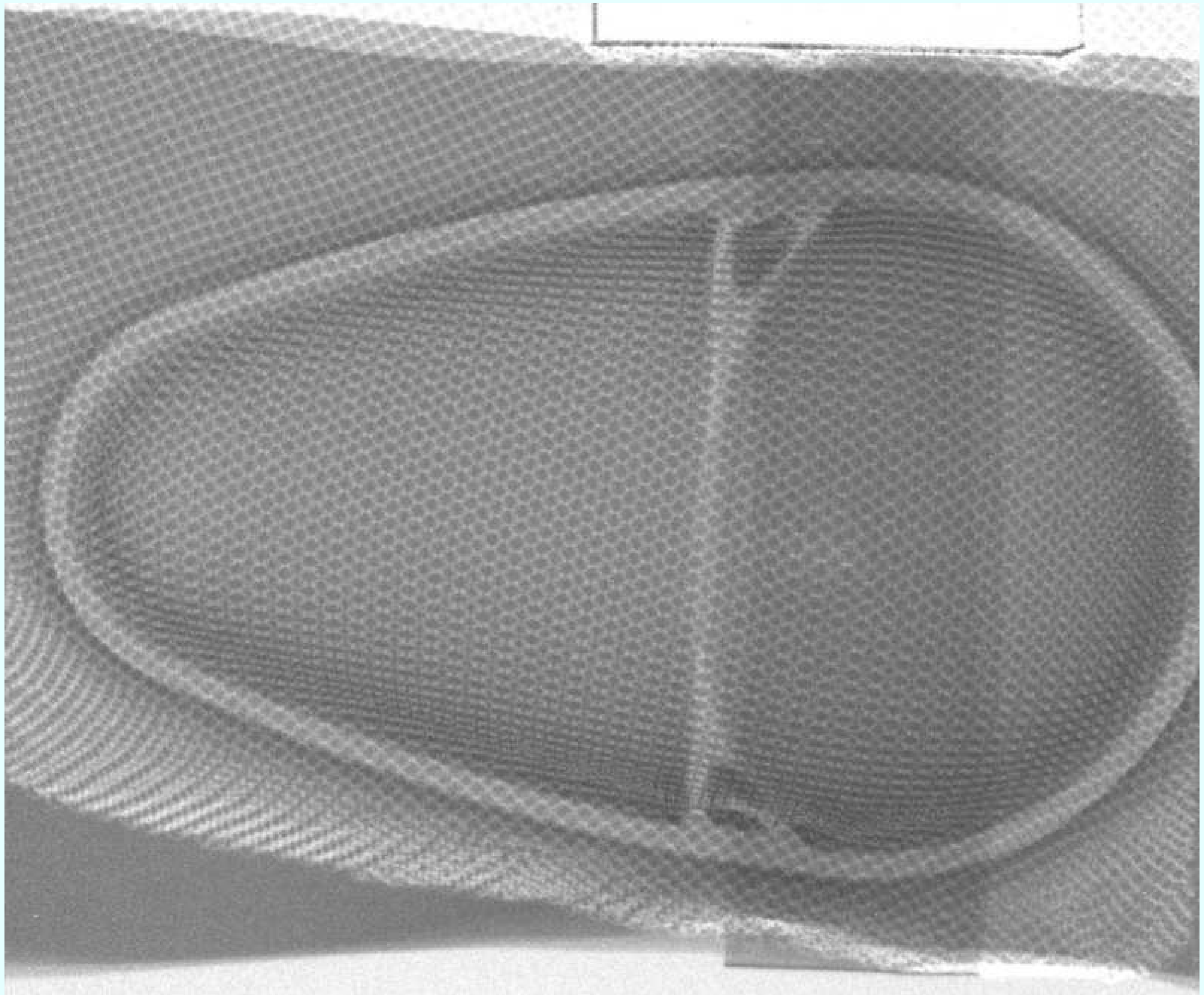

The combination of both images reveals the shape of the rubber foam as well as the embedded chain mail.

Comparison and combination of X-ray and neutron images

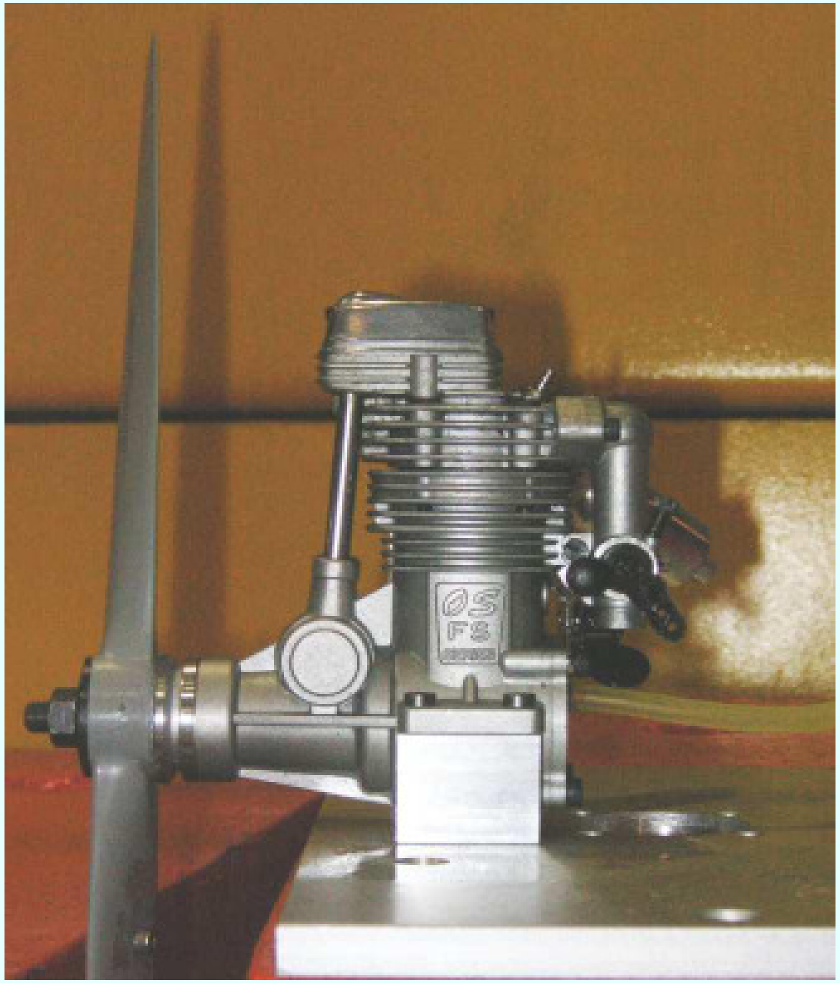

A toy plane combustion engine with a plastic propeller is another good example for the different properties of X-rays and neutrons.

Comparison and combination of X-ray and neutron images

The X-rays easily penetrate the plastic propeller, still penetrate the Aluminium well, but are heavily attenuated by steel parts.

Comparison and combination of X-ray and neutron images

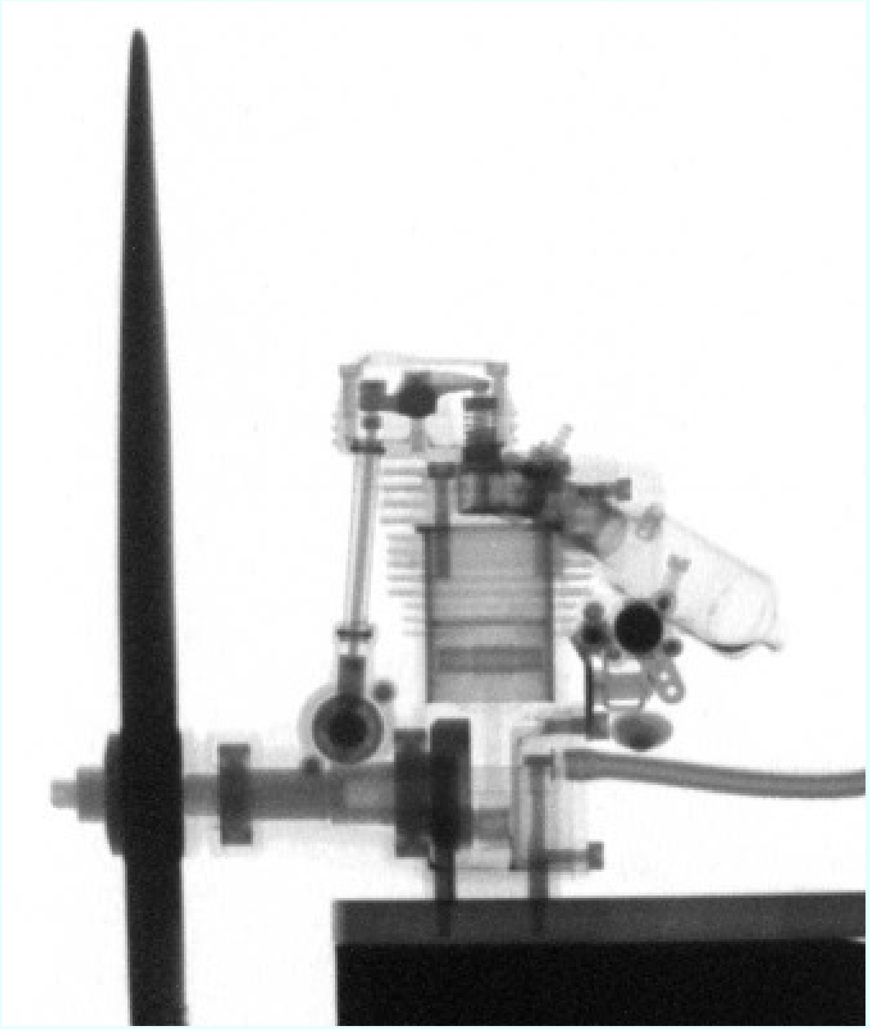

Aluminium is very transparent for neutrons, steel is better penetrated than by X-rays, but plastic is very opaque..

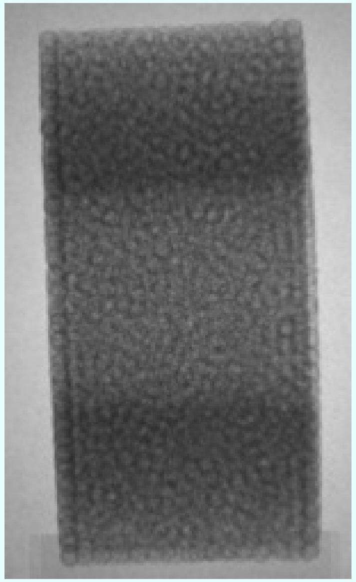
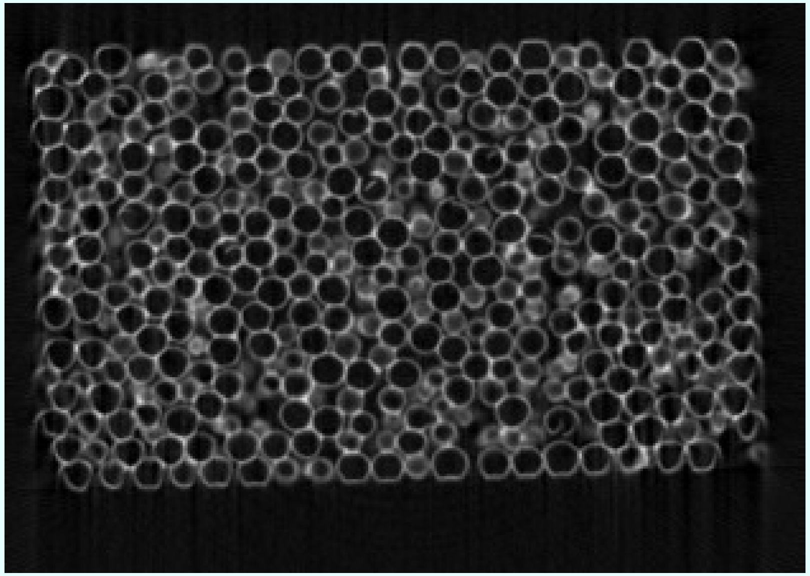
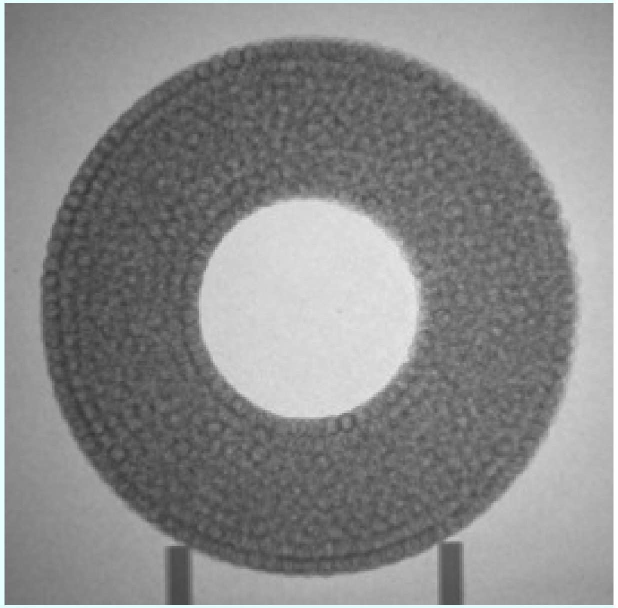
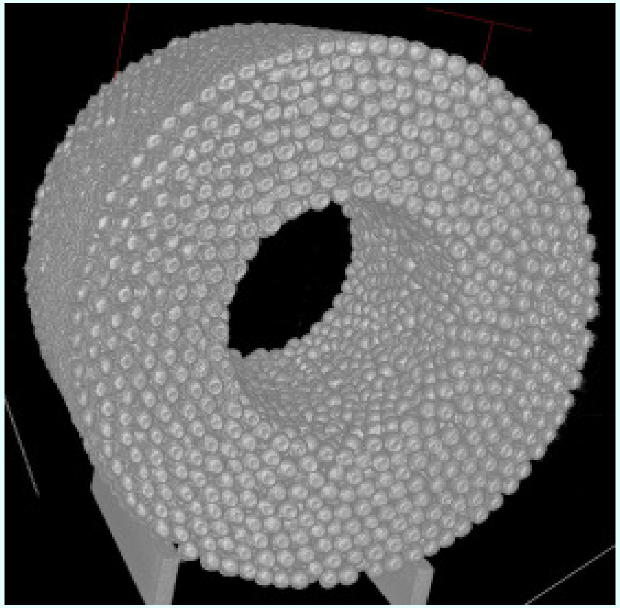
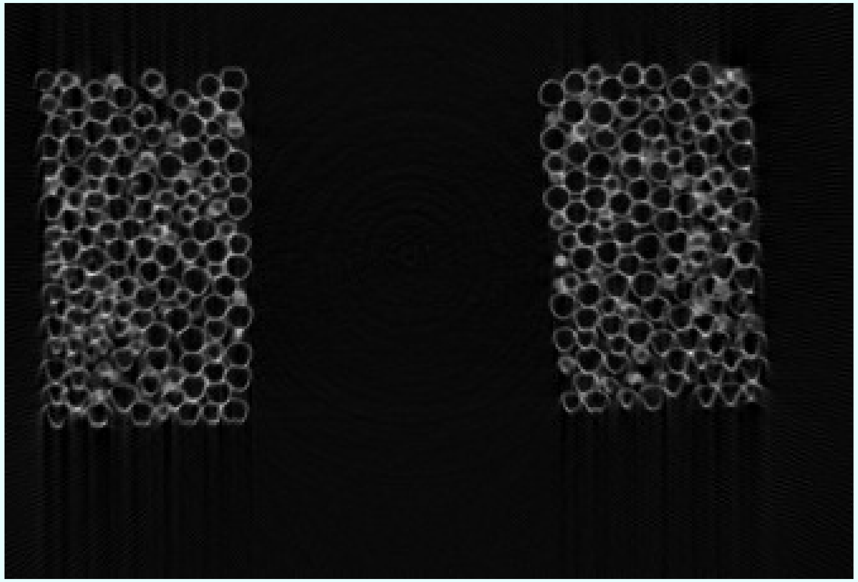

Radiography and tomography of a hollow spheres catalyst

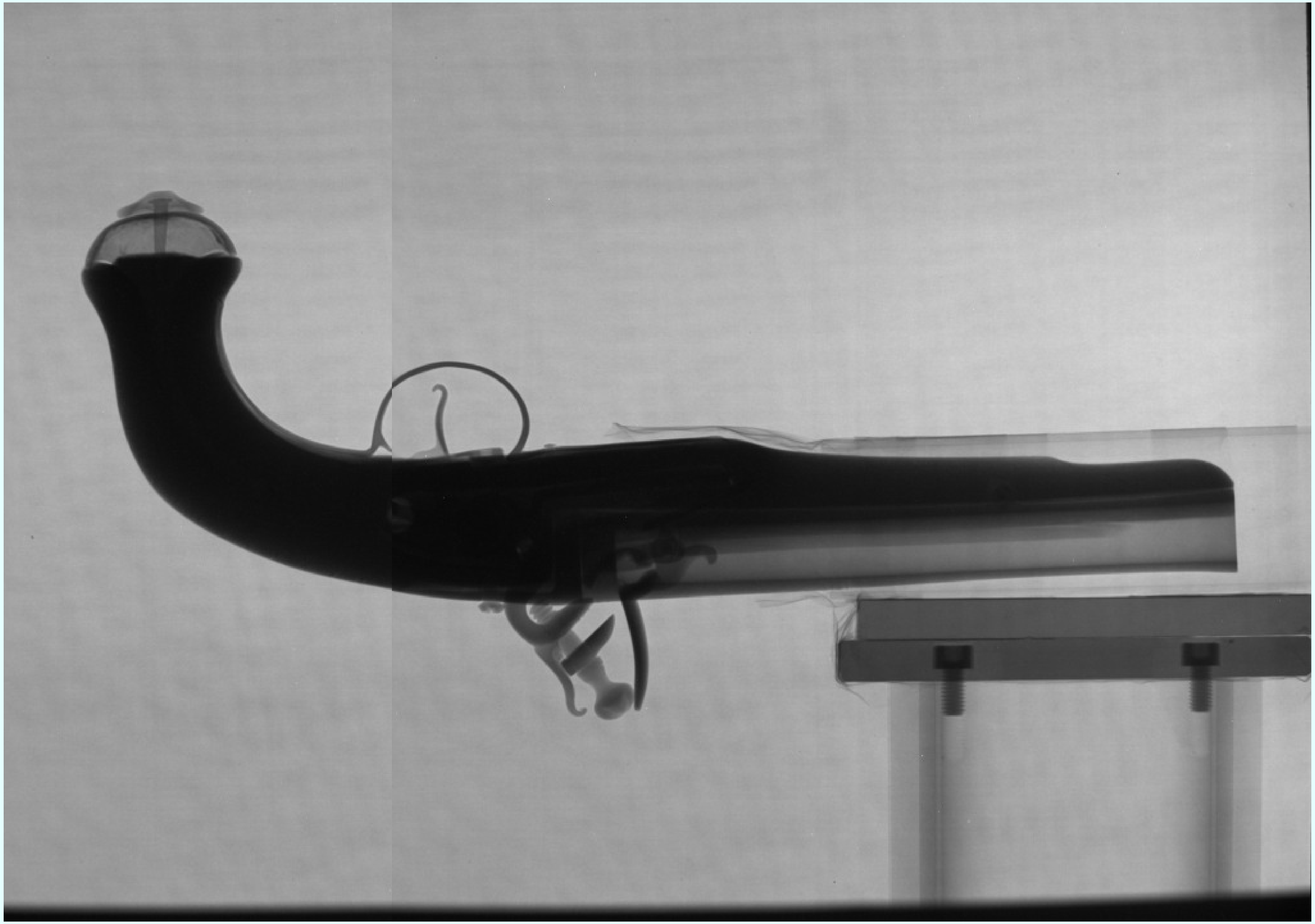

Historic dueling pistol from the posession of President Monroe, 5th President of the USA

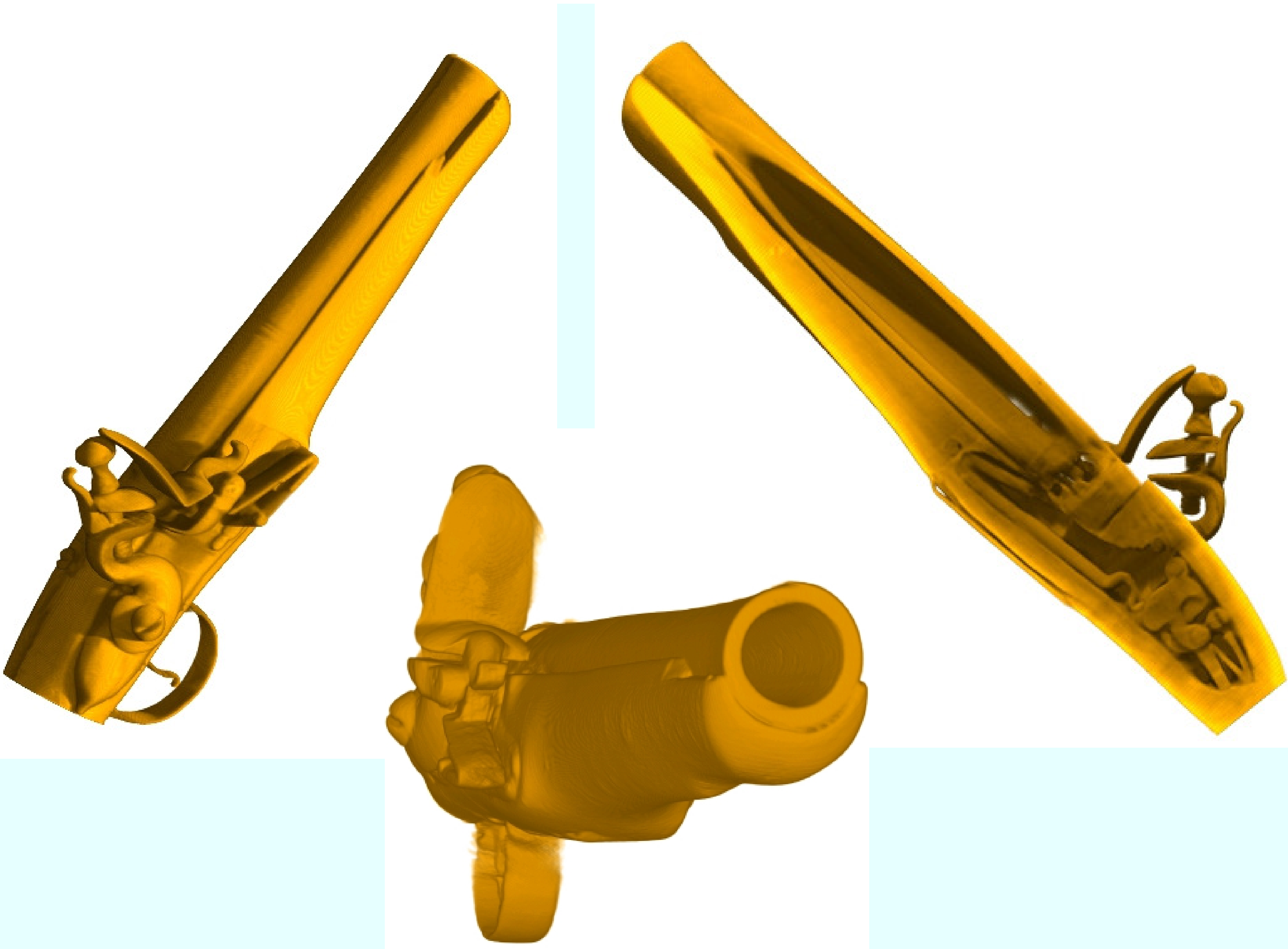

3D tomographic reconstruction, view to internal mechanism

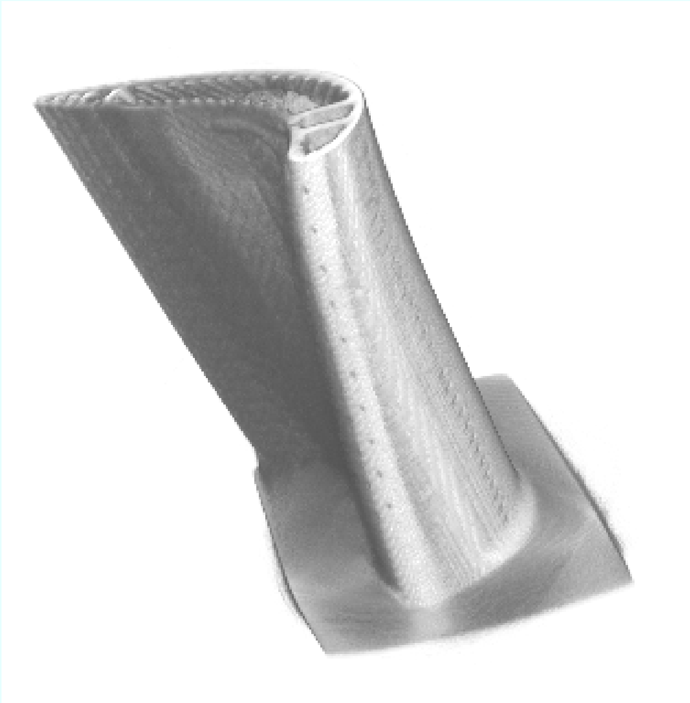

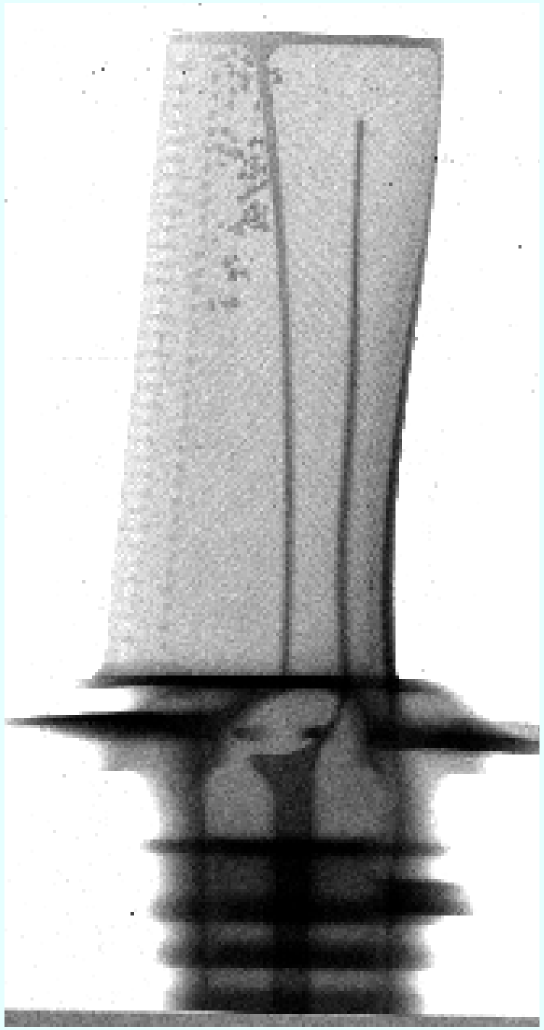

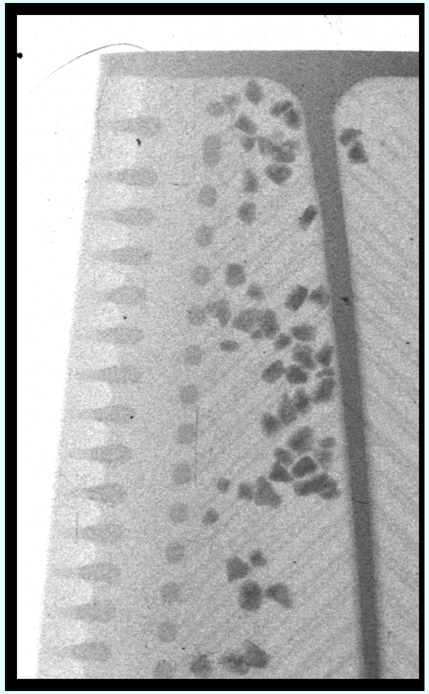

Turbinenschaufel: Tomographie und Radiographie

(Messung PSI)

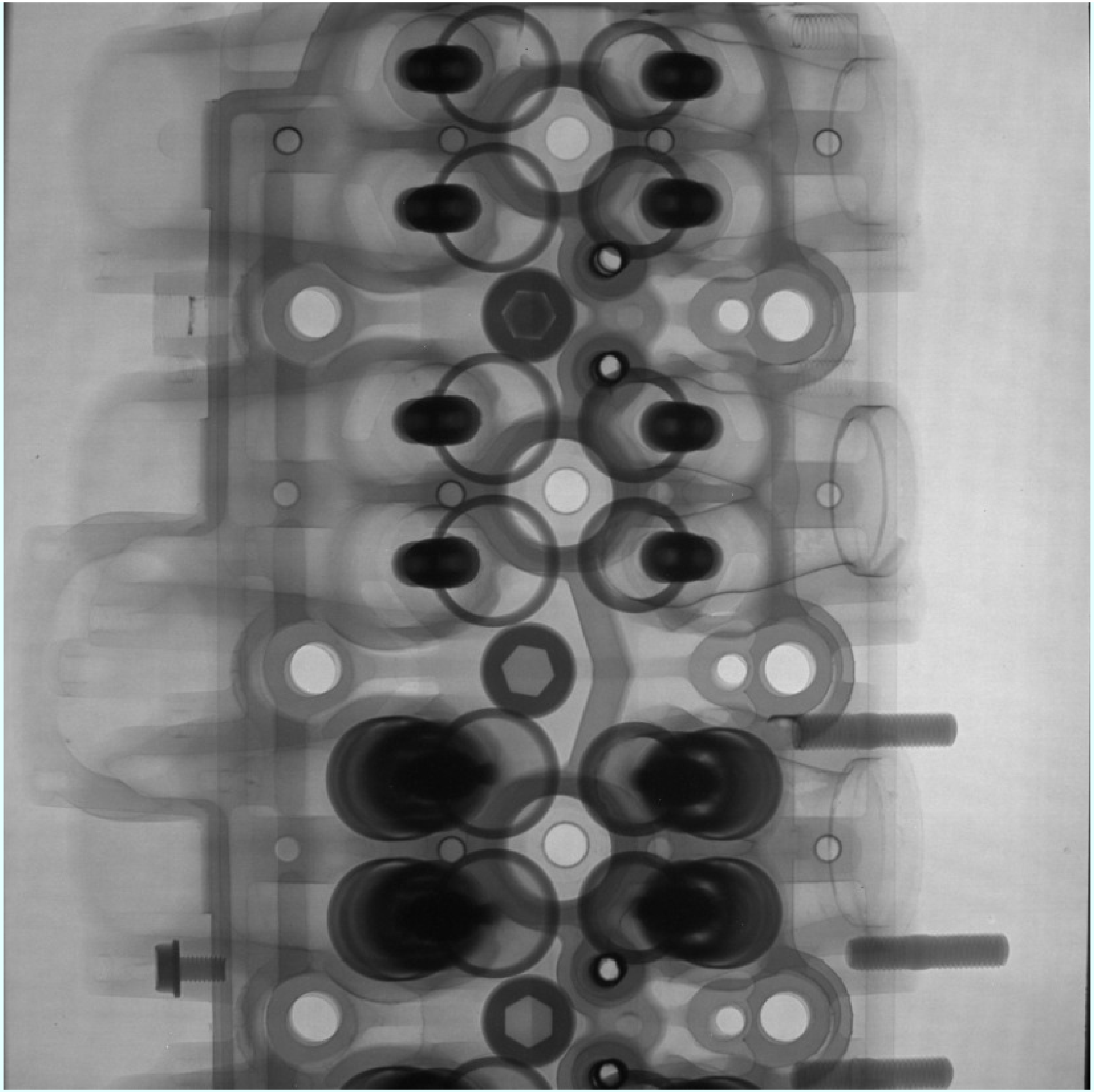

A motor block of a
four-piston
motor cycle engine.

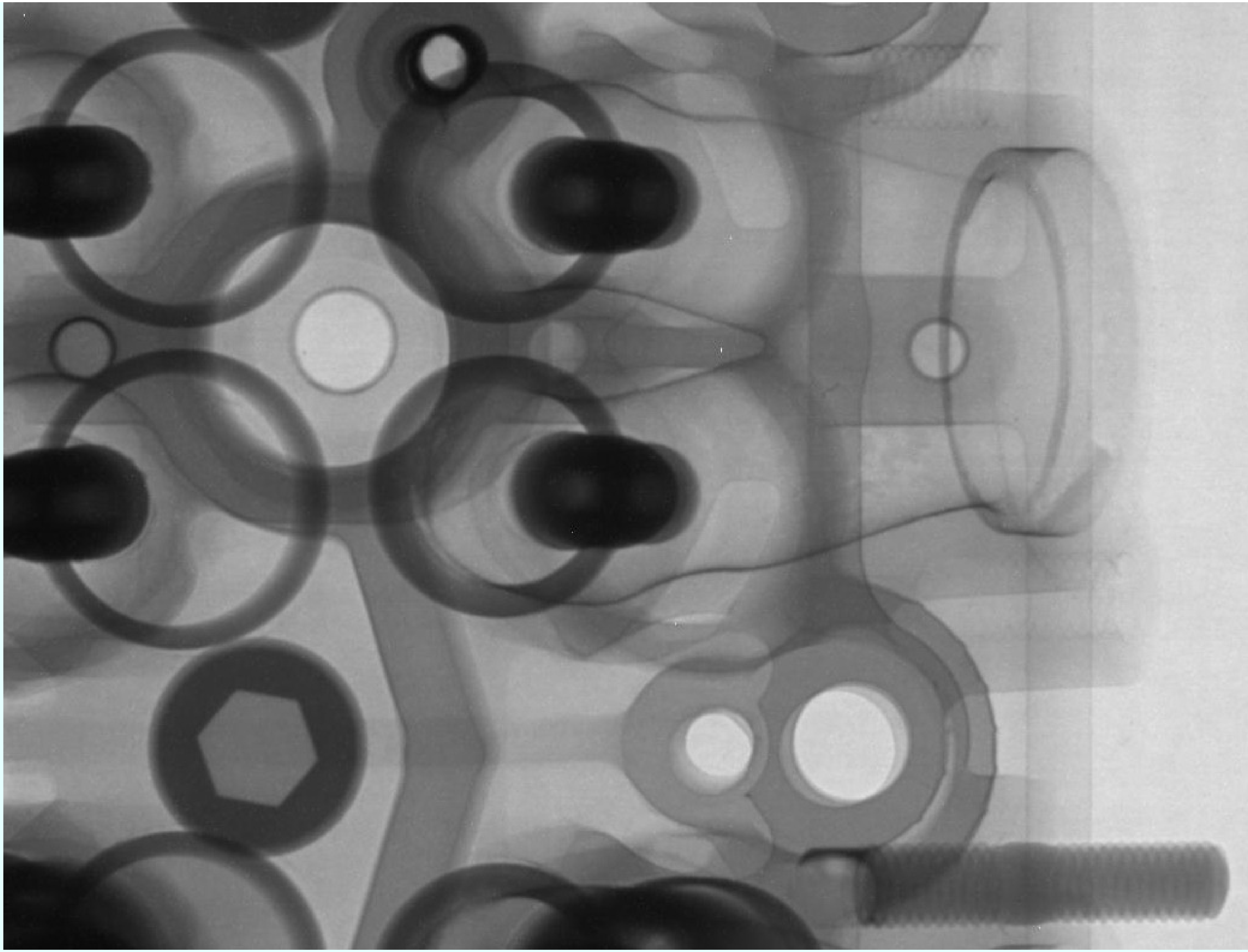

Cutout of the motor block.

Examination of water ingress into temperature sensors

NTC sensor in two-part injection mold

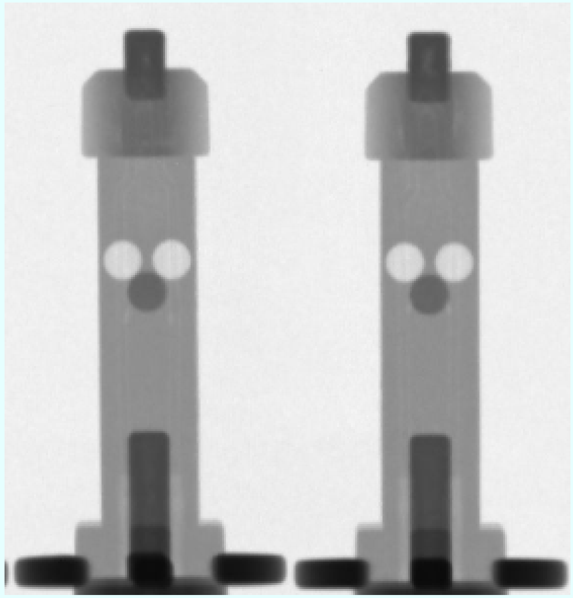

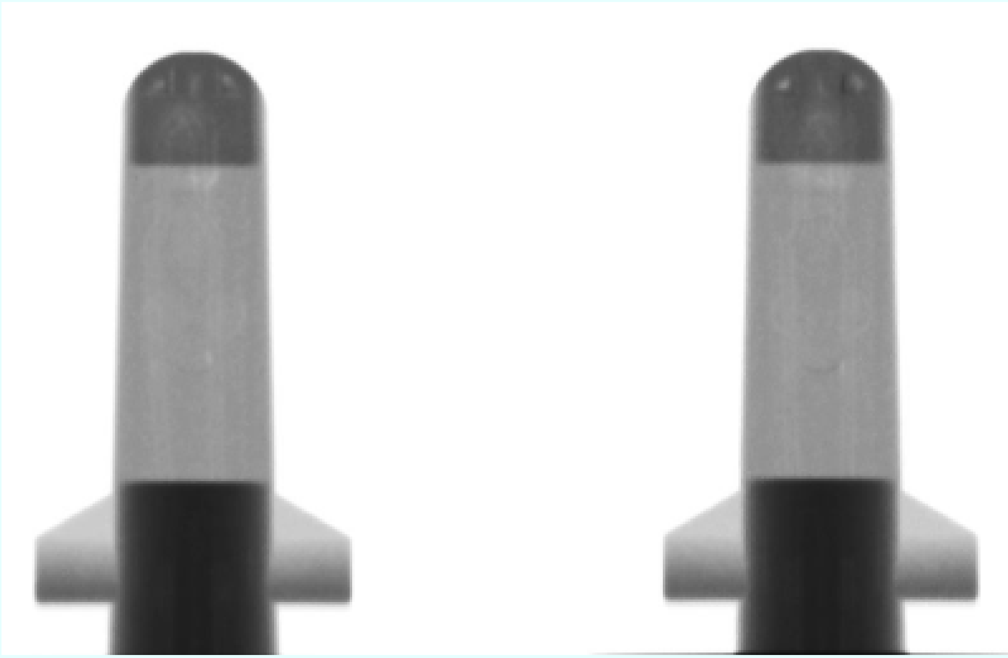

Inner injection mold

Outer injection mold added

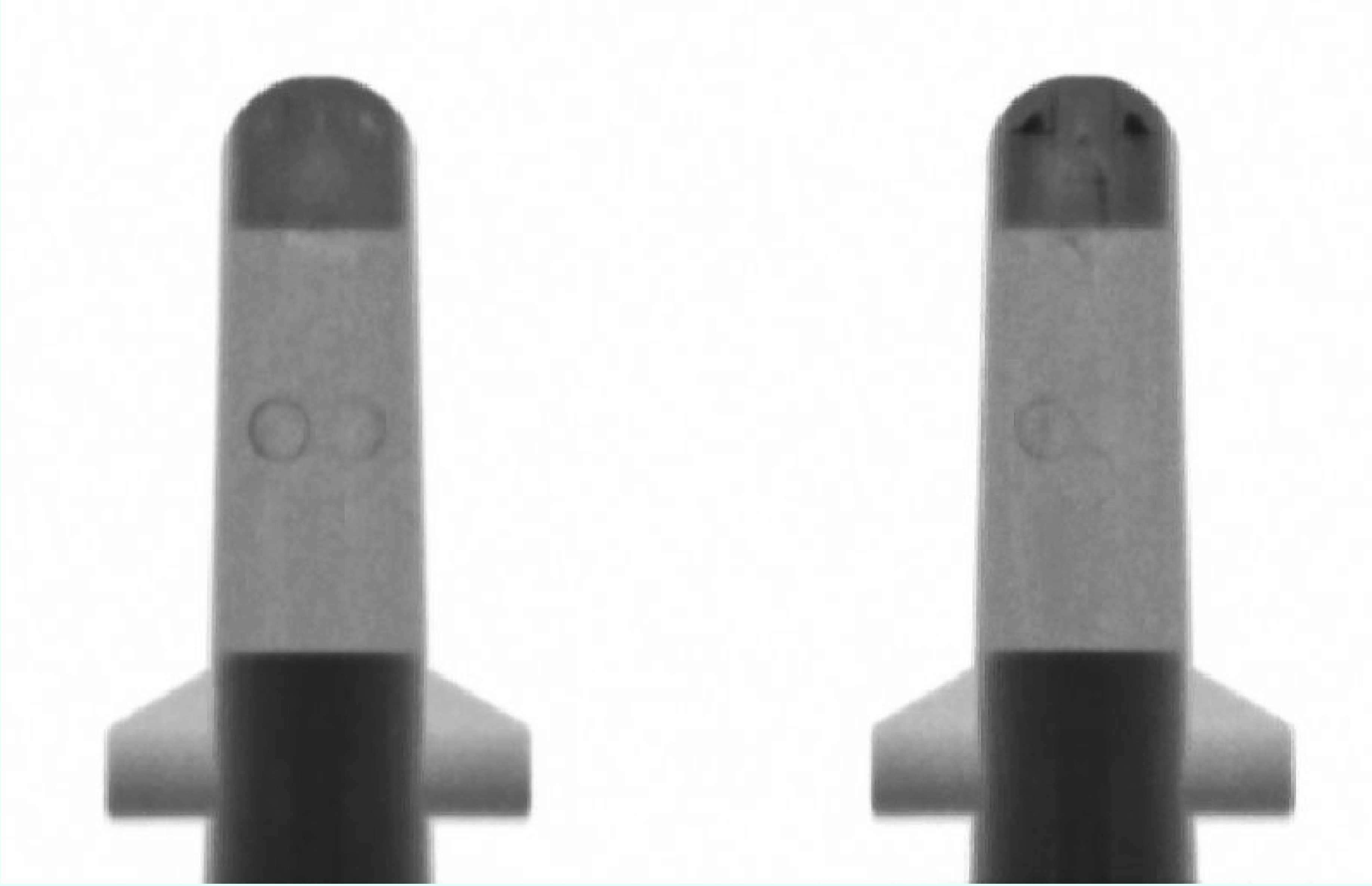

Sensors are put into a Gadolinium contrast agent, first evacuated, then pressurized to force the agent into cracks

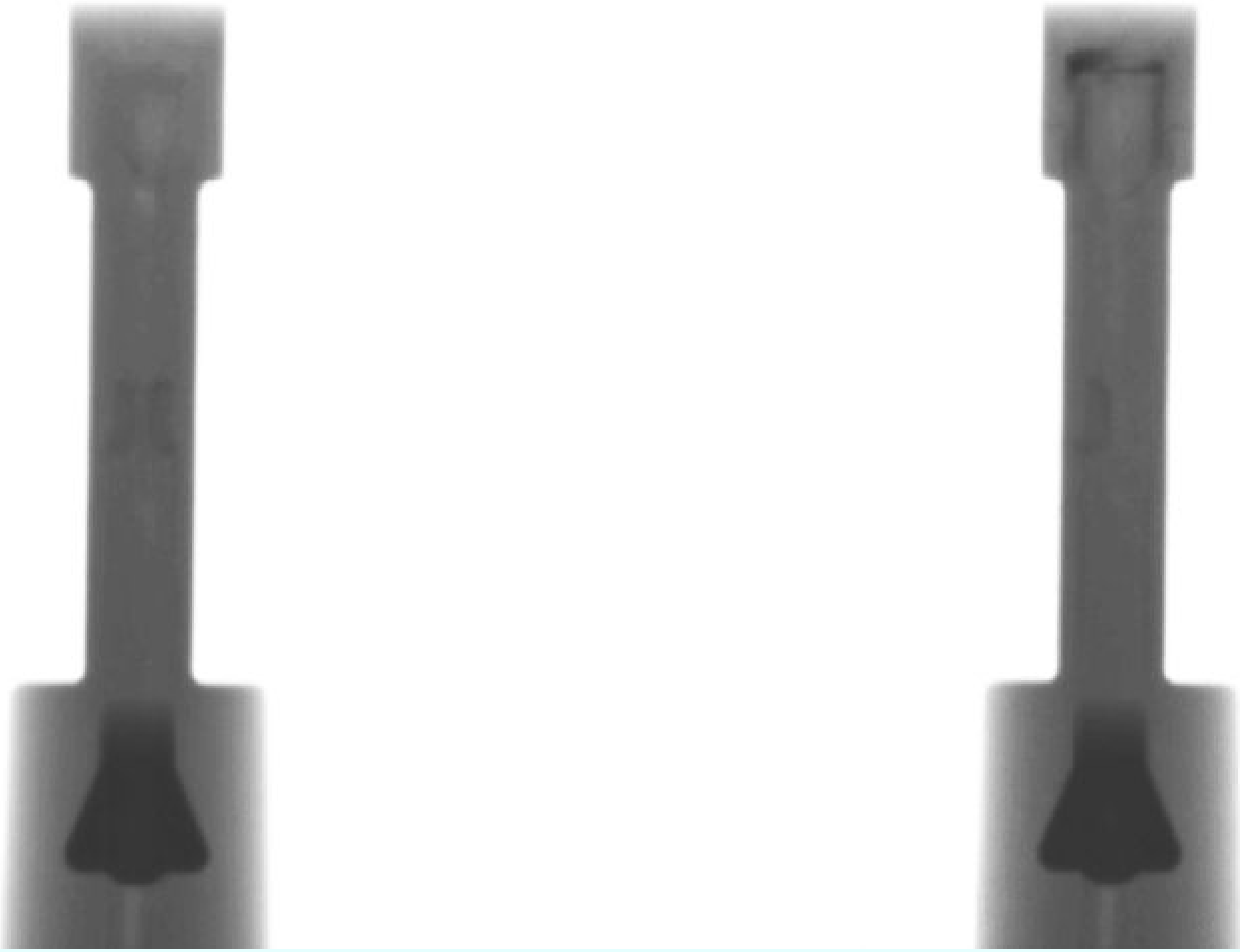

Sensors are put into a Gadolinium contrast agent, first evacuated, then pressurized to force the agent into cracks.

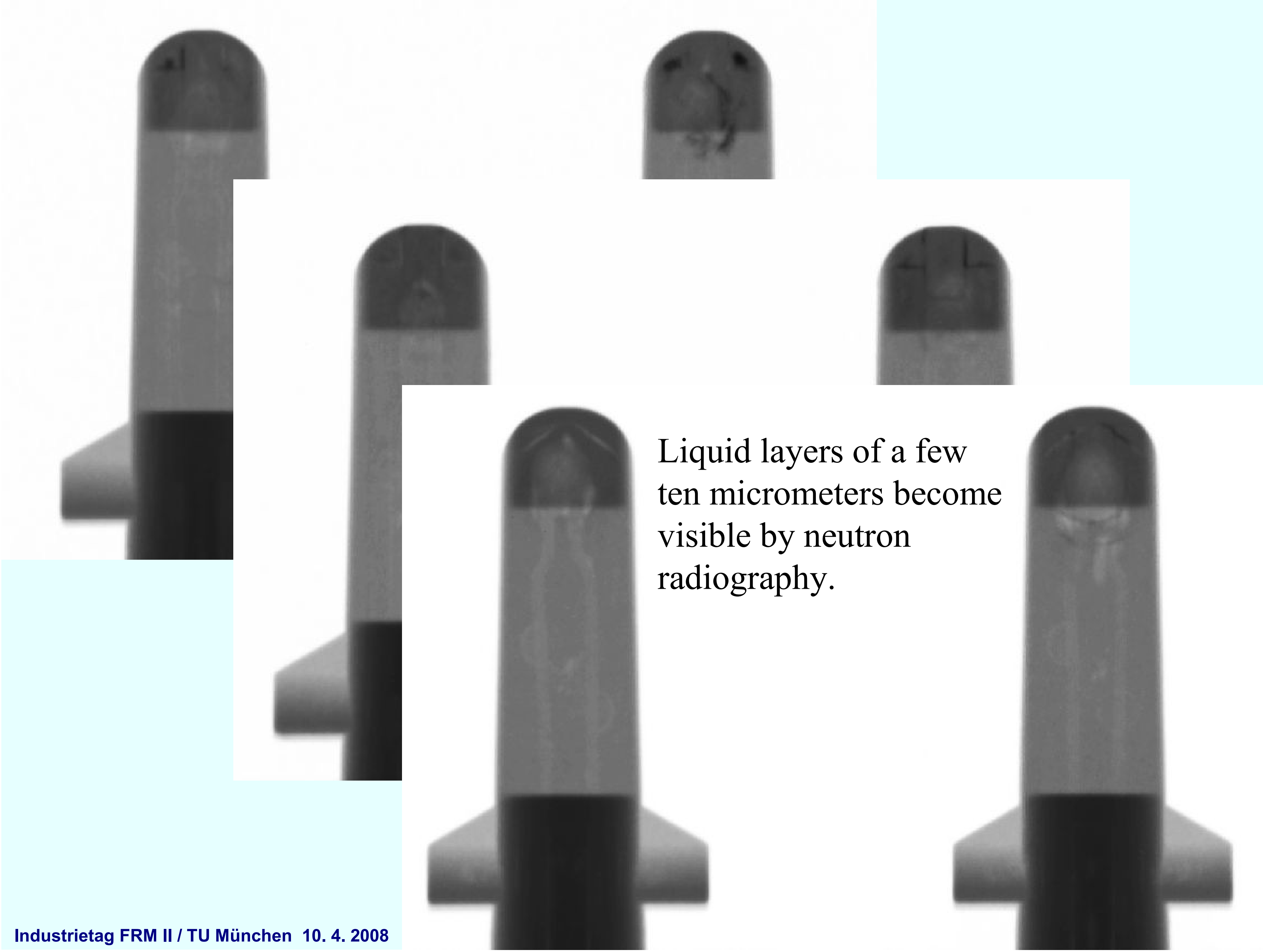

Liquid layers of a few ten micrometers become visible by neutron radiography.

Measurements on a BMW engine at NEUTROGRAPH, ILL

150 individual images were recorded as an on-chip accumulation of a 200 microseconds exposure each.

The total exposure time for the full run was in the order of 18 minutes only.

The field of view was 24 cm * 24 cm.

The observation area could be varied by displacement of the full set-up.

First-time visualisation of the oil cooling of the pistons!

Valves
(two behind each other)

Oil spreads on the piston bottom

Oil jet ejected from below onto the piston bottom

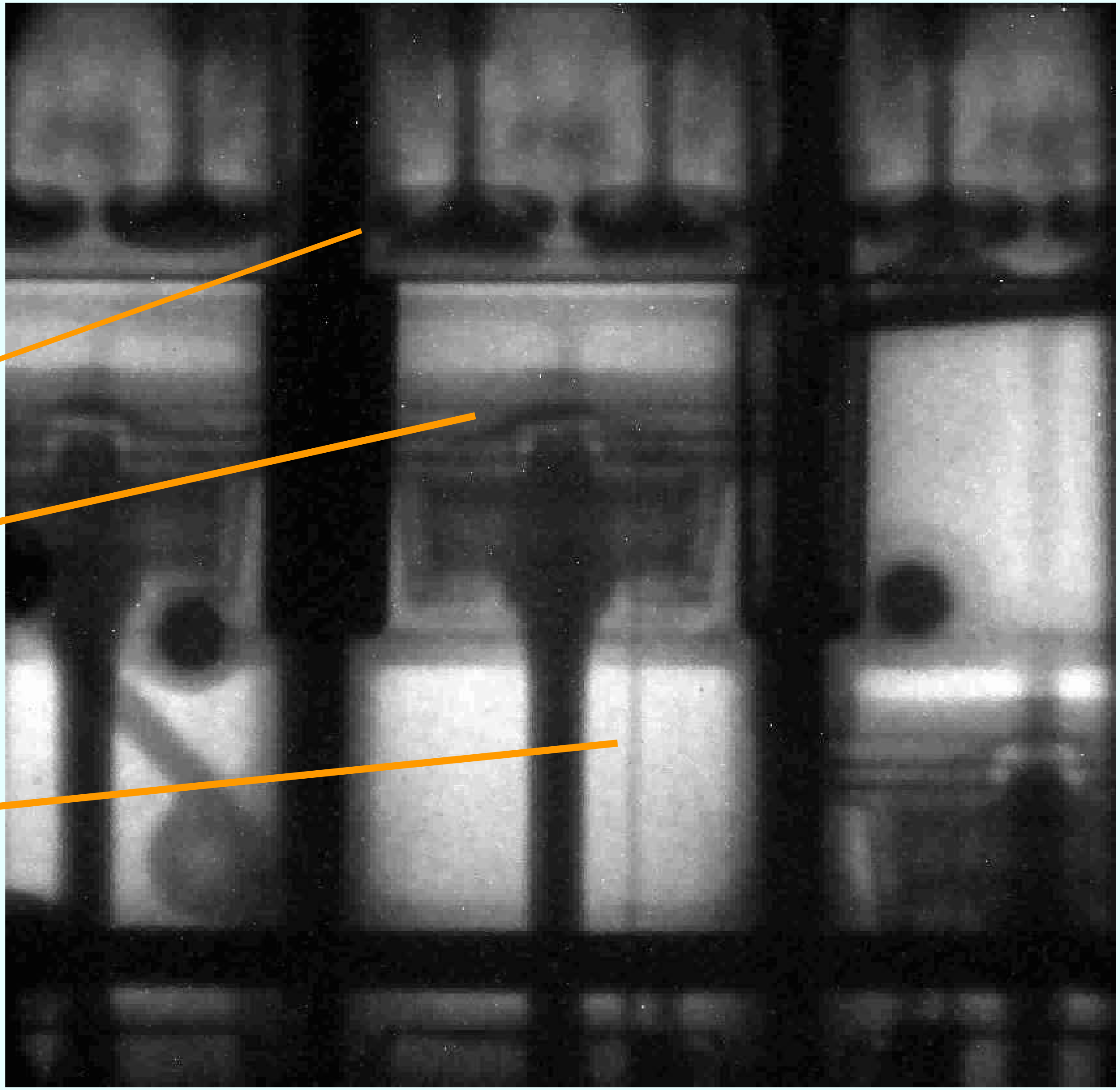

Measurements at ANTARES, FRM-II

The ANTARES facility at FRM-II offers a lower flux (10^8 n/cm^{2}s), but higher collimation (L/D=400).

The time window was extended to 1 ms,
the rotation speed was reduced to 600 rpm,
which is well below the nominal idle speed of the engine.

The images show more motion unsharpness,
but better definition on the stationary parts.

At this rotation speed, the oil pump did not produce its nominal pressure,
the oil pressure was pulsed and produced blobs in the cooling oil jet.

Measurements at ANTARES, FRM-II

Static radiography

of the engine,

with horizontal
pressure tubes and
vertical backflow tubes
empty

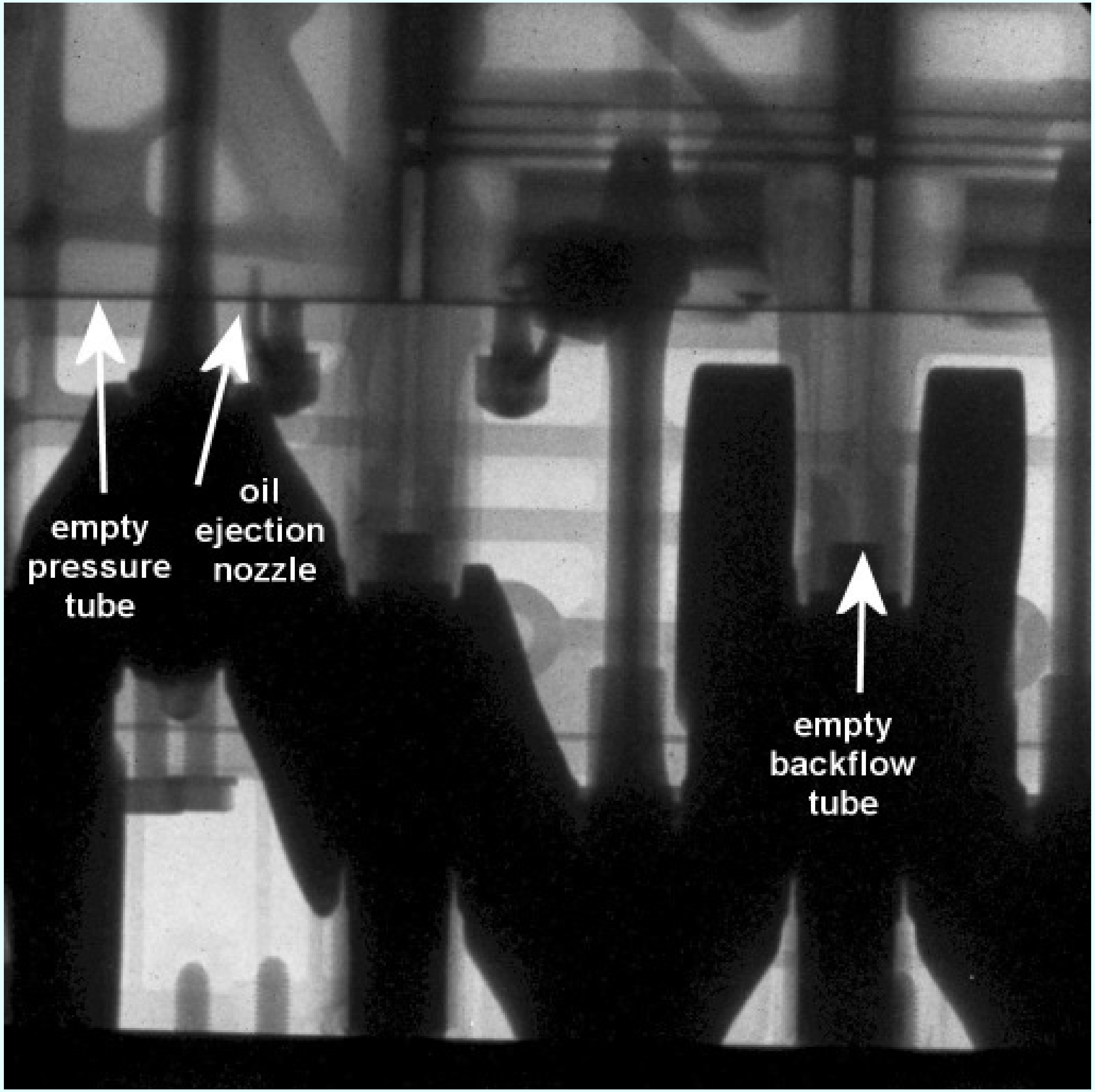

Measurements at ANTARES, FRM-II

Dynamic radiography of the engine,

with oil filled horizontal pressure tubes and vertical backflow tubes,

and an oil blob within the oil jet to the piston bottom

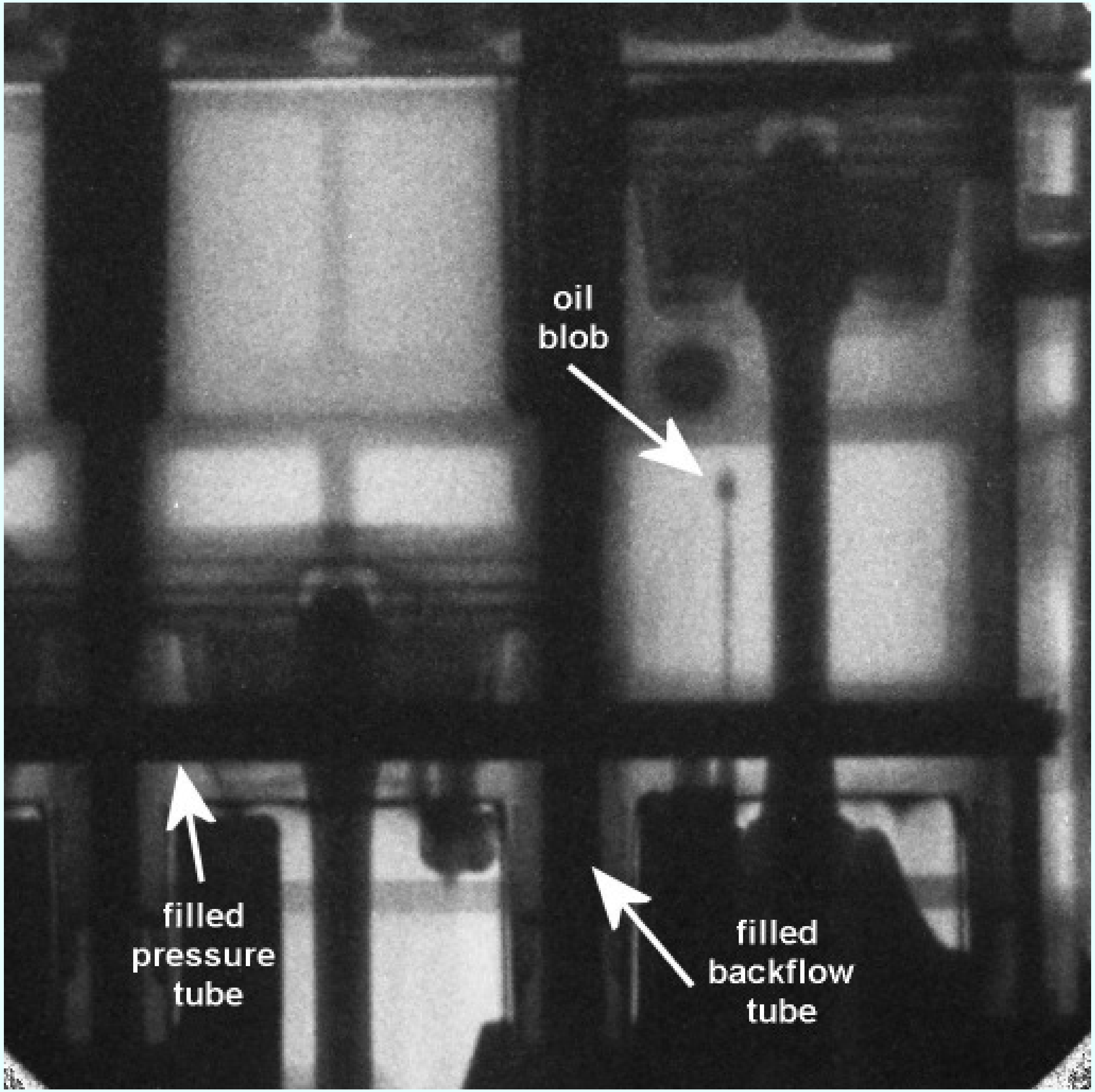

Blobs in jet

Oil curtains detaching

Oil curtains detaching

Detection of imprinted car chassis numbers in smooth-polished metal sheets

E. Calzada, H. Li
TU München FRM-II / Physik E21

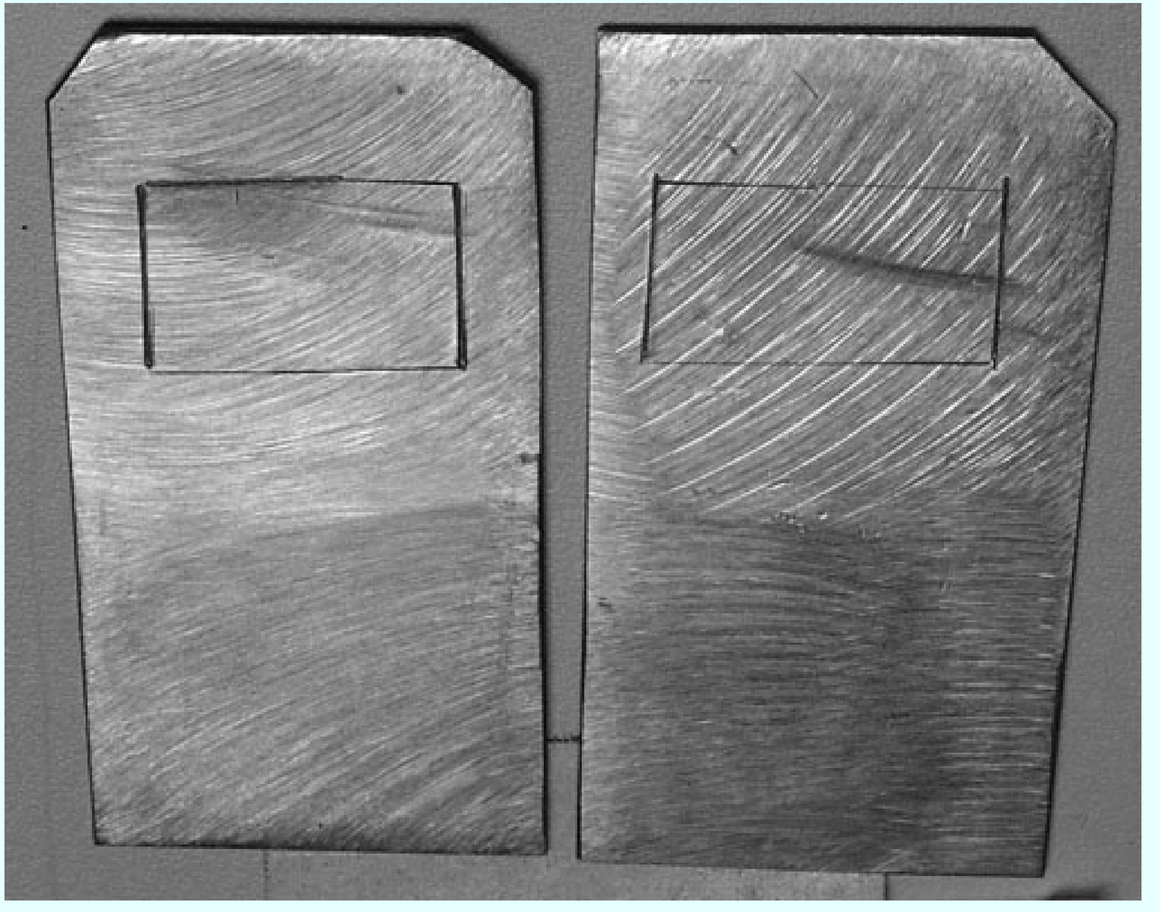

The police brought us two smooth-polished metal sheets, where originally the car chassis numbers had been imprinted.

Nothing is visible on the surface, but deep in the metal, the structure has been altered…

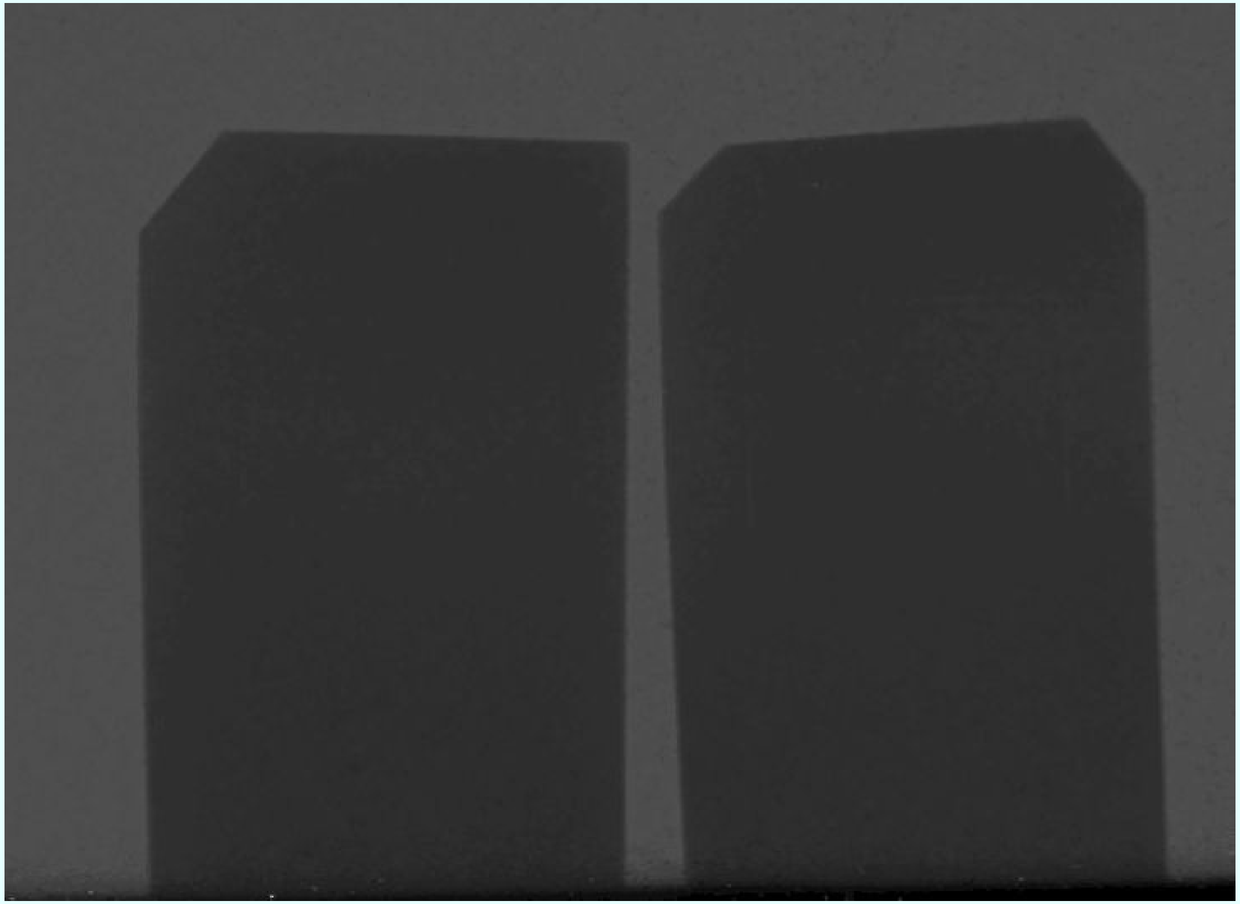

The normal radiography shows nothing at all.

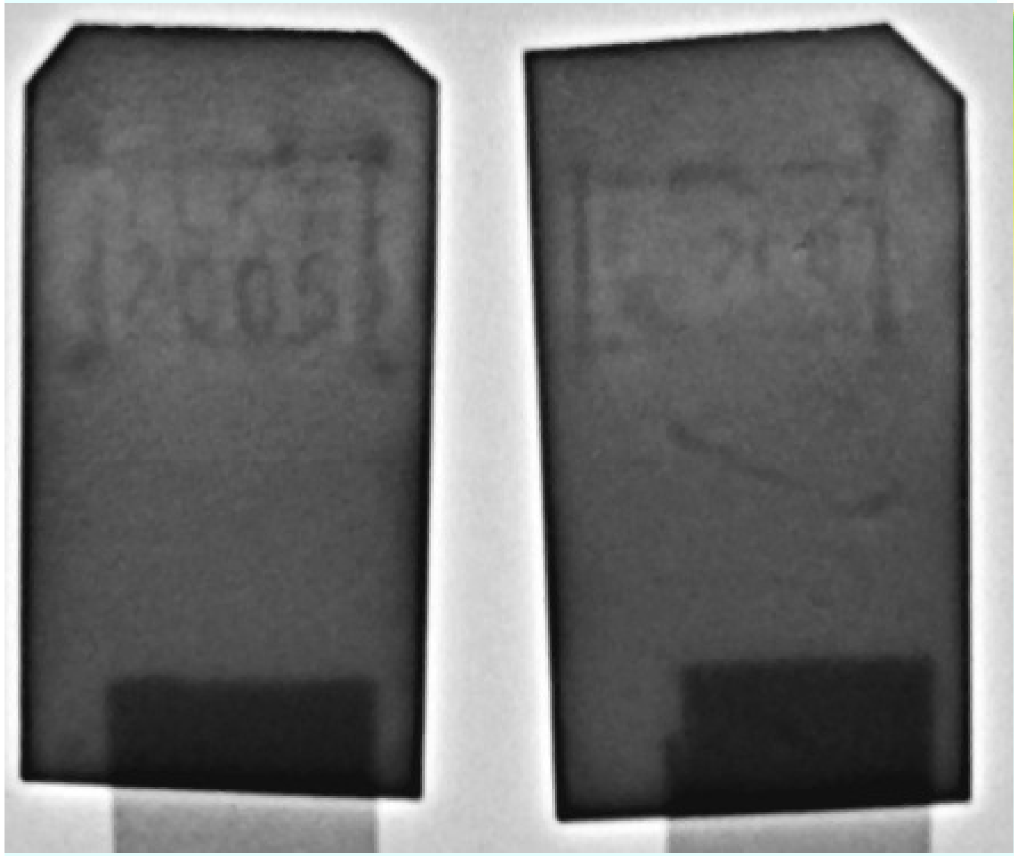

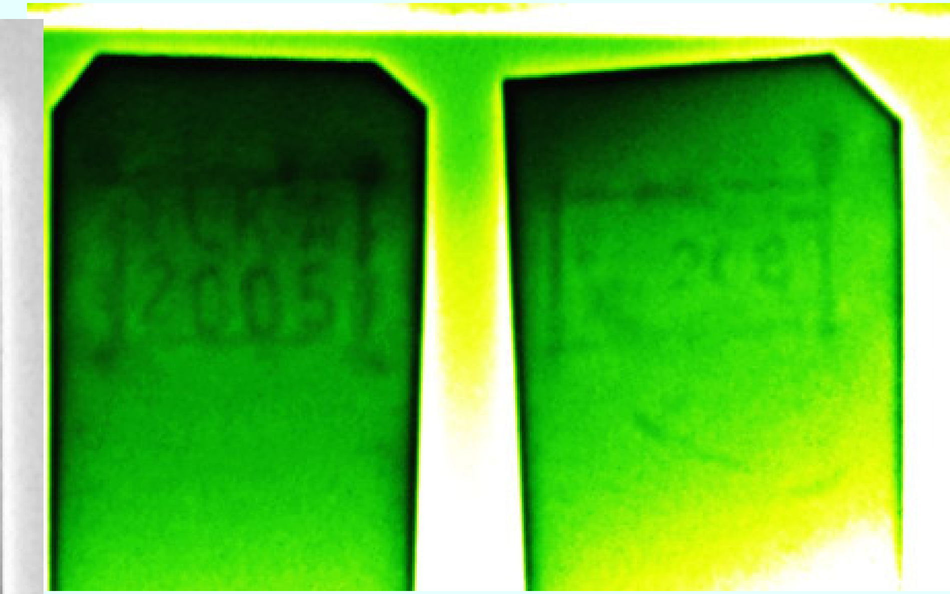

But with a 7 mm pinhole, and 2 meters distance to the detector…

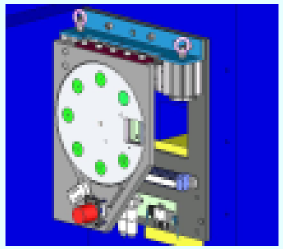

Neutron Imaging:

Detection of texture alteration in steel and Al parts using Small Angle Scattering in Neutron Radiography and Computed Tomography

B. Schillinger, E. Calzada, M. Hofmann, H. Li
TU München FRM-II and Physics E21

A. Steuwer, R. Gähler
Institut Laue-Langevin, Grenoble
L. Edwards
The Open University , Milton Keynes

Cold expanded fastener holes

- The primary source of aircraft fatigue is at joints.
- Cold expansion increases joint durability.
- Quantification of the benefits of cold expansion requires accurate reliable residual stress estimation.

The cold expansion process

- The most common method is FTI split sleeve expansion.
- At present, air worthiness authorities do not allow the benefits of cold expansion to be included in design calculations.

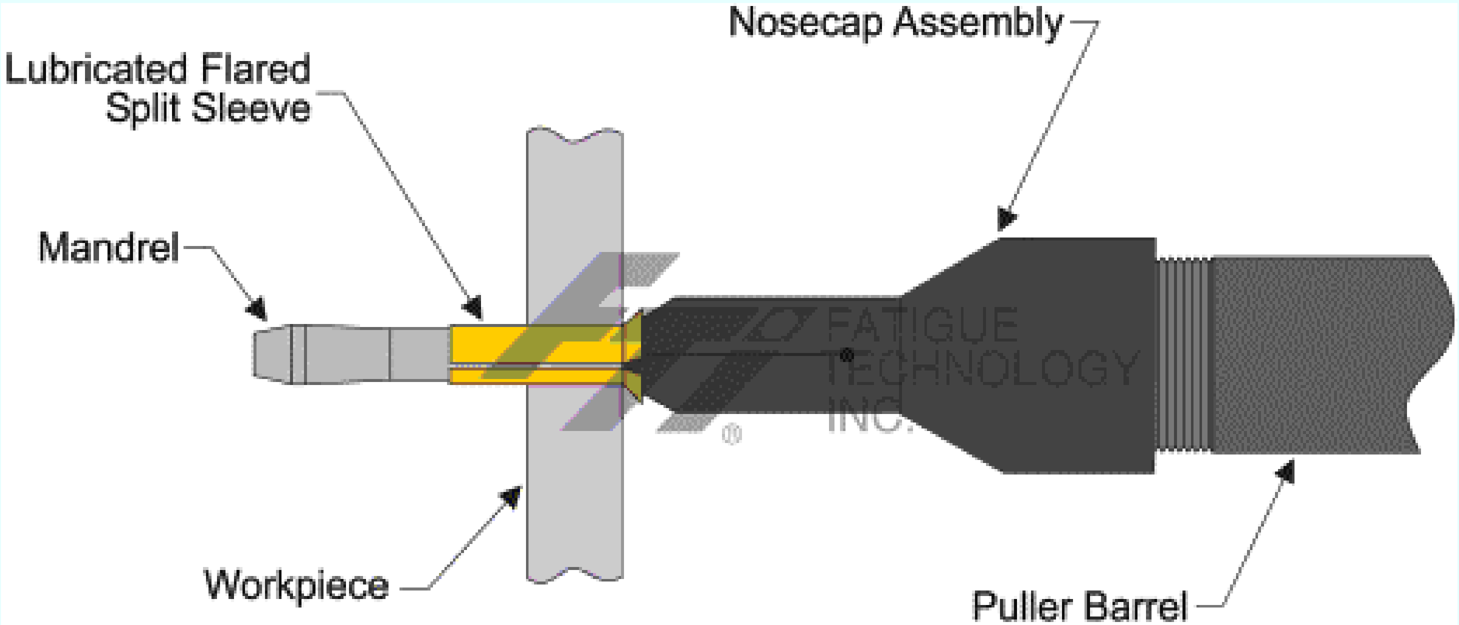

Picture:*http://www.fatiguetech.com/products/splitsleeve.html*

The Split Sleeve Cold Expansion Process

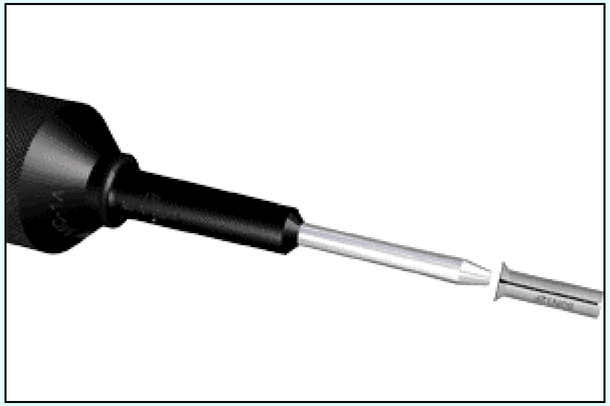

. **Step 1** After verifying the starting hole size, slip the pre-lubricated split sleeve onto the mandrel, which is attached to the hydraulic puller unit.

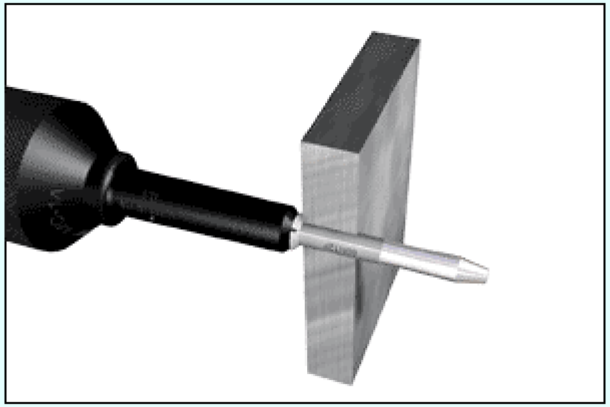

. **Step 2.**Insert the mandrel and sleeve through the hole with the nosecap held firmly against the work piece

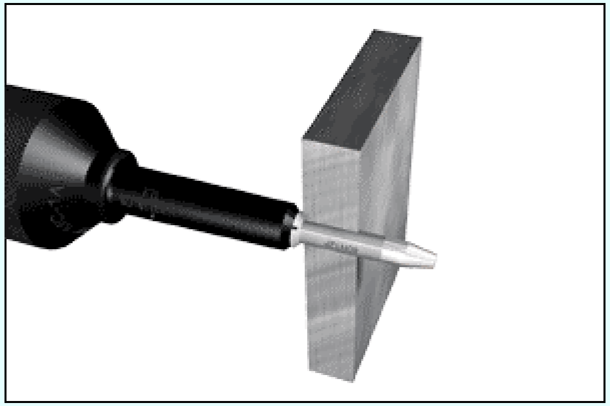

Step 3. Activate the puller unit. The mandrel is drawn through the sleeve and the hole. The combined thickness of the sleeve and the mandrel major diameter radially expand the hole. The lubricated sleeve reduces the pull force required, protects the hole, and allows the mandrel to exert radial forces through the entire thickness of the material.

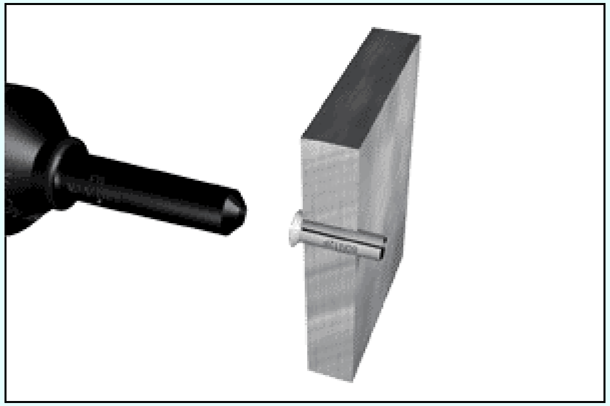

Step 4. Remove and discard sleeve

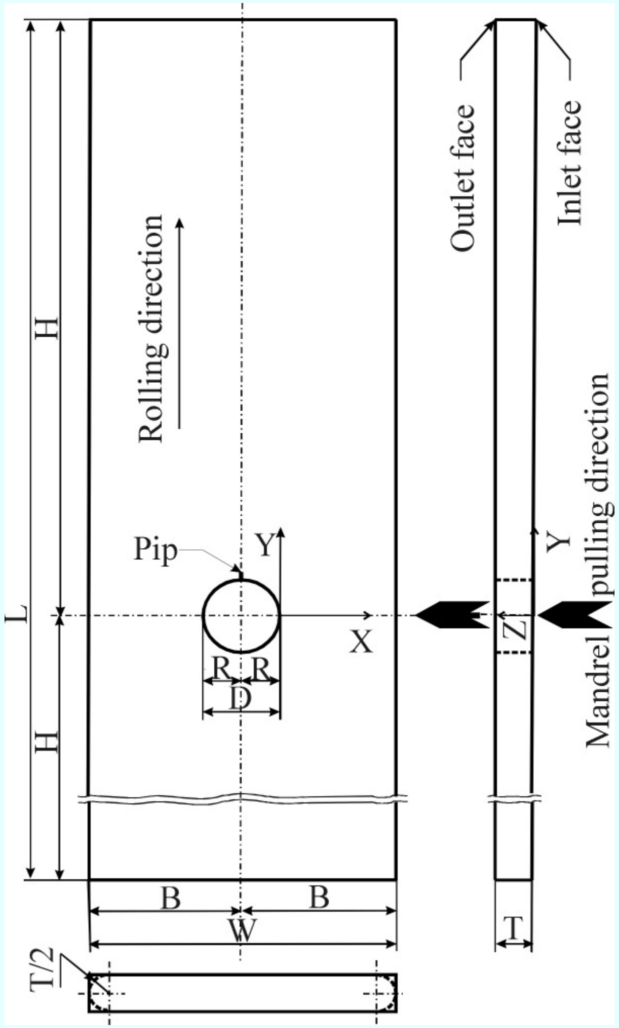

Test sample:

Aluminium sheet

Rolled out along the longitudinal direction

180 mm length, 40 mm width, 5 mm thickness

Initial hole drilled with diameter 9.52mm (3/8inch)

Cold expansion (4%) to 10 mm diameter

Strain measurements with synchrotron radiation, neutrons, and simulated data

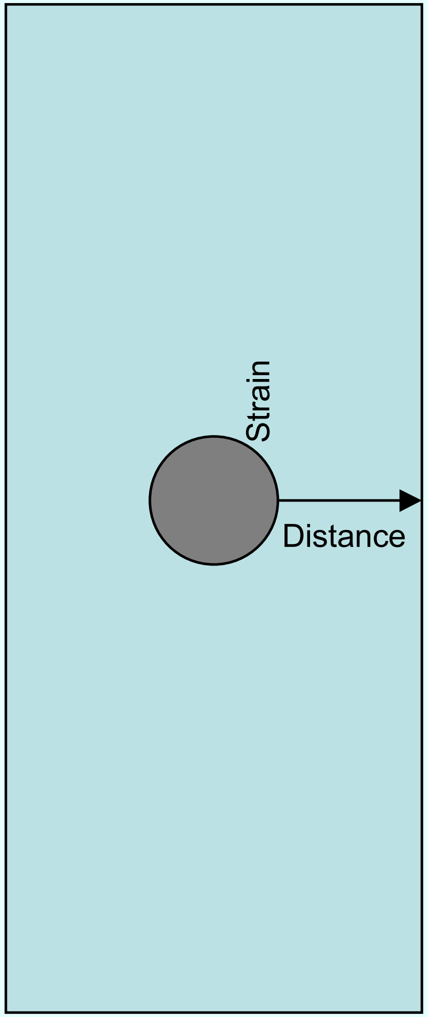

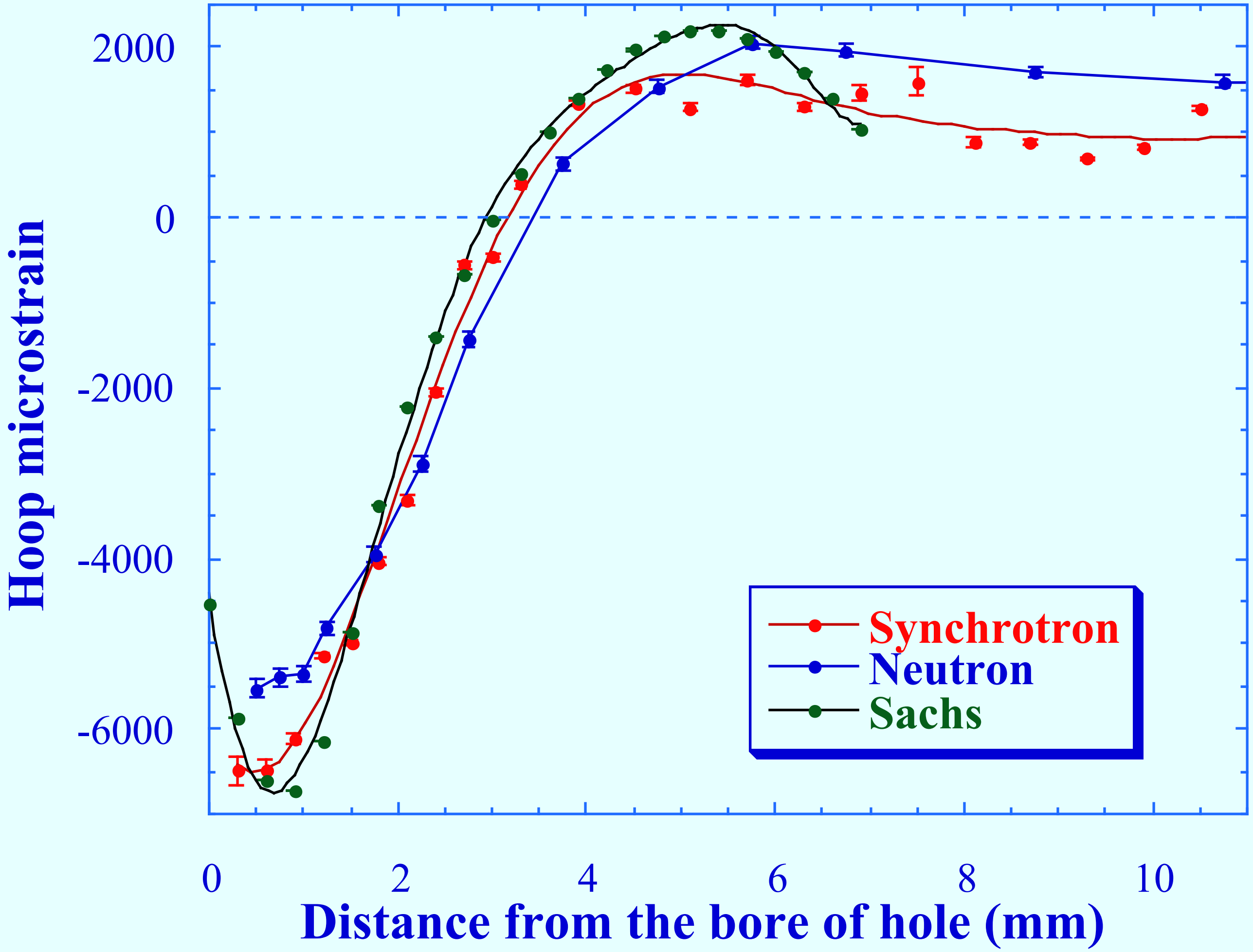

Measurement of a 3D computed tomography of the test sample

• Distance sample to detector was approx. 50 cms.

• 400 projections recorded for calculation of the tomography

• The tomography delivers a range interval of gray values for the attenuation of Aluminium

• For visualisation of the 3D tomography, nearly the whole attenuation range for Aluminium is set transparent, only the most attenuating part is set visible.

•The expanded area at the hole rim produces increased small angle scattering,
which in turn leads to increased attenuation of the transmitted beam.
The area clearly shows up in the computed tomography.

•Surprise: Even a wave structure resulting from the rolling of the Aluminium sheet is visible!

Piece of tape

Pieces of glue

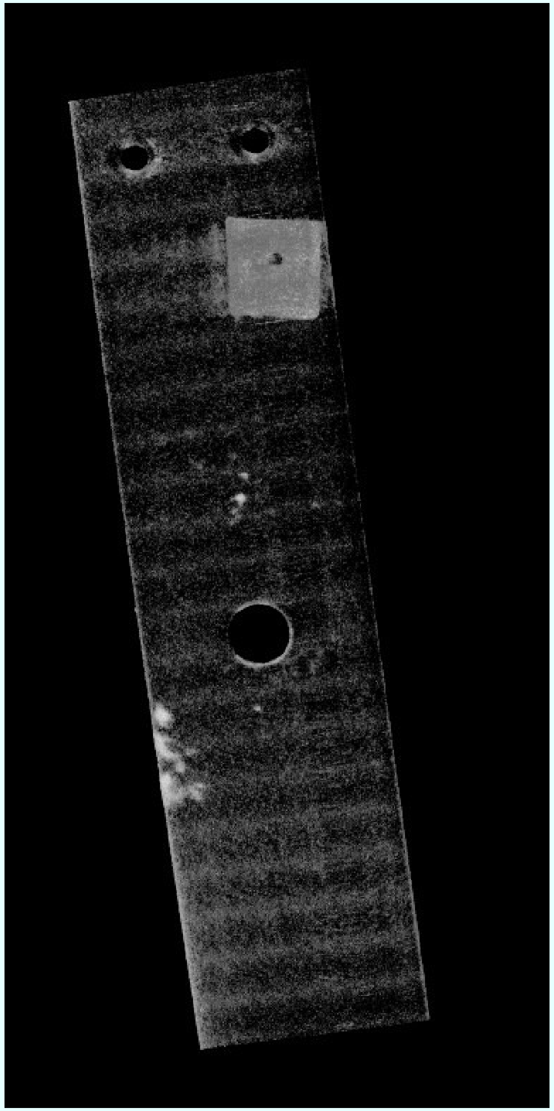

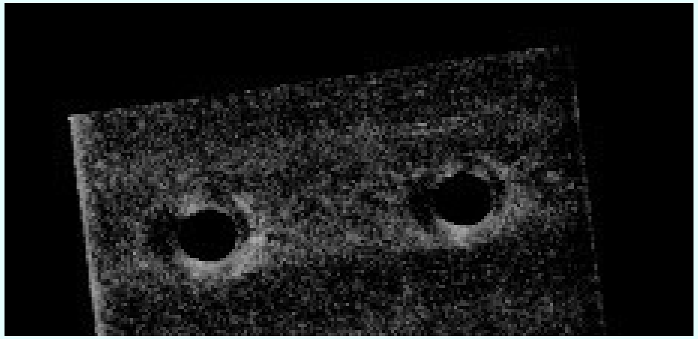

Ordinary holes with phased edges

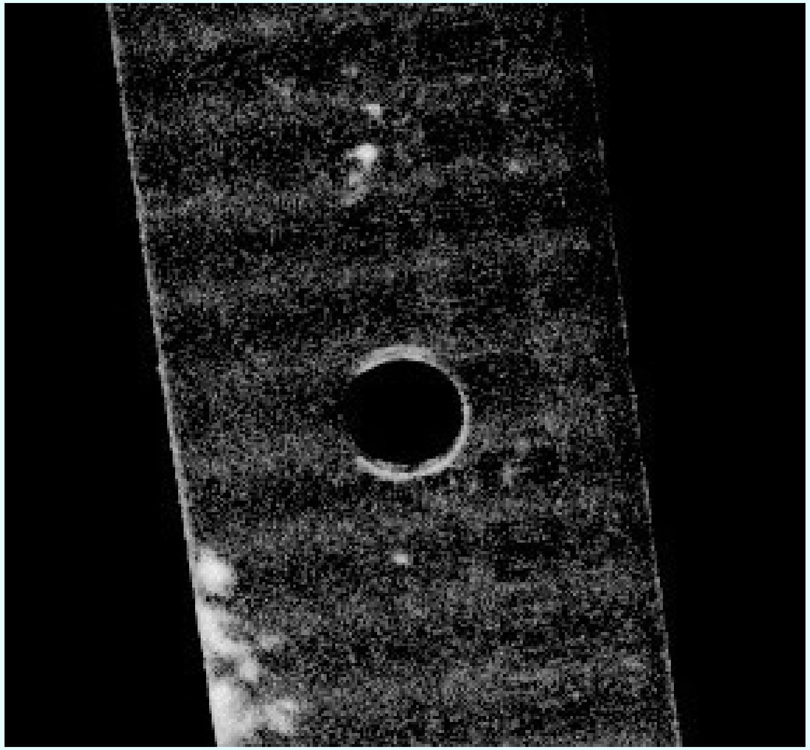

Widened hole compressed Edges.

The widening was asymmetric.

Surprise: Even a wave structure resulting from the rolling of the Aluminium sheet is visible!

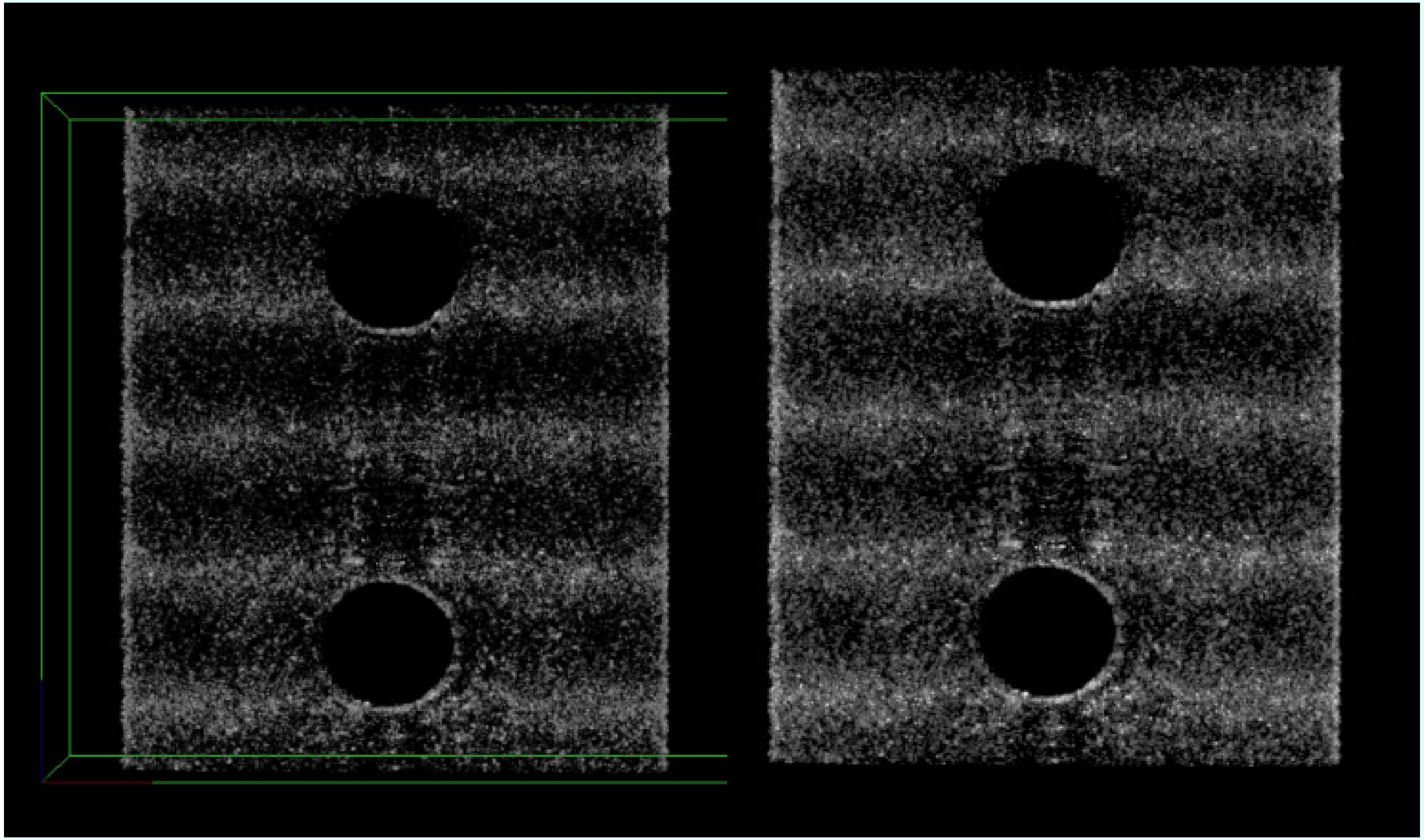

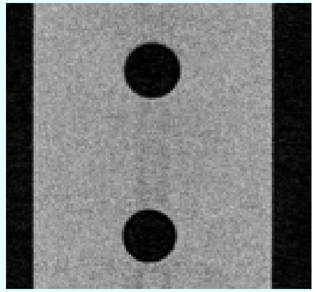

Above: Normal full view of the piece.

Second hole drilled for second tomography.

This was recorded with a smaller detector with less dynamics and sensitivity.
The distance to the detector was only 25 cms, but still, the difference is clearly visible!

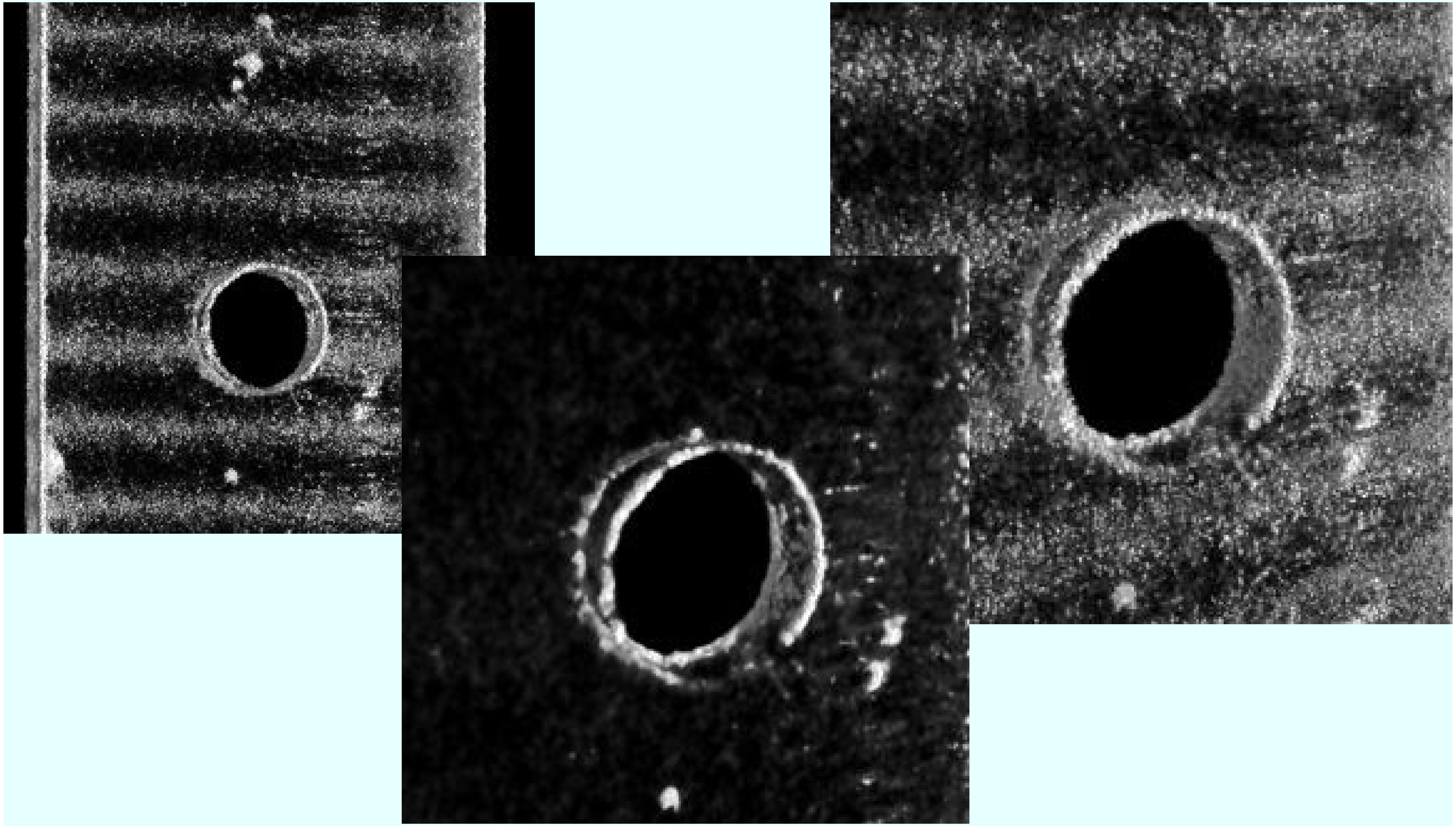

These pictures show more clearly that they represent a true 3D tomography.

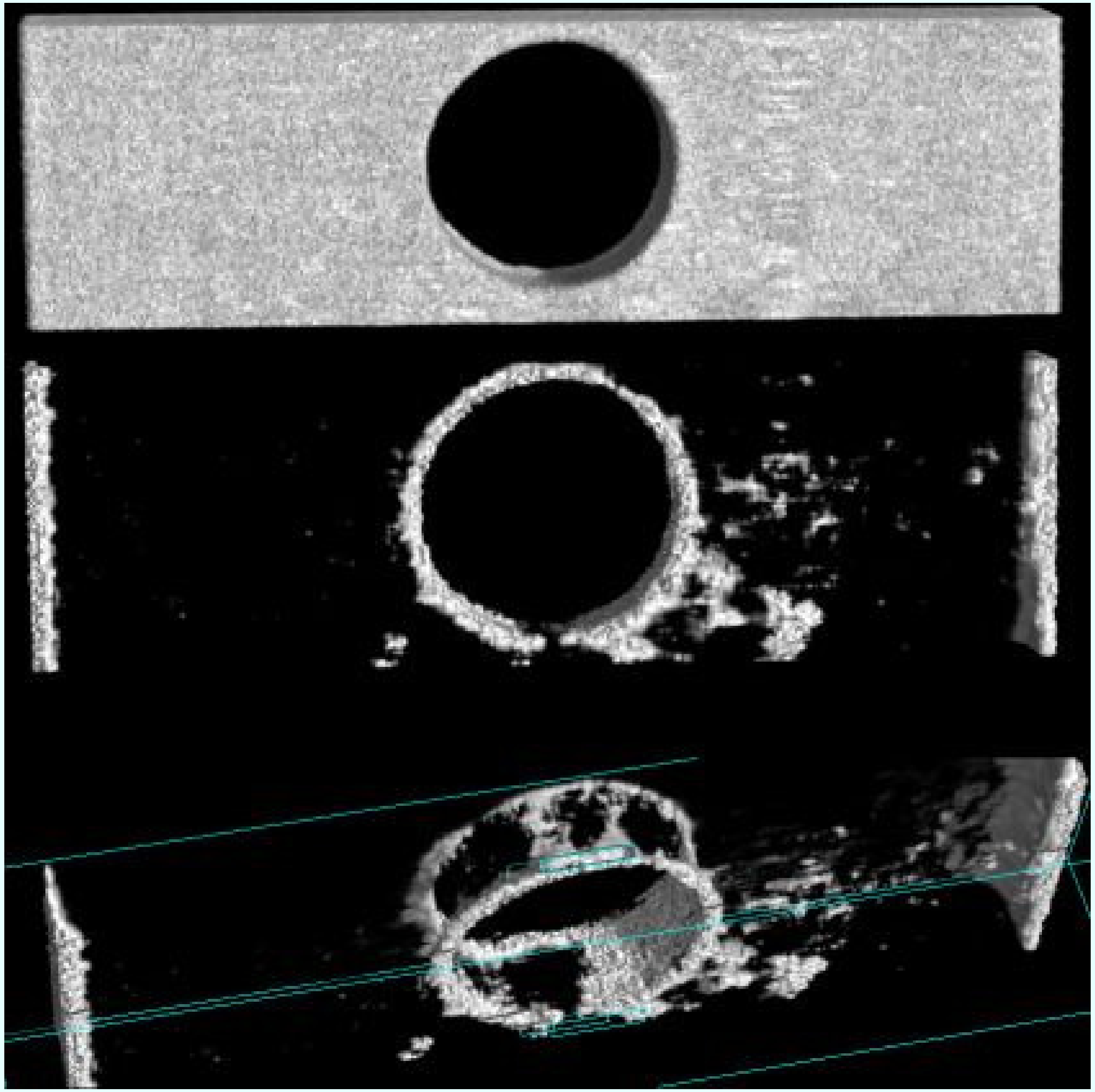

The edge of deformed material segmented in 3D.

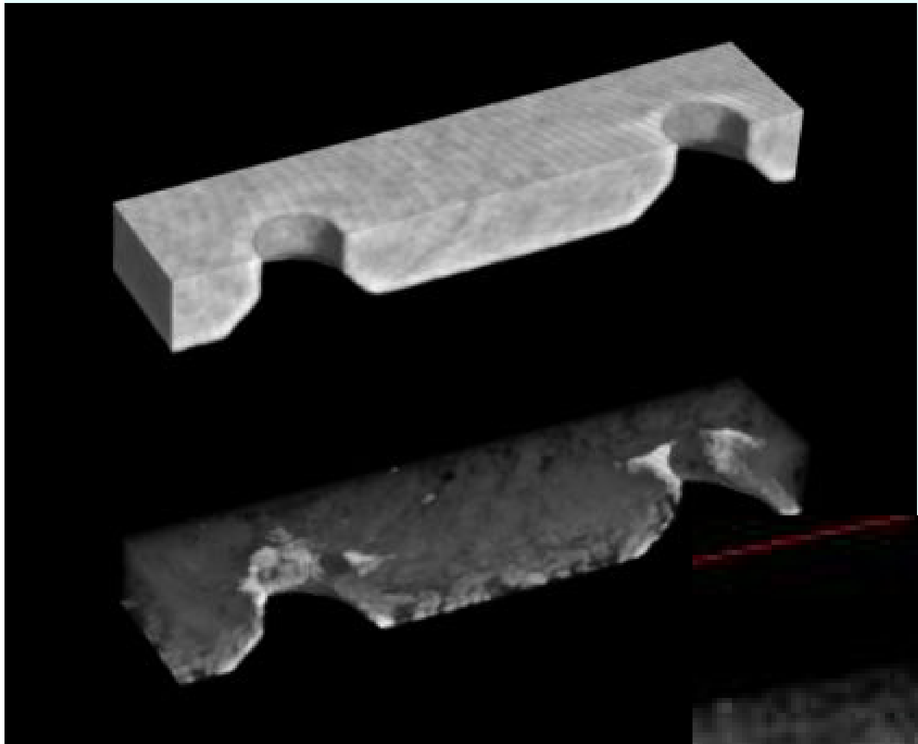

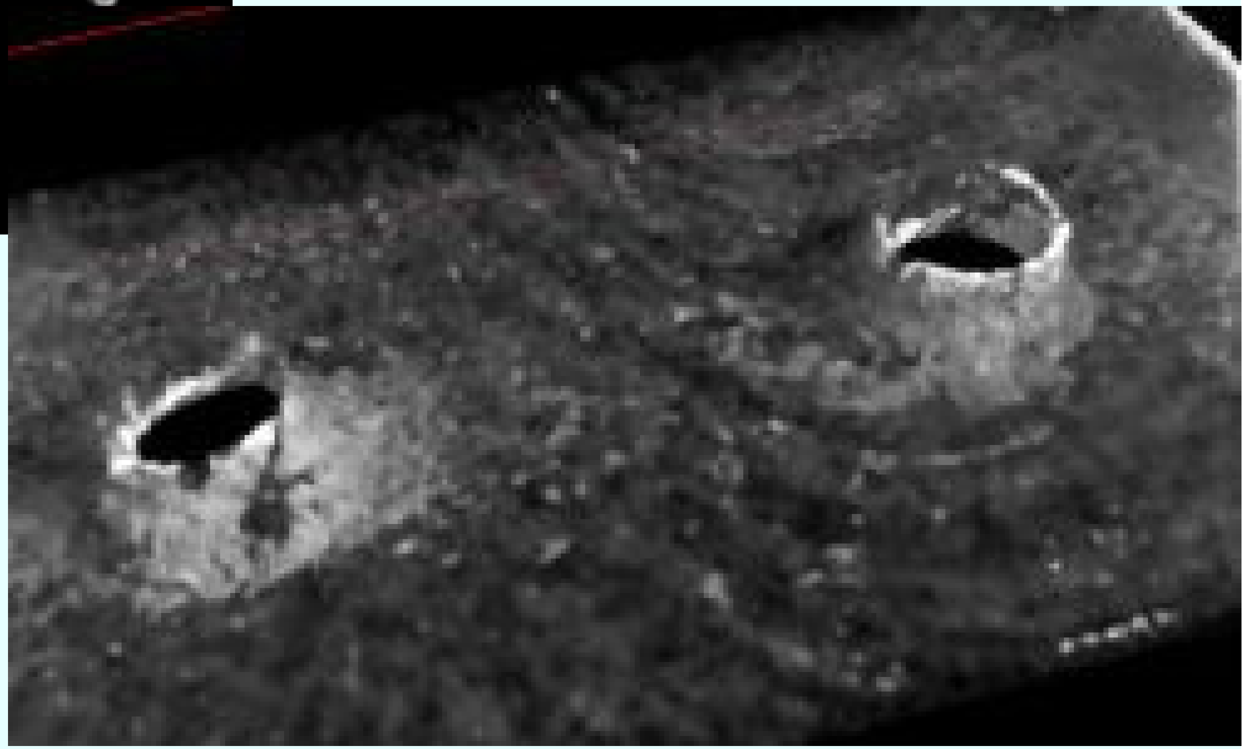

The phased holes on the top:
material deformed by the drill at
the fringes.

Phase Contrast Radiography with X-Rays and Synchrotron Light

X-ray image of a genetically engineered mouse (source: www.xrt.com.au):

Conventional radiography

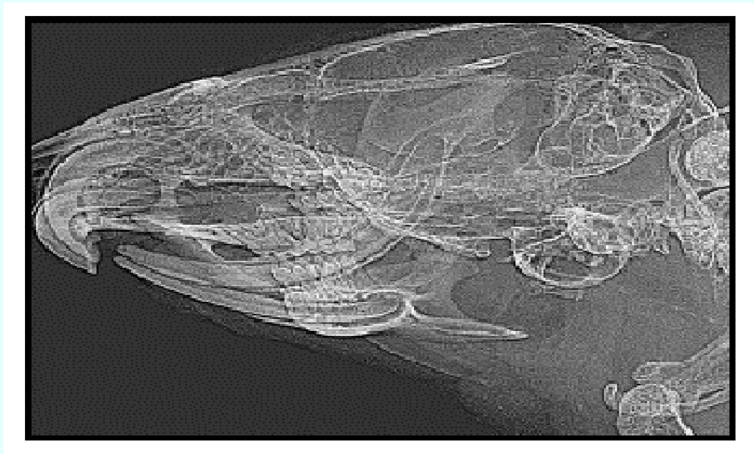

Phase contrast radiography

Refraction of a wave by a medium

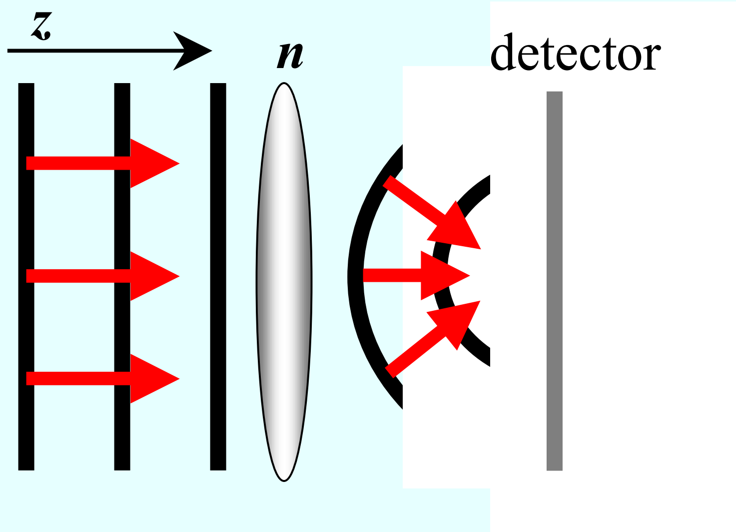

Refractive index:

phase shift absorption

$$n = 1 - \delta - i\beta$$

Angular deviation of the normal: $\Delta\alpha \propto \lambda \left| \nabla_{\perp} \varphi \right|$

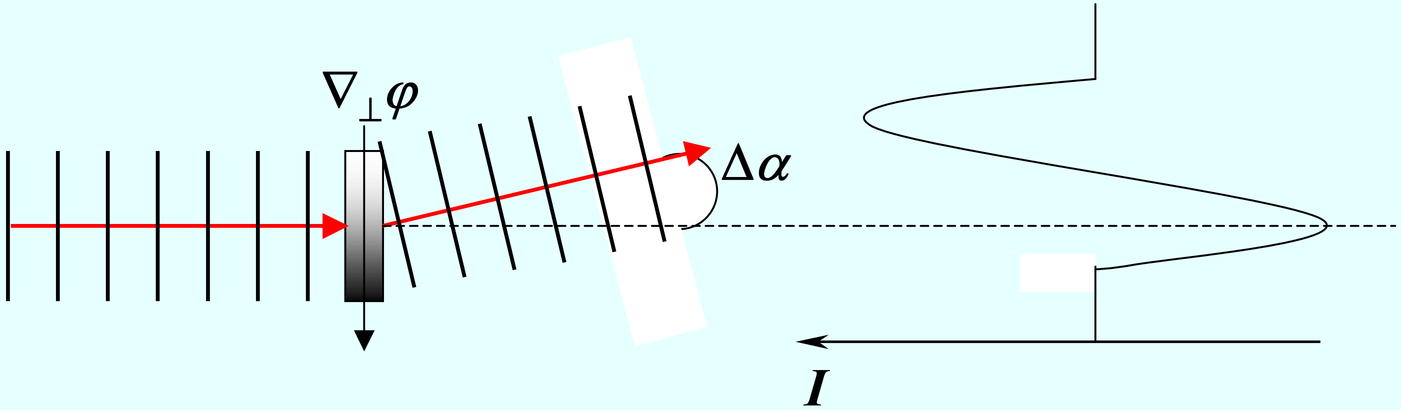

Phase object with gradient

Requirements for Phase Contrast

1. Neutron beam with a high lateral spatial coherence length.
2. The detector plane must be in the near field region.

Schematic of a phase contrast radiography setup:

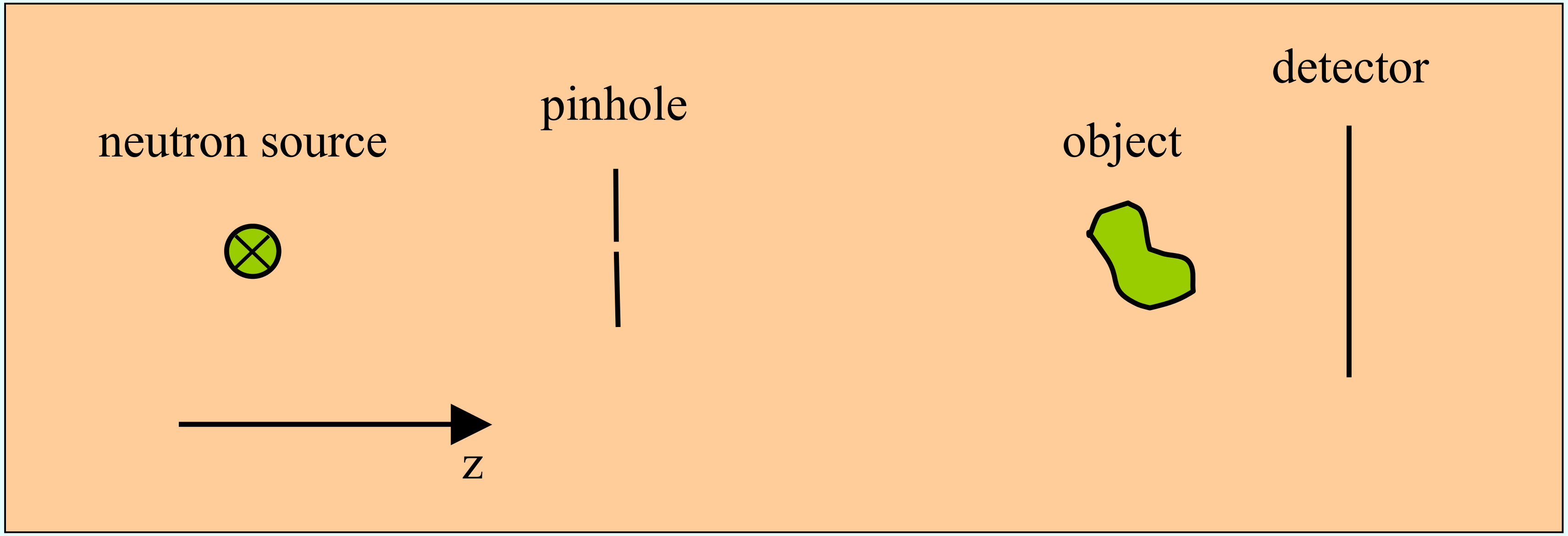

The small pinhole results in low intensity and large exposure times!
(several minutes to hours per radiograph)

Beam Characteristics

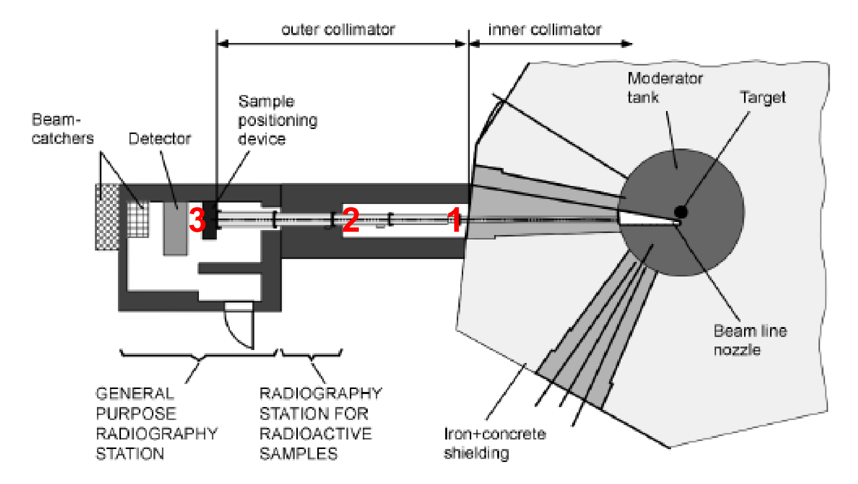

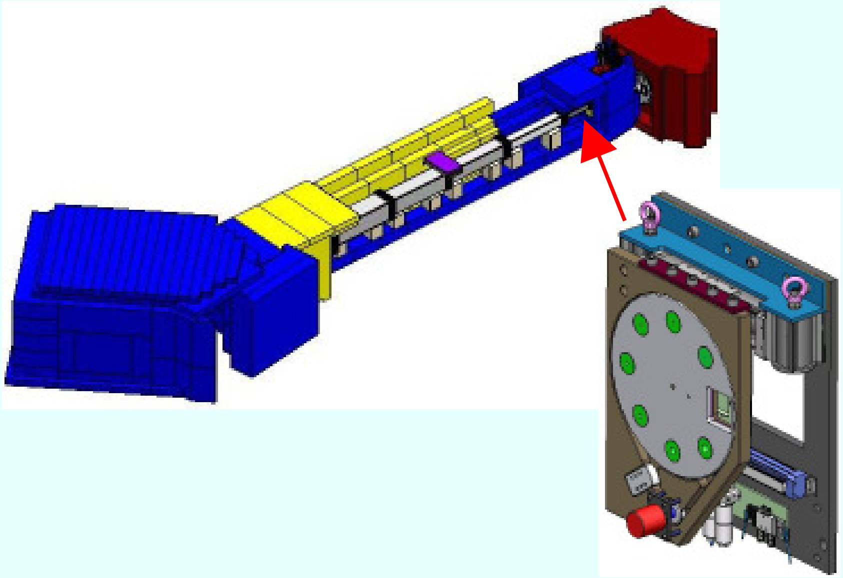

	NEUTRA Pos. 3	ANTARES
Energy of the neutrons	thermal neutrons	cold neutrons
Distance from the pinhole position [mm]	6675	13600
L/D-ratio without pinhole	550	400
L/D-ratio with 0.5mm pinhole	13350	27200
Neutron flux with 0.5mm pinhole [$cm^{-2}s^{-1}$]	3.64E+03	2.3E+04
Beam diameter with 0.5mm pinhole [mm]	36.3	290

For the long sample-to detector-distance at ANTARES, a 2 mm pinhole is sufficient.

With the resulting intensity, a good phase contrast image takes about 7-10 minutes, making phase contrast tomography possible.

Investigations on metal foams

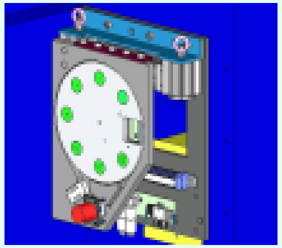

information about the average bubble size,
standard deviation, homogeneity of the distribution of the bubbles

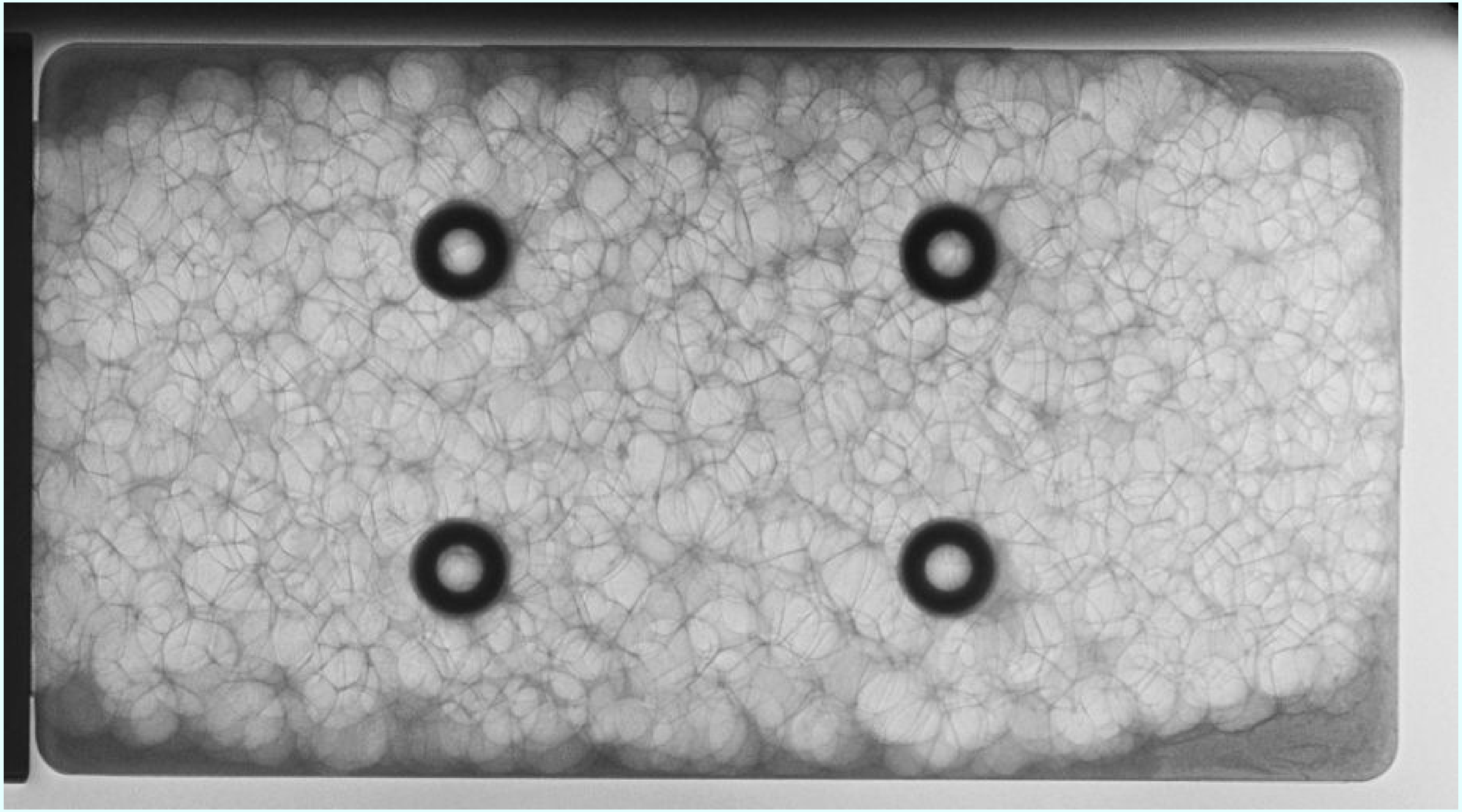

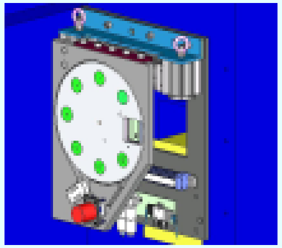

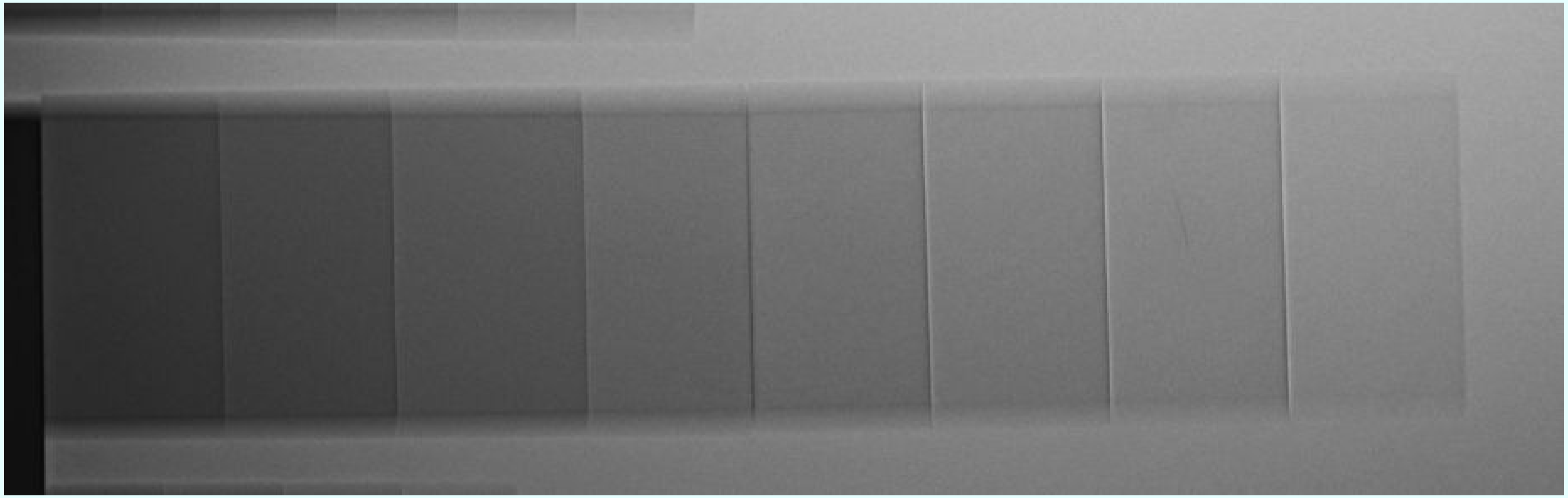

On a massive step wedge, we can even see the bright and dark part of the edge enhancement!

Step wedge made from one Aluminium alloy, with surrounding casting of a different Aluminium alloy with different index of refraction.

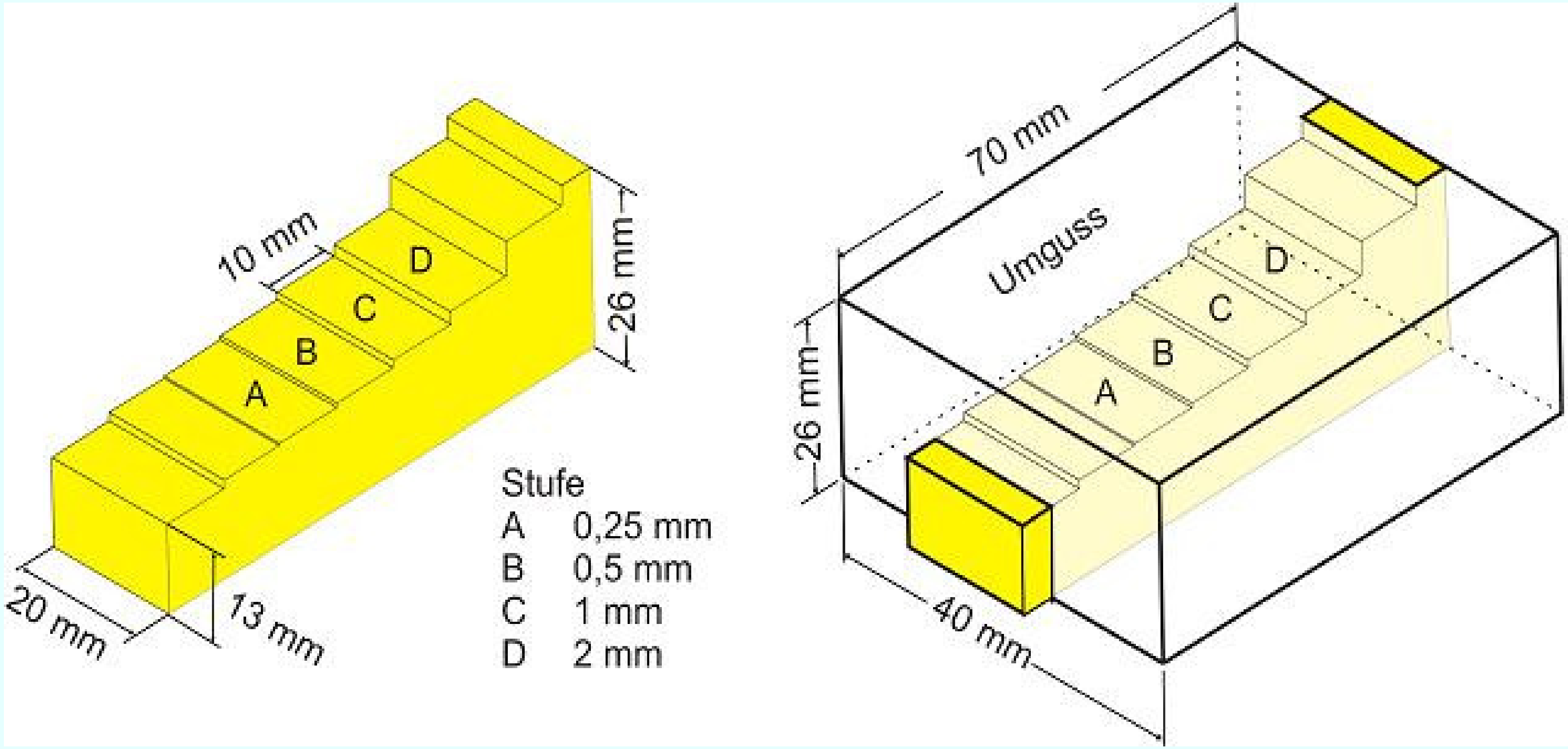

Aluminium foam and step wedge with surrounding.

The standard radiograph (left) shows only air gaps, the phase contrast radiograph shows the material interface!

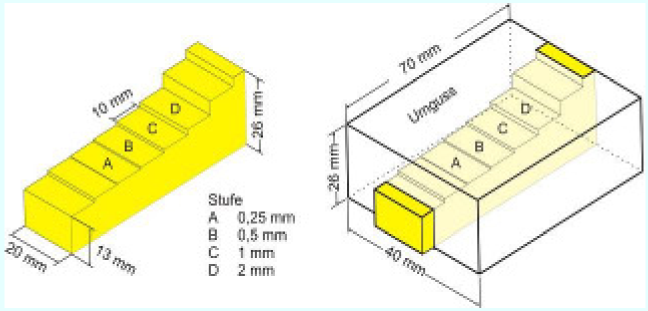

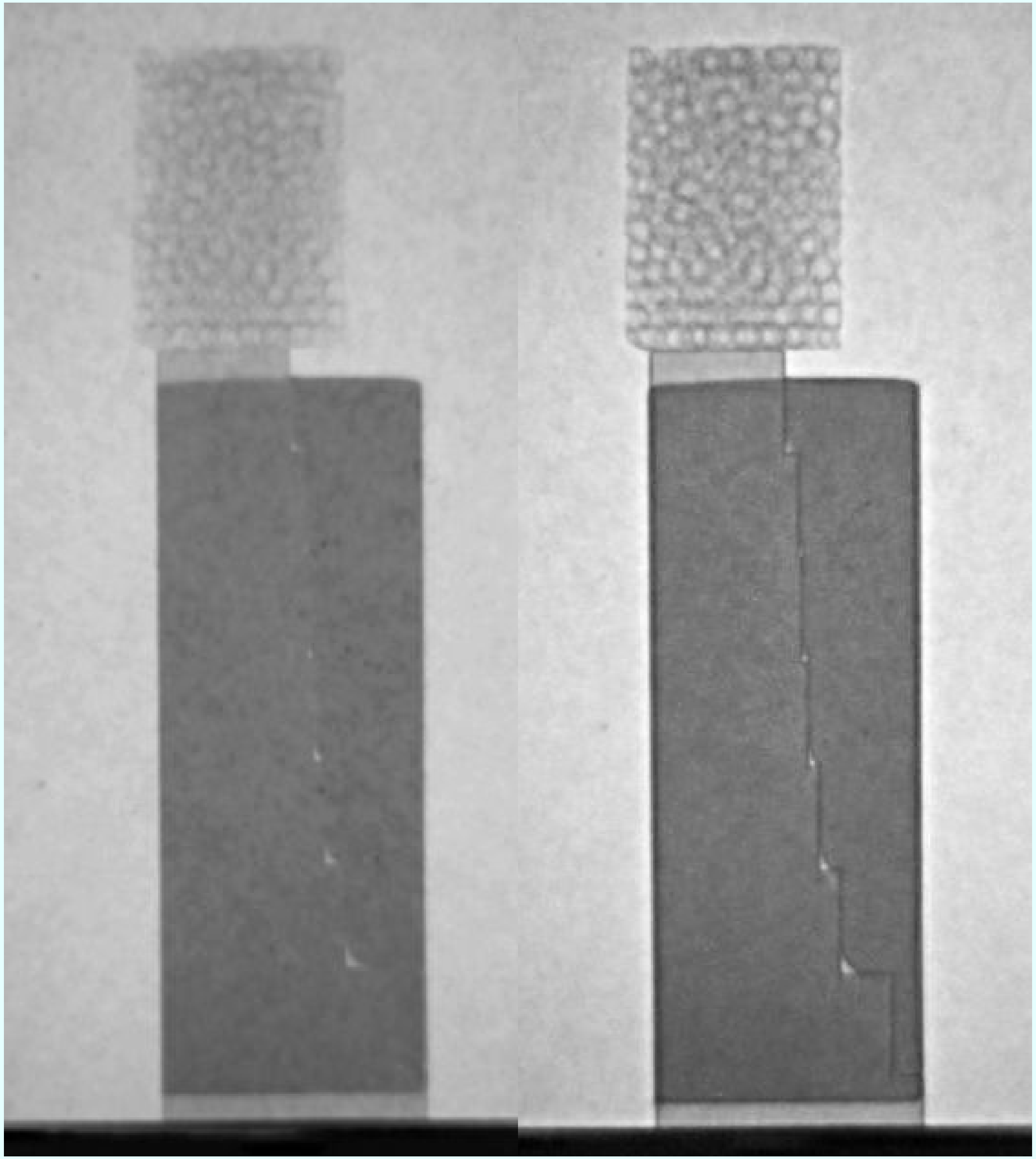

90° rotated view:
The standard radiograph (left) shows no difference between the Aluminium alloys, the phase contrast radiograph shows the material interface!

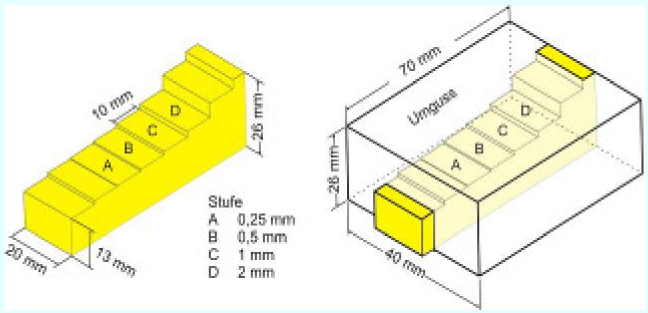

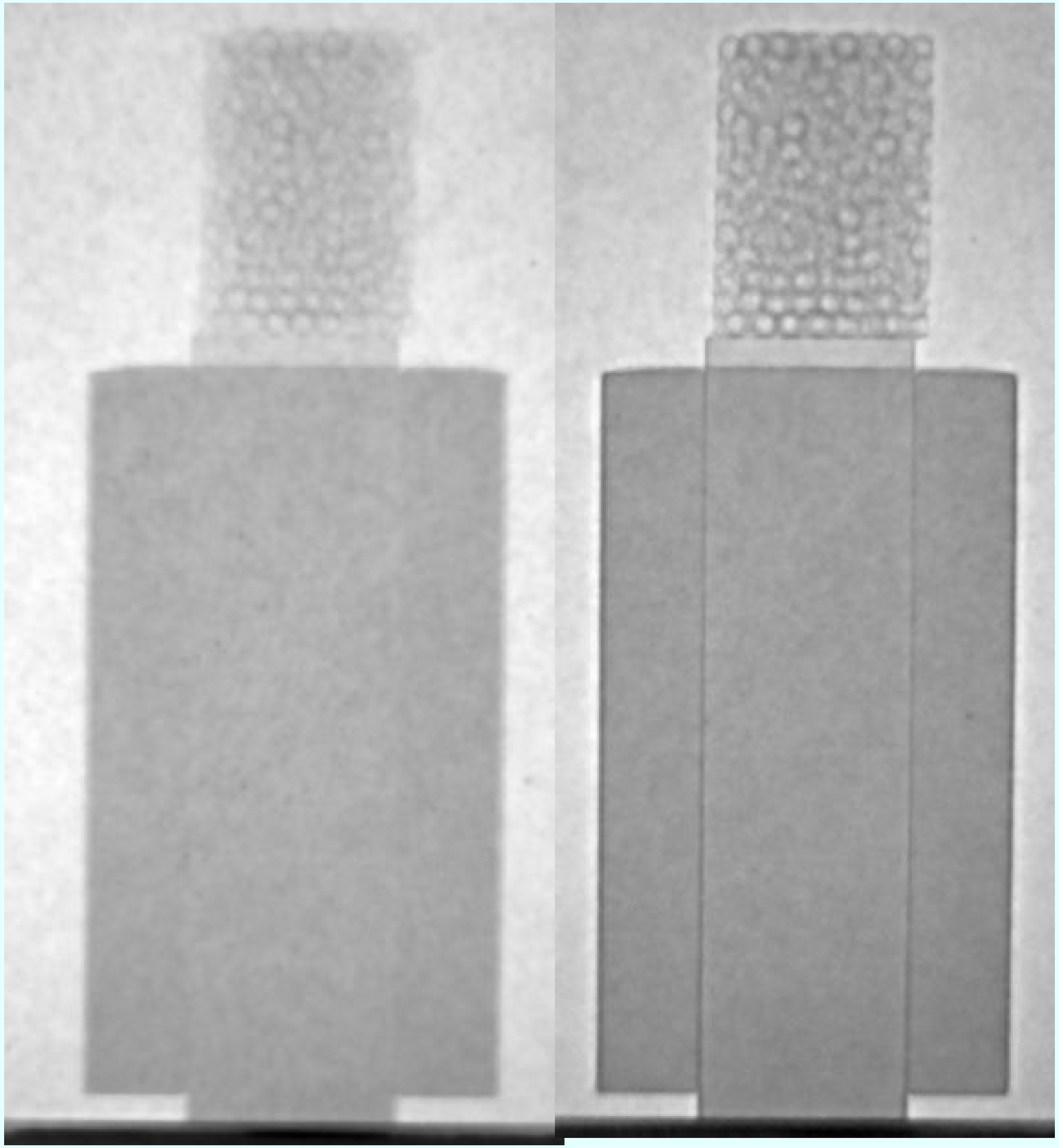

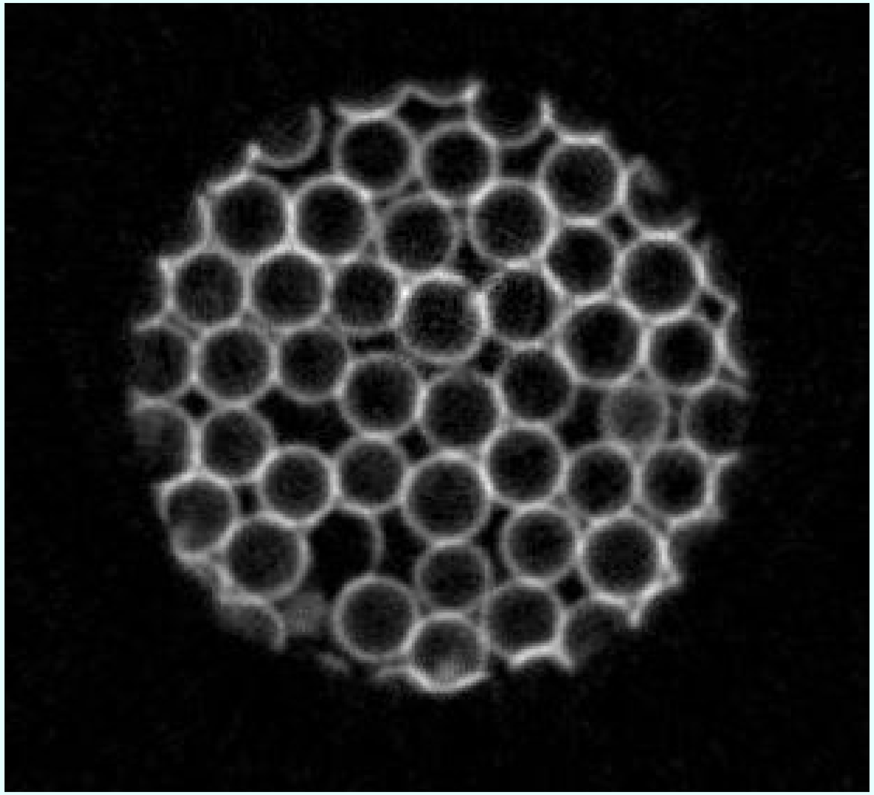

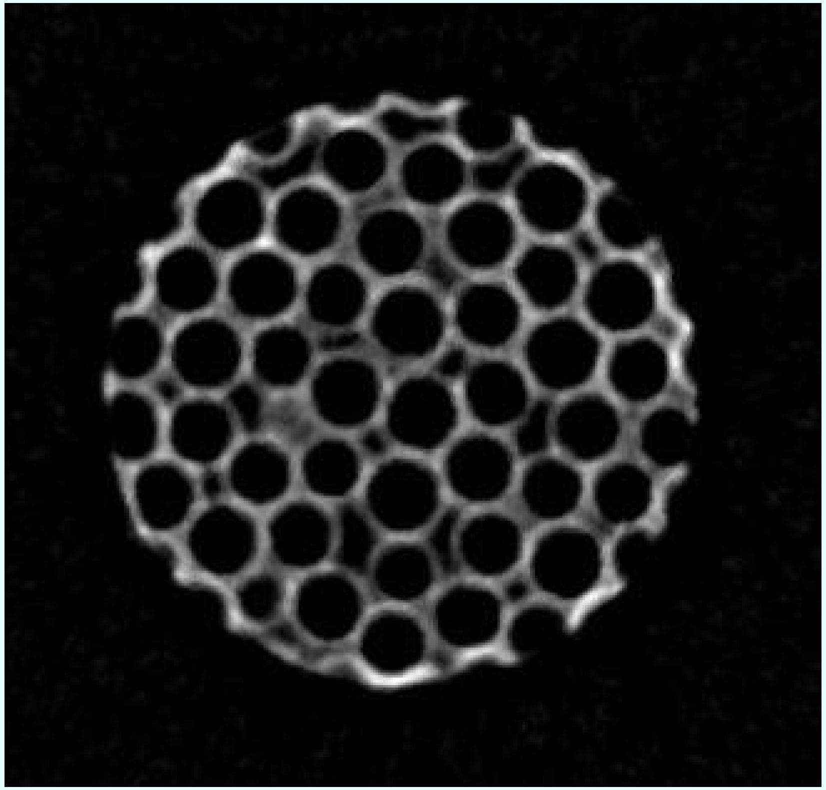

Aluminium foam

Left: **Standard Tomography**

Continuous grey scale for material thickness

Right: **Phase contrast tomography**

Strong edge enhancement

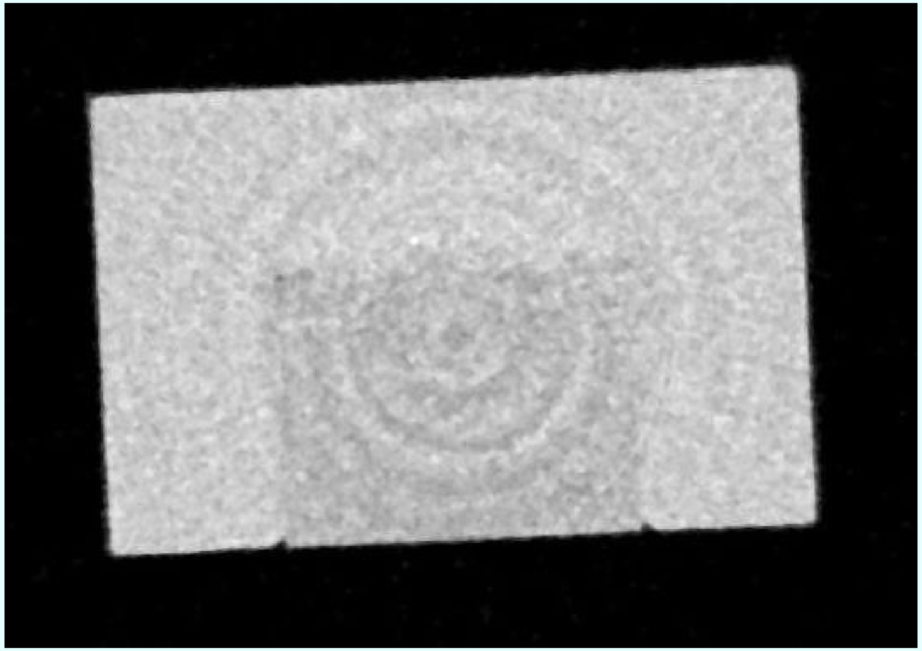 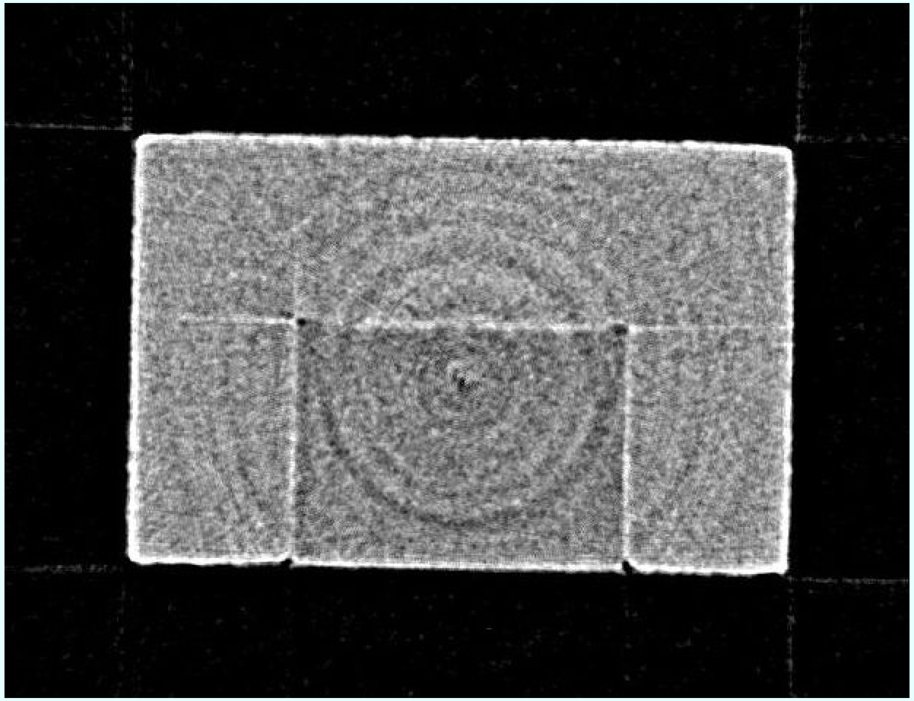

Aluminium step wedge with surrounding casting

Left: **Standard Tomography**

Nearly identical attenuation for both alloys

Right: **Phase contrast tomography**

Strong edge enhancement but new reconstruction artefacts!

Biomechanics: Pulmonary System

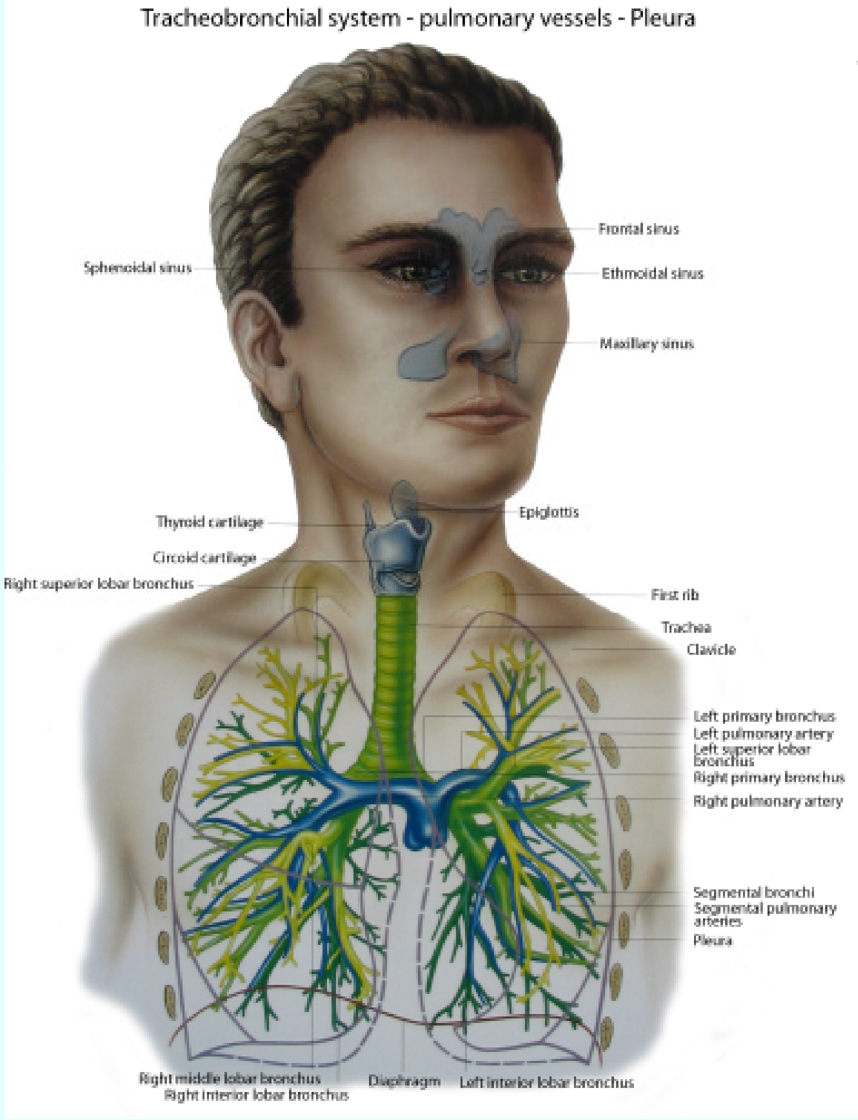

"**Terra Incognita**" with high potential clinical relevance

Bridging the gap of different scales and physical areas

Trachea
Ø 18mm

T. Bronchus
Ø 1.09

T. bronchiole
Ø 0.6

Alveoli
Ø 0.28
(Weibel 1963)

Fluid – Structure

Fluid – Liquid Lining – Structure

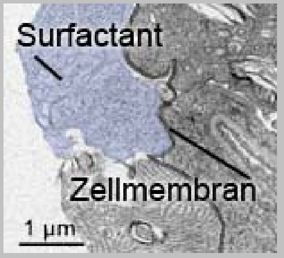

- Patients in hospitals often suffer lung damage when on long-time artificial respiration

- This is due to insufficient fine-tuning of the respiration pressure

- The exact composition of the lung is of yet poorly understood

- A numerical model of a lung is to be developed to simulate the air flow

- X-ray tomography cannot deliver fine data due to lack of contrast

- But neutrons proved rather successful in a first attempt….

- For the experiment, lungs are extracted from “recently deceased” rats.

- The lungs are confined in an Aluminium cylinder to simulate the ribcage

- They are inflated by 20-30 mbar air pressure

- For some lungs, 0.15 ml of a contrast agent containg Gadolinium were injected into the main air tube (windpipe)

- One lung was inflated without container

Scales to bridge

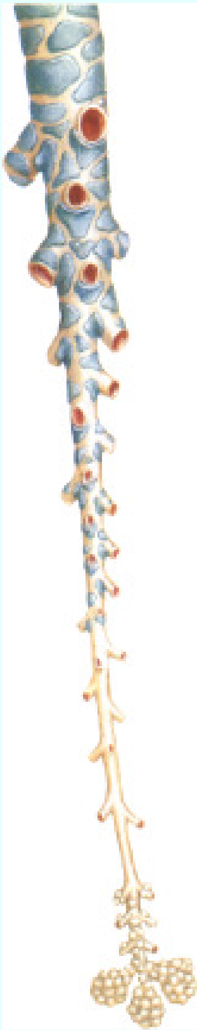

Trachea

Generation: 1
Number: 1
Diameter: 18 mm
Area: 2.6 cm^2
Reynolds No.: 4350

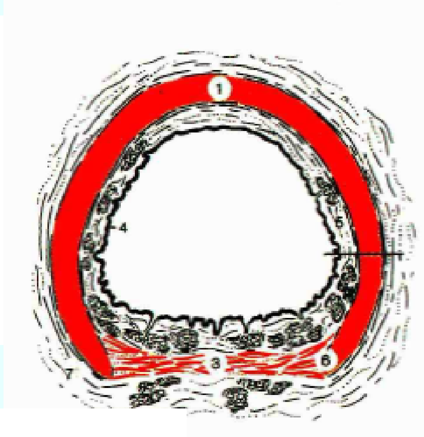

T. Bronchus

Generation: 11
Number: 2050
Diameter: 1.09 mm
Area: 19 cm^2
Reynolds No. 34

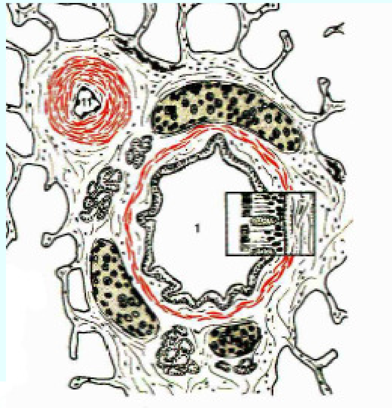

Alveolar duct

Generation: 22
Number: 4.19 x 10^6
Diameter: 0.41 mm
Area: 5900 cm^2
Reynolds No.: 0.04

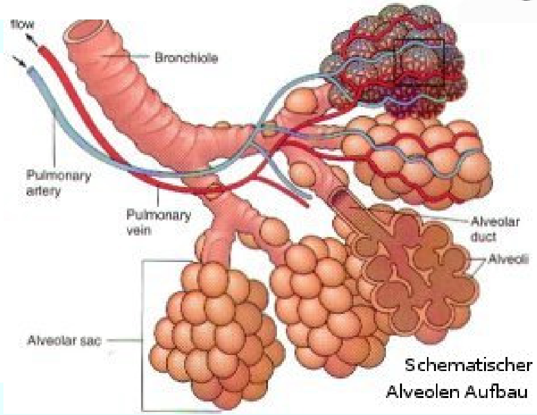

Weibel et al.

Neutron computed tomography on rat lungs

lung inflated inside
Al container

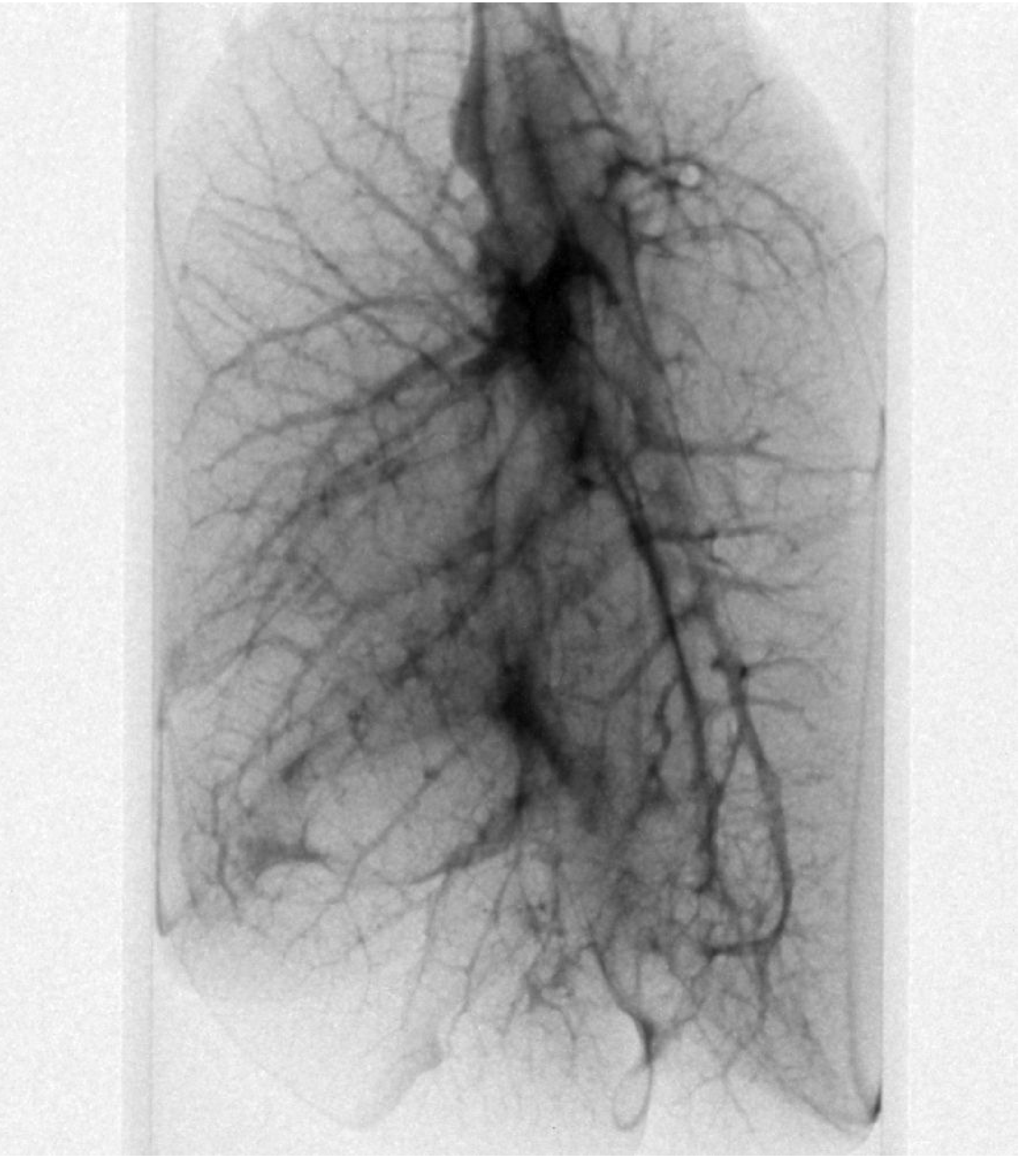

Neutron computed tomography on rat lungs

lung inflated inside
Al container

Neutron computed tomography on rat lungs

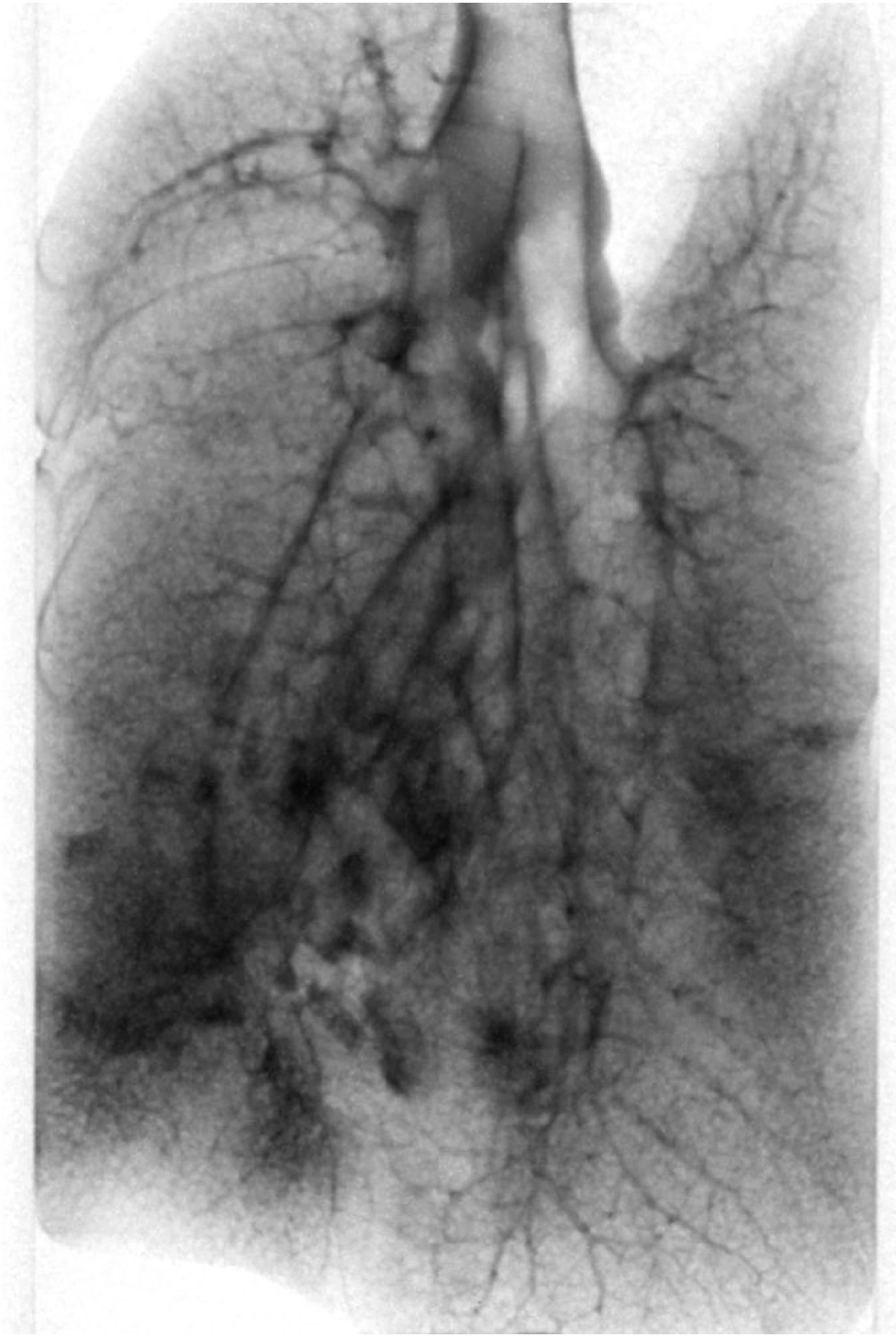

lung inflated inside
Al container with Gd
Contrast agent

Neutron computed tomography on rat lungs

lung fully inflated
without confining
container

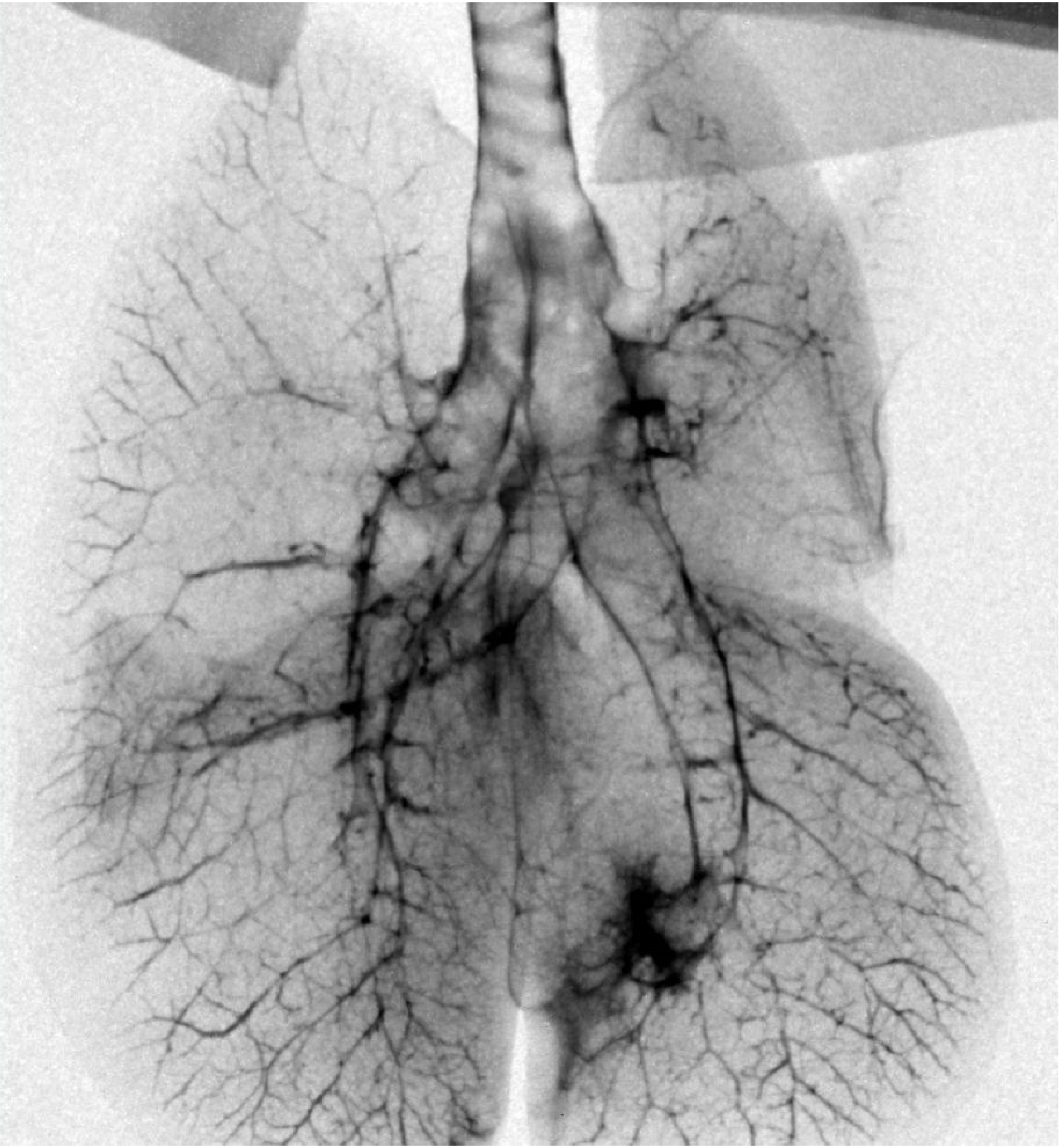

Neutron computed tomography on rat lungs

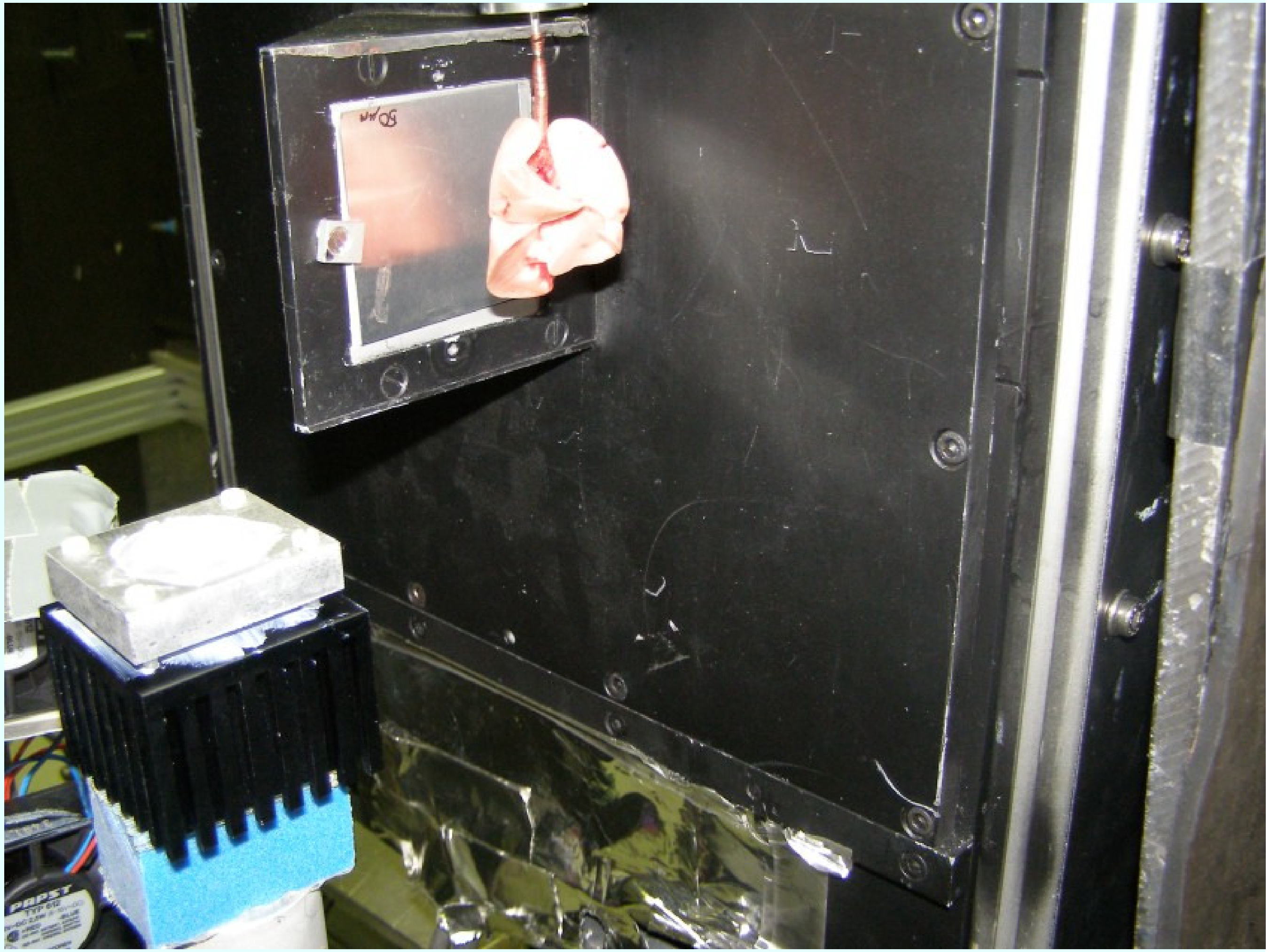

lung fully inflated
without container

Neutron computed tomography on rat lungs

lung fully inflated
in a non-confining
Container for the
CT scan

Tomography
of the lung

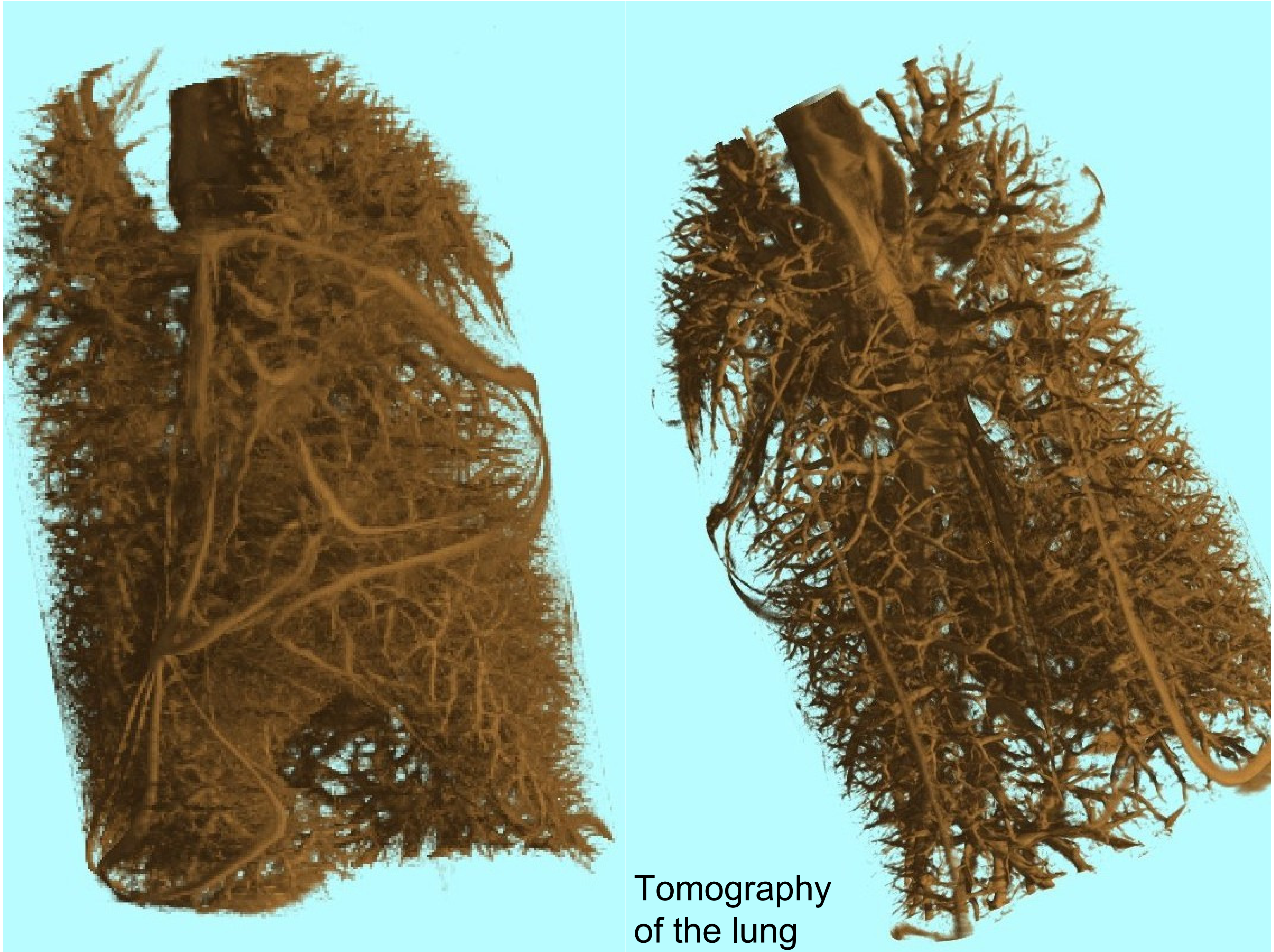

Tomography
of the lung

Neutron computed tomography on rat lungs

Tomography of the lung with Gd contrast agent

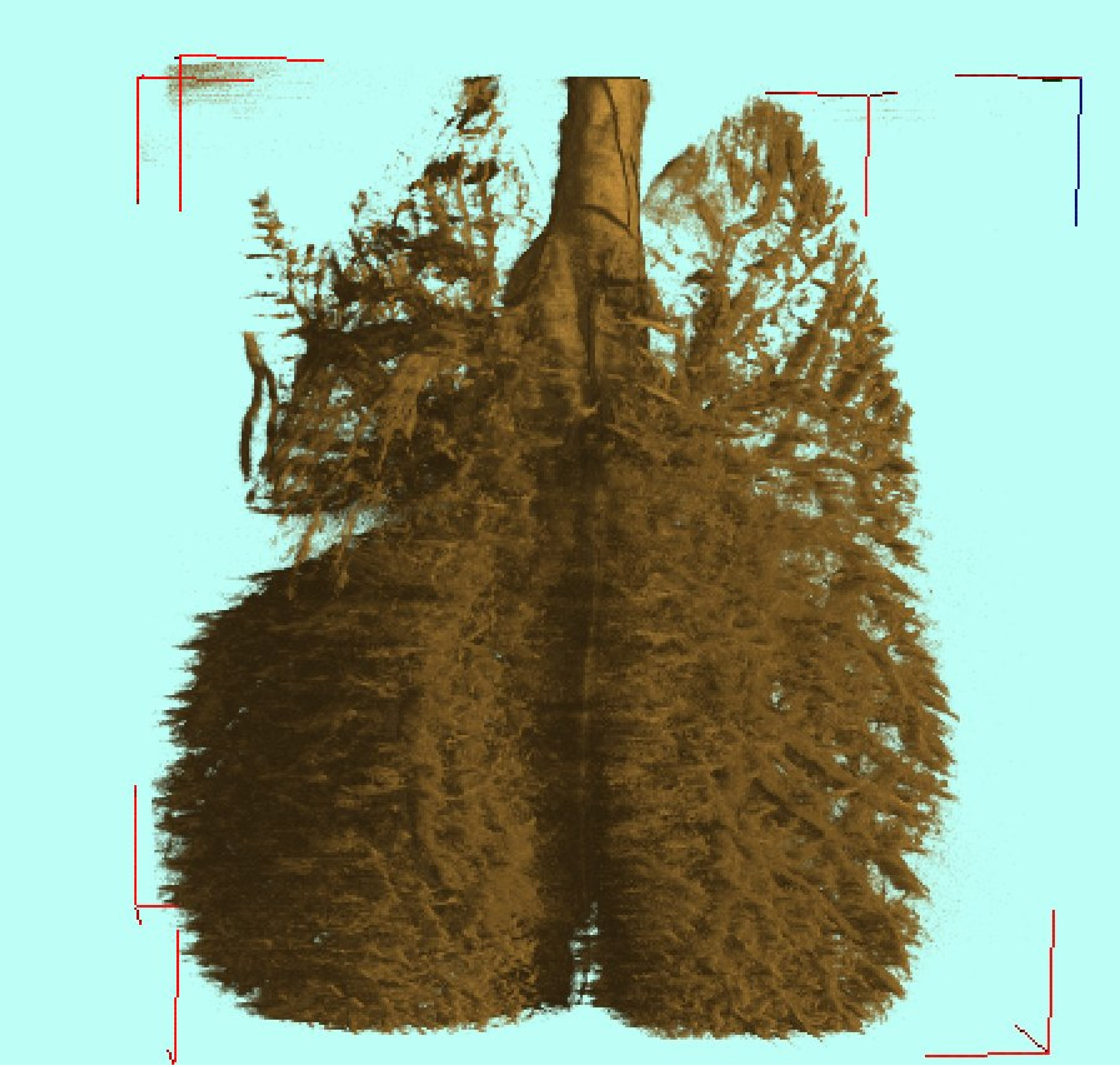

Die Neutronen-CT-Anlage ANTARES steht der Industrie für Messungen zur Verfügung.

(Da wir ein staatliches Institut sind und kein Wirtschaftsunternehmen, darf ich hier werben!)

Da wir die Anlage in staatlichem Auftrag zur Verfügung stellen, arbeiten wir nicht kostendeckend, wodurch wir günstige Preise anbieten können.

Industriekunden bekommen bevorzugten kurzfristigen Zugang.

Haben Sie Fragen?

Kontakt:

Dr. Burkhard Schillinger
TU München – FRM-II
Lichtenbergstr.1
85747 Garching bei München

Tel. 089/289-12185
Fax -14997
Burkhard.Schillinger@frm2.tum.de
www.frm2.tum.de